TITLE:

Identification of 153 new loci associated with heel bone mineral density and functional involvement of GPC6 in osteoporosis

AUTHOR LIST AND AFFILIATIONS

John P Kemp[1,2§], John A Morris[3,4§], Carolina Medina-Gomez[5,6§], Vincenzo Forgetta[3], Nicole M Warrington[1,7], Scott E Youlten[8,9], Jie Zheng[2], Celia L Gregson[10], Elin Grundberg[4], Katerina Trajanoska[5,6], John G Logan[11], Andrea S Pollard[11], Penny C Sparkes[11], Elena J Ghirardello[11], Rebecca Allen[11], Victoria D Leitch[11], Natalie C Butterfield[11], Davide Komla-Ebri[11], Anne-Tounsia Adoum[11], Katharine F Curry[11], Jacqueline K White[12], Fiona Kussy[12], Keelin M Greenlaw[3], Changjiang Xu[13], Nicholas C Harvey[14,15], Cyrus Cooper[14,15,16], David J Adams[12], Celia MT Greenwood[3,4,17,18], Matthew T Maurano[19], Stephen Kaptoge[20,21], Fernando Rivadeneira[5,6], Jonathan H Tobias[10], Peter I Croucher[8,9,22], Cheryl L Ackert-Bicknell[23], JH Duncan Bassett[11], Graham R Williams[11], J Brent Richards [3,4,24#*], David M Evans[1,2#*]

[1] University of Queensland Diamantina Institute, Translational Research Institute, Brisbane, Queensland, Australia

[2] MRC Integrative Epidemiology Unit, University of Bristol, UK

[3] Centre for Clinical Epidemiology, Lady Davis Institute, Jewish General Hospital, McGill University, Montréal, Québec, Canada

[4] Department of Human Genetics, McGill University, Montréal, Québec, Canada

[5] Department of Internal Medicine, Erasmus Medical Center, Rotterdam, The Netherlands

[6] Department of Epidemiology, Erasmus Medical Center, Rotterdam, The Netherlands

[7] Division of Obstetrics and Gynaecology, The University of Western Australia, Perth, Australia

[8] Garvan Institute of Medical Research, 384 Victoria Street, Sydney, New South Wales, Australia

[9] St Vincent's Clinical School, University of New South Wales, Sydney, New South Wales, Australia

[10] Musculoskeletal Research Unit, Department of Translational Health Sciences, University of Bristol, Bristol, UK

[11] Molecular Endocrinology Laboratory, Department of Medicine, Imperial College London, London, UK

[12] Wellcome Trust Sanger Institute, Wellcome Trust Genome Campus, Hinxton, Cambridgeshire, UK

[13] Donnelly Center for Cellular and Biomedical Research, University of Toronto, Toronto, Canada

[14] MRC Lifecourse Epidemiology Unit, University of Southampton, Southampton, UK

[15] NIHR Southampton Biomedical Research Centre, University of Southampton and University Hospital Southampton NHS Foundation Trust, Southampton, UK

[16] NIHR Oxford Biomedical Research Centre, University of Oxford, Oxford, UK

[17] Gerald Bronfman Department of Oncology, McGill University, Montréal, Québec, Canada

[18] Department of Epidemiology, Biostatistics & Occupational Health, McGill University, Montréal, Québec, Canada

[19] Department of Pathology and Institute for Systems Genetics, New York University Langone Medical Center, New York, New York, USA

[20] Department of Public Health and Primary Care, University of Cambridge, Cambridge, UK

[21] Strangeways Research Laboratory, Worts' Causeway, Cambridge, UK

[22] School of Biotechnology and Biomolecular Sciences, University of New South Wales, Sydney, New South Wales 2015, Australia

[23] Center for Musculoskeletal Research, Department of Orthopaedics, University of Rochester, Rochester, NY, USA

[24] Department of Twin Research and Genetic Epidemiology, King's College London, London, United Kingdom

[§]**These authors contributed equally to this work:**

John P Kemp, John A Morris and Carolina Medina-Gomez

[#]**These authors jointly supervised this work.**

J Brent Richards and David M Evans

*Address for correspondence:

David M Evans

University of Queensland Diamantina Institute

Level 8, 37 Kent St

Translational Research Institute

Woolloongabba, QLD, 4201

AUSTRALIA

Email: d.evans1@uq.edu.au

Brent Richards

H413, Jewish General Hospital,

3755 Cote Ste Catherine, Montreal, QC, H3T1E2

CANADA

Email: brent.richards@mcgill.ca

Key Words: bone mineral density, genome-wide association, *GPC6*, osteoporosis, UK Biobank, ultrasound

ABSTRACT

Osteoporosis is a common disease diagnosed primarily by measurement of bone mineral density (BMD). We undertook a genome-wide association study in 142,487 individuals from the UK Biobank to identify loci associated with BMD estimated by quantitative ultrasound of the heel ("eBMD"). We identified 307 conditionally independent SNPs attaining genome-wide significance at 203 loci, explaining approximately 12% of the phenotypic variance. These included 153 novel loci, and several rare variants with large effect sizes. To investigate underlying mechanisms we undertook: 1) bioinformatic, functional genomic annotation and human osteoblast expression studies; 2) gene function prediction; 3) skeletal phenotyping of 120 knockout mice with deletions of genes adjacent to lead independent SNPs; and 4) analysis of gene expression in mouse osteoblasts, osteocytes and osteoclasts. These studies strongly implicate *GPC6* as a novel determinant of BMD and also identify abnormal skeletal phenotypes in knockout mice for a further 100 prioritized genes.

INTRODUCTION

Osteoporosis is a common age-related disorder characterised by low bone mass and deterioration in bone micro-architecture leading to an increase in skeletal fragility and fracture risk. Low bone mineral density (BMD) is a strong risk factor for osteoporosis and is a key indicator for its diagnosis and treatment [1]. BMD is highly heritable [2], and genome-wide association studies (GWAS) have identified common variants at 73 loci associated with the trait, including many significantly associated with fracture risk [3,4]. Recently, deep imputation based on whole-genome sequencing, has also identified low frequency variants of large effect associated with BMD and fracture risk [4]. Despite these advances, common and rare variants only explain 5.8% of the total phenotypic variance in BMD [3,4].

Most previous genetic studies of BMD have analysed data derived from dual energy X-ray absorptiometry (DXA). However, DXA is expensive and consequently the largest GWAS to date of DXA-derived BMD includes only 32,965 individuals[4], compromising the ability to detect genetic loci. An alternative method of estimating BMD that is quick, safe, relatively inexpensive and can therefore be assessed in very large samples of individuals, is derived from ultrasound, typically at the heel calcaneus (referred to as estimated BMD "eBMD" in this manuscript). Measures of eBMD derived from ultrasound are highly heritable (in the order of 50% to 80%) [5-8], are independently associated with fracture risk [9,10], and are moderately correlated with DXA derived BMD at the hip and spine (r = 0.4 to 0.6) [11]. A previous GWAS that used heel ultrasound parameters (N = 15,514) identified variants at nine loci, including seven previously associated with lumbar spine/hip BMD [12].

Since genetic loci associated with BMD are strongly enriched for the targets of clinically relevant osteoporosis therapies[13,14], the discovery of new genetic loci and the biological pathways they implicate may help identify drug targets for the prevention and treatment of fragility fracture. In order to identify novel genetic determinants of BMD, we performed genome-wide association in the UK Biobank Study, which has measured eBMD and genome-wide genotypes on 142,487 individuals. We subsequently performed three systematic and complementary approaches to prioritize genes for functional validation (**Supplementary Fig. 1**).

RESULTS

Genome-wide Association Study of eBMD

BMD was measured by quantitative ultrasound of the heel, a non-invasive estimate of BMD (eBMD) that predicts fracture [9,10]. After stringent quality control of both eBMD and genome-wide genotypes (see Online Methods and **Supplementary Fig. 2**), data were available from 142,487 individuals (53% women) (**Supplementary Table 1**). We tested the additive effect of 17,166,351 single nucleotide polymorphisms (SNPs) with minor allele frequency (MAF) > 0.1% and imputation quality (info) score >0.4 on eBMD, controlling for age, sex and genotyping array. In total, 307 conditionally independent SNPs at 203 loci surpassed our revised genome-wide significant threshold ($P \leq 6.6 \times 10^{-9}$, which accounts for the larger number of independent SNPs deeply imputed in the UK Biobank, see Online Methods) and jointly explained ~12% of the variance in eBMD (**Supplementary Fig. 3, Supplementary Table 2**). Together the 307 SNPs explained about a third of eBMD SNP heritability estimated by BOLT-REML ($h^2_{SNP} = 0.36$). Although there was substantial inflation of the test statistics relative to the null ($\lambda_{GC} = 1.37$), linkage disequilibrium (LD) score regression[15] indicated that the majority of inflation was due to polygenicity rather than population stratification (LD Score regression intercept = 1.05). Of the 203 loci identified, 153 (75%) regions had not been implicated in previous GWAS of BMD (**Supplementary Table 2, Supplementary Fig. 3**).[3,4,16-22] Interestingly, the list of novel associations included multiple variants (e.g. SNPs at *TBX1*, *ZNRF3*) for which there was extremely strong evidence of association with heel eBMD (i.e. $P < 10^{-30}$), but little evidence of association ($p > 0.05$ any trait) in the previous GEFOS-Seq GWAS of DXA derived BMD[4] (**Supplementary Table 3**).

Our study also replicated SNPs in 55 out of 73 regions (>75%) that had been reported as genome-wide significant in previous GWAS of BMD at other body sites (i.e. $P < 0.05$ and consistent direction of effect), and we replicated all genome-wide significant loci identified in a previous GWAS of ultrasound heel eBMD[12] (**Supplementary Table 4**). Our list of known BMD associated SNPs is deliberately broad and comprehensive in terms of previous GWAS. This comprehensive inclusion policy, however, means that we have also incorporated the results of some smaller GWAS studies that may include false positives. When we restrict our attention to the 64 SNPs reported in the large Estrada et al (2012) GEFOS meta-analysis[3] (which are unlikely to represent type 1 errors), we replicate 54 of 64 (84%) SNPs. Possible reasons for non-replicating loci include site specificity, differences in phenotype (ultrasound derived versus DXA derived BMD), differences in ancestral population between studies, and type 1 error in the smaller previous study.

Notably, across six loci (*RSPO3*, *LINC00326*, *CPED1*, *MPP7*, *KCNMA1*, *TMEM263*), there were SNPs that exhibited different directions of effect in the current eBMD study compared to previous BMD studies. In the case of the SNPs at *CPED1*, these also showed an association with fracture in UK Biobank (see below), but in the direction predicted by eBMD rather than the direction predicted by BMD in previous studies (i.e. alleles that predispose to low eBMD are associated with increased risk of fracture). Although these opposite directions of association are harder to explain, differences in the phenotype measured by DXA and ultrasound technologies are likely to be responsible. For example, whereas heel ultrasound primarily measures trabecular bone, DXA-based BMD measurements reflect a combination of trabecular and cortical bone. In addition, ultrasound-based measurements are independent of bone size, while areal BMD as measured by DXA is not fully size corrected. In fact, of the six loci showing opposite associations between DXA BMD and eBMD, three also showed strong associations with height in the GIANT consortium in the same direction of DXA BMD[23], suggesting that the latter relationships may partly have reflected size effects (although it must be noted that several other concordant eBMD and DXA BMD associated loci also showed associations with height). Whereas bone size and bone mass generally show a strong positive correlation, genetic influences leading to greater bone size might be inversely related to trabecular bone density at certain sites, due to reduced mechanical

strain as a consequence of a larger and hence stronger skeleton. However, despite these few discrepancies, overall there was a strong positive correlation between estimated effect size for the genome-wide significant heel eBMD SNPs in the present UK Biobank Study and estimated effect sizes for DXA-derived BMD at other skeletal sites in our previous GEFOS-Seq study (femoral neck: Pearson's r = 0.64 (0.57 – 0.71); lumbar spine: r = 0.69 (0.62 – 0.75); forearm: r = 0.49 (0.39 – 0.58)) (**Fig. 1**)[4]. Adjusting for weight had little effect on the genome-wide significant results, save for partially attenuating the strength of association between eBMD and known adiposity variants (**Supplementary Table 5**).

Since we employed a large sample size and genotyped and/or imputed low frequency variants (MAF <1%), we next assessed the allelic architecture of eBMD (**Fig 2**). We found a strong relationship between MAF and effect size, which in general followed the statistical power of our study design. The variants of largest effect (where each allele increased eBMD by 0.44 standard deviations [SD], $P = 5 \times 10^{-11}$) were in the gene *IGHMBP2* (within 0.5Mb of known variants in *LRP5*) and the known *EN1* and *WNT16/CPED1* loci. We also detected several rare (MAF <1%) and low frequency variants (1% < MAF < 5%) in novel loci including rare variants near the genes *BMP5* and *BMPR2*. Comparing the mean absolute effect sizes of genome-wide significant variants, we found a 6.5-fold difference in effects attributed to rare compared to common variants.

Sex-specific analyses across the genome and tests of sex heterogeneity at genome-wide significant SNPs revealed a single variant rs17307280 at *FAM9B* on the X chromosome that was significantly associated with eBMD in men only (**Supplementary Fig. 4**, **Supplementary Table 6**) (heterogeneity $P = 1.4 \times 10^{-11}$), replicating previous results from Estrada et al.[3]

Effects on Fracture

We tested the relationship between eBMD-associated SNPs and fracture. We identified 14,492 individuals (58% women) in UK Biobank reporting a previous fracture, irrespective of the trauma mechanism, since high-trauma fractures are predicted by low BMD and are predictive of future low-trauma fracture, suggesting a shared aetiology [24,25]. In total, we observed that twelve eBMD SNPs were associated with fracture, after control for multiple testing ($P \leq 1.6 \times 10^{-4}$). Sensitivity analyses, including only 8,540 individuals (69% women) reporting a fracture resulting from a simple fall (i.e. from standing height), were consistent with these findings (**Table 1**). Of these twelve loci, variants at *AQP1* and *SLC8A1* have not been associated with BMD or risk of fracture previously (although both SNPs show nominal association ($P < 0.01$) with DXA derived measures of BMD in the previous GEFOS-Seq study[4] (**Fig. 1**, **Supplementary Table 3**)). Genome-wide significant eBMD variants showed an inverse relationship between their effect on eBMD and odds of fracture (**Supplementary Fig. 5**).

Shared Genetic Factors

We tested whether eBMD had a shared genetic aetiology with 247 other diseases and biomedically relevant traits using LD score regression[26] as implemented in LDHub[27]. This method estimates the degree of shared genetic risk factors between two diseases or traits, although it says nothing about how this shared genetic aetiology arises (i.e. whether one variable causes the other or whether the relationship between eBMD and the other variable is mediated by an underlying variable like body mass index which is itself partially genetic). **Fig. 3** shows that genetically increased eBMD was strongly and negatively correlated with fracture (r_g = -0.47, 95% CI: -0.59, -0.35). Further, measures of BMD at other skeletal sites showed moderate positive genetic correlations with eBMD (**Fig. 3**) consistent with the concordant directions observed at the genome-wide significant loci (**Fig. 1**).

We also tested to see whether eBMD was genetically correlated with a range of other complex traits and diseases (**Supplementary Table 7**; **Fig. 3**). We observed that eBMD was

weakly and negatively correlated with HDL, LDL, height, age at menarche and rheumatoid arthritis (**Fig. 3**). On the other hand, eBMD was weakly positively genetically correlated with body mass index (BMI), waist circumference, waist-hip ratio, coronary heart disease and type 2 diabetes. These findings support a shared genetic etiology of several common traits and diseases with eBMD, as has been shown previously between BMD, adiposity and type 2 diabetes through Mendelian randomization[28,29].

Gene Prioritization

Strategy One: Bioinformatic, Statistical and Functional Genomics in Humans

We used several bioinformatics and statistical genetics tools to prioritize likely candidate genes and variants. These included the Variant Effect Predictor software[30] to identify deleterious coding variation at genome-wide significant loci (**Supplementary Table 8**), the FINEMAP software to create configurations of plausible causal SNPs around each conditionally independent lead SNP (**Supplementary Table 9**), ENCODE maps of DNase I hypersensitivity sites (DHS) [31,32] and contextual analysis of transcription factor occupancy (CATO) scores[4] to identify SNPs perturbing transcription factor activity, and *cis*-eQTL evidence in human osteoblasts [33] (**Supplementary Table 10**). These results are fully described in the **Supplementary Note**.

Strategy Two: Data-Driven Expression-Prioritized Integration

The second gene prioritization approach applied the DEPICT computational tool[34]. We identified 273 genes as most likely to be driving the eBMD association signals (false discovery rate (FDR) < 0.05). Among these 273 genes are several with an established role in bone metabolism including *BMP2, LRP5, EN1*, *RUNX2, JAG1, ESR1, COL21A1* and *SOST* (**Supplementary Table 11**).

We next tested the DEPICT prioritized genes for enriched expression in any of 209 Medical Subject Heading (MeSH) tissue and cell type annotations[34]. 62 tissue or cell type annotations were identified (at a FDR of 5%) among the entries defined from the medical subject heading tissue and cell annotations (**Supplementary Table 12, Supplementary Fig. 6**). The strongest evidence of enriched expression of the genes mapping to eBMD loci came from chondrocytes and cartilage, although systems other than the musculoskeletal system were also overrepresented (i.e., cardiovascular system [7/12 significant entries], membranes tissue [6/7 significant entries] and connective tissue cells [5/7 significant entries]).

The DEPICT prioritized genes were also tested for enriched gene sets, which identified more than 1,000 significantly enriched (FDR 5%) gene sets. After clustering in 35 *'meta gene-sets'*, most clusters were related to skeletal growth (e.g. regulation of mineralized tissue development, vertebral fusion, abnormal craniofacial development, cartilage development) or to signalling pathways involved in bone biology (e.g. mesenchymal stem cell differentiation, BMP or WNT signalling). More global biological processes were also highlighted (e.g. transcription factor binding and regulation, chromatin remodelling complex or cell development) (**Supplementary Fig. 7**).

Meta-analysis gene-set enrichment of variant associations (MAGENTA) software produced similar results implicating gene sets involved in bone mineralization and development, Cadherin, WNT and Hedgehog signalling pathways, as well as other pathways worthy of further investigation (oncogenic pathways, melanogenesis etc) (**Supplementary Table 13**).

All genes prioritized by DEPICT were tested for expression in mouse osteoblasts, osteoclasts and osteocytes. Among the 273 genes prioritized, 241 had mouse homologs (the majority that did not have a known homologue were long non-coding RNAs), 92% were expressed in osteoblasts, 66% in osteoclasts, and 83% in osteocytes (**Supplementary Table 14**). Taken together, 95.4% of these genes were expressed in at least one of the three

cell types. This represents a substantial enrichment of genes expressed in osteoblast, osteocyte and osteoclasts ($P < 0.0001$ for each of osteoblasts, osteocytes and osteoclasts).

We then investigated whether a skeletal phenotype had been reported in the International Mouse Phenotyping Consortium (IMPC: http://www.mousephenotype.org) or Mouse Genome Informatics (MGI: http://www.informatics.jax.org) databases in knockout mice harbouring a deletion of any of the prioritized genes. 189 (78%) of the 241 DEPICT-prioritized genes had mouse knockout phenotype data available and 62 (33%) of these had skeletal abnormalities (**Supplementary Table 14**).

Strategy Three: Deep Phenotyping of Murine Knockouts of Selected Genes within 1MB of Lead SNPs

The third gene prioritization approach identified all genes within 1MB of lead SNPs at associated eBMD loci. These genes were compared with knockout mice generated at the Wellcome Trust Sanger Institute for the IMPC [35]. Knockout mice had been generated for 120 of the prioritized genes and bespoke skeletal phenotyping was undertaken as part of the Origins of Bone and Cartilage Disease (OBCD) Program [36]. Specifically, we performed both structural and functional analysis of skeletal samples using digital x-ray microradiography, micro-CT and biomechanical testing. Results were compared with normal reference data from >250 controls with identical C57BL/6 genetic background. 43 (36%) of these 120 prioritized genes had significantly abnormal bone structure, representing a 2-fold enrichment compared to previous analysis of 100 unselected knockout mice [36] ($\chi^2 = 8.359$, $P = 0.0038$) (**Supplementary Table 15**).

***GPC6* Findings**

These parallel strategies identified 100 genes with an abnormal skeletal phenotype when disrupted in mutant mice (**Supplementary Table 14**, **Supplementary Table 15**). However, all three gene prioritization strategies identified *GPC6* and, therefore this gene was selected for further study (**Supplementary Table 16**).

GPC6 encodes a member of the glycosylphosphatidylinositol-anchored, membrane-bound heparan sulfate proteoglycan protein family. Loss of function mutations in *GPC6* result in omodysplasia-1 (MIM 258315) a rare autosomal recessive skeletal dysplasia characterized by short limbed dwarfism with craniofacial dysmorphism, indicating a role for *GPC6* in skeletal biology[37], although the gene has not previously been implicated in osteoporosis.

Our bioinformatics pipeline provided evidence for a functional association at the *GPC6* locus. A single SNP in *GPC6*, rs1933784, in high linkage disequilibrium with the conditionally independent lead SNP rs147720516 at this locus ($r^2 > 0.9$), is a plausible causal and functional variant. We observed that rs1933784 is a low frequency SNP (MAF = 0.05) significantly associated with eBMD ($P = 2.3 \times 10^{-10}$), with a high causal probability ($\log_{10}$ Bayes factor = 2.4), and lies within DHS in several cell types (**Supplementary Table 16**). The rs1933784 variant also shows some evidence of association with expression of *GPC6* in osteoblasts ($P = 4.7 \times 10^{-3}$) (**Supplementary Table 16**).

GPC6 was identified by DEPICT as the most likely gene responsible for the association at this locus. *Gpc6* is expressed in osteoblasts and osteocytes in mice (**Supplementary Table 14**). *Gpc6* had a similar level of enrichment (1.76 log fold-enrichment) in osteocytes when compared to genes known to play a key role in the skeleton, such as *Lrp5* (1.95 log fold-enrichment) (**Supplementary Fig. 8**), an important receptor that influences bone mass through canonical Wnt-signalling, and *Runx2* (1.73 log fold-enrichment), a key transcription factor in osteoblast differentiation.

Adult female *Gpc6*$^{-/-}$ mice were analyzed and results compared to >250 wild type controls of identical C57BL/6 background. Consistent with the phenotype of omodysplasia-1, *Gpc6*$^{-/-}$ mice, had femurs and vertebrae that were shorter than wild type (-1.95 and -2.17 SD, permuted *P* = 0.06, *P* = 0.016 respectively). *Gpc6*$^{-/-}$ mice also had increased femoral bone mineral content (+2.4 SD, permuted P = $3x10^{-4}$), and increased cortical thickness (+2.3 SD, permuted P = $5x10^{-3}$). The biomechanical consequence of these structural abnormalities was an increase in yield load (+2.1SD, permuted P = $8x10^{-3}$) which reflects an increased material elasticity (**Fig. 4**). While the phenotype of *Gpc6*$^{-/-}$ mice is consistent with human omodysplasia-1, no information is available regarding adult manifestations of the condition. Thus further studies in *Gpc6*$^{-/-}$ mice are required to characterize the cellular and molecular mechanisms underlying the role of GPC6 in the pathogenesis of osteoporosis.

Finally, we queried 87 separate GWAS using the web-utility "PhenoScanner", where full genome-wide summary statistics were available for the conditionally independent genome-wide significant SNPs for eBMD (rs72635657, rs147720516) at the *GPC6* locus, for any associations with a p-value <0.05[38]. We identified one association at a p-value <0.05, for rs72635657 with femoral neck BMD (P = 0.015). We also searched the NHGRI-EBI catalogue[39] of published genome-wide association studies for the gene *GPC6* (accessed 22nd March 2017). SNPs in the region of *GPC6* had previously shown evidence of association with Attention Deficit Hyperactivity Disorder, FEV1 following bronchodilation, alzheimer's disease, neuroticism and lower facial height although the lead SNPs reported in these scans were not in appreciable linkage disequilibrium with the lead conditionally independent SNPs in the present study (all $r^2 < 0.1$).

DISCUSSION

In this study, we have increased the number of genetic loci associated with BMD in humans almost threefold and doubled the amount of variance explained for this trait. Further, we have demonstrated that several BMD associated variants also influence risk of fracture. We have prioritized genes for future study and provided functional evidence that *GPC6* plays a role in BMD and the pathophysiology of osteoporosis.

Our findings provide clear evidence that the genetic architecture of BMD is highly polygenic. The effect sizes observed follow a close relationship with MAF within the limits of the statistical power of the study. This suggests that further low-frequency and rare variants of moderate to large effect will be identified in future studies, which will likely be helpful to understand cellular and molecular mechanisms. Drug targets supported by evidence from human genetics are more likely to result in clinically useful therapies in general, and this has been demonstrated for musculoskeletal conditions [13,14]. Thus, our findings will be helpful in identifying pathways and proteins amenable to pharmacologic manipulation to decrease the burden of fracture in the population.

GPC6 encodes a glypican that may serve as a novel drug target for osteoporosis care since it is a cell-surface protein involved in signalling, whose loss of function leads to increased bone mineral content, likely due to increased cortical bone and a resultant increased elasticity. GPC6 is a member of the glypican family (GPC1-6) of glycosylphosphatidylinositol-anchored, membrane-bound heparan sulfate proteoglycan core proteins that are involved in cellular growth control and differentiation. Mutations of *GPC3*, *GPC4* and *GPC6* result in developmental skeletal abnormalities but limited or no information is available from affected adults (OMIM 312870, OMIM 258315). The heparan sulfate proteoglycans attached to the GPC6 core protein regulate skeletal signalling pathways involved in bone formation and mineralization, including those mediated by fibroblast growth factors, vascular endothelial growth factor, Hedgehog, and bone morphogenetic protein pathways [40]. In addition, the adult high bone mass phenotype and increased cortical bone thickness identified in *Gpc6*$^{-/-}$ mice in these studies is consistent with the recently identified direct role for GPC6 in the modulation of Wnt signalling [41,42], which is the key regulator of osteoblastic bone formation and is associated with BMD in humans. Overall, these findings suggest a number of possible new pharmacological targets that include not only the core protein GPC6, but also the heparan sulphate synthetic (EXT1-2) and modification enzymes (NDST1-4, GLCE, HS2ST, and HS6ST1-3) that specifically regulate growth factor binding and activity. The availability of global and tissue-specific *Gpc6*$^{-/-}$ mice [35] now provides the opportunity to test these possibilities directly. However we caution that whilst GPC6 and associated proteins appear to be promising targets for pharmacotherapy, other factors will need to be considered before these molecules are confirmed to be suitable candidates for pharmacological manipulation (e.g. likelihood of unintended side effects etc).

There are several limitations to our study. First, despite the high concordance between the loci identified using ultrasound derived measures of BMD and previous studies utilizing DXA derived BMD, there were some notable differences. Our study did not replicate associations at 18 known BMD loci from previous studies. Also, our list of genome-wide significant variants included some that were strongly related to eBMD at the heel, but have not been found in previous studies utilizing DXA derived BMD measures at other body sites in considerably smaller sample sizes. For some of these loci such as *TBX1*, this may simply be a consequence of the associated variants having neither been genotyped nor tagged well in previous studies. For other loci it may reflect genetic influences that are specific to the heel (e.g. genetic responses of the heel to ground reaction forces) that are not present at other body sites. Interestingly, we identified variants at six loci where the direction of effect was opposite between heel eBMD and DXA derived BMD at other sites, although notably at *CPED1* the variants also showed association with risk of fracture in the direction consistent

with the heel eBMD association. Whilst the reason behind these differences is unclear, the implication is that ultrasound measures of the heel capture aspects of bone structure beyond those obtained by central DXA, and is consistent with previous observations that ultrasound measures of the heel predict risk of osteoporotic fracture over and above hip BMD[43].

Second, our study does not provide a definitive biological mechanism through which variants at genome-wide significant loci causally affect eBMD. Our eQTL analyses were not consistent with SNP effects being mediated through osteoblast expression at a majority of loci. This is likely because at least some of the identified eBMD-associated SNPs may act on cell types other than osteoblasts, such as osteocytes and osteoclasts. Further, the relatively small sample size of 95 individuals in the osteoblast eQTL experiment may have led to uncertain estimates. Last, the expression of genes in culture may reflect different biological processes than those *in vivo*. Whilst differences in gene expression are not the only mechanism through which the functional effects of an association can be mediated, we expect that large scale genetical genomics studies investigating the pattern of genetic association in osteoblasts, osteocytes and osteoclasts will facilitate answers to how these eBMD associations are mediated in the not too distant future.

Third, our study had limited ability to detect very rare variants (i.e. MAF <0.1%) or rare variants of small effect (MAF <1% and effect size <0.05 SD). Finally, our study has only investigated the genetic aetiology of osteoporosis in European individuals. It is likely that the study of populations of different ancestry will reveal novel loci important in the regulation of BMD, as has been shown in the study of other conditions[44].

In summary, our findings shed light on the pathophysiologic mechanisms that underlie BMD and fracture risk in humans. Proteins identified and prioritized by these studies have identified signalling pathways that represent new drug targets for the prevention and treatment of osteoporosis- a major health care priority.

ACKNOWLEDGEMENTS

We thank Pak Sham for helpful discussions and Marcus Schull for assistance with high performance computing.

This work was supported by a Medical Research Council Programme Grant (MC_UU_12013/4 to D.M.E); a Wellcome Trust Strategic Award (grant number 101123) and a Wellcome Trust Project Grant (grant number 094134) (awarded to G.R.W, J.H.D.B and P.I.C); the Netherlands Organization for Health Research and Development ZonMw VIDI 016.136.367 (funding F.R, C.M-G, K.T), and the mobility stimuli plan of the European Union Erasmus Mundus Action 2: ERAWEB programme funding (K.T); the NIAMS/NIH (AR060981 and AR060234 to C.L.A.B).

We thank research nurses and assistants at the Departments of Surgical and Medical Sciences, Uppsala University, Sweden for large-scale collection of bone samples and culture of primary osteoblasts. This part of the work was supported by Genome Quebec, Genome Canada, and the Canadian Institutes of Health Research (CIHR). We would like to thank Thomas Winkler for providing invaluable technical support for the EasyStrata Software used in this manuscript.

N.M.W. is supported by a National Health and Medical Research Council Early Career Fellowship (APP1104818). E.G. was supported by the Swedish Research Council. J.A.M is supported by funding from the Réseau de Médecine Génétique Appliquée (RMGA) and the Fonds de Recherche du Québec - Santé (FRQS). C.M.T.G is supported by the Natural Sciences and Engineering Research Council of Canada. P.I.C is supported by Mrs Janice Gibson and the Ernest Heine Family Foundation. C.L.G is funded by Arthritis Research UK (ref 20000). J.B.R. is funded by the Canadian Institutes of Health Research, the Fonds du Recherche Québec Santé and the Jewish General Hospital. D.M.E. is funded by an Australian Research Council Future Fellowship (FT130101709).

This research has been conducted using the UK Biobank Resource (Application number 12703). Access to the UK Biobank study data was funded by University of Queensland Early Career Researcher Grant (2014002959).

URLS

Mouse Phenotyping Consortium (IMPC: http://www.mousephenotype.org)

Mouse Genome Informatics (MGI: http://www.informatics.jax.org)

The Origins of Bone and Cartilage Disease study (OBCD: http://www.boneandcartilage.com)

UK Biobank (UKBB: http://www.ukbiobank.ac.uk/)

GEnetic Factors for OSteoporosis Consortium (GEFOS: http://www.gefos.org/)

AUTHOR CONTRIBUTIONS

Conceived and designed experiments: S.K., F.R., J.H.T., P.I.C., C.L.A-B., J.H.D.B., G.R.W., J.B.R., D.M.E.

Performed statistical Analysis: J.P.K., J.A.M., C.M-G., V.F., N.M.W., S.E.Y., J.Z., K.T., K.G., C.X., C.M.T.G., C.L.A-B., J.D.B., G.R.W.

Wrote the paper: J.P.K., J.A.M., C.M-G., V.F., N.M.W., S.E.Y, C.L.G., K.T., C.M.T.G., M.T.M, S.K., F.R., J.H.T., P.I.C., C.L.A-B., J.H.D.B., G.R.W., J.B.R., D.M.E.

Generation of mouse models and/or functional experiments: S.E.Y., E.J.G., J.G.L., A.S.P., P.C.S., R.A., V.D.L., N.C.B., D.K-E., A-T.A., K.F.C., J.K.W., F.K., D.J.A, P.I.C, C.L.A-B, J.H.D.B, G.R.W.

Generation of heel eBMD Data: N.C.H., C.C.

Lead analysts: J.P.K., J.A.M., C.M.G.

Jointly supervised research: J.B.R., D.M.E

Revised and reviewed the paper: All authors.

COMPETING FINANCIAL INTERESTS STATEMENT

Authors declare no competing financial interests.

REFERENCES

1. Cauley, J.A. *et al.* Long-term risk of incident vertebral fractures. *JAMA* **298**, 2761-7 (2007).
2. Liu, C.T. *et al.* Heritability of prevalent vertebral fracture and volumetric bone mineral density and geometry at the lumbar spine in three generations of the Framingham study. *J Bone Miner Res* **27**, 954-8 (2012).
3. Estrada, K. *et al.* Genome-wide meta-analysis identifies 56 bone mineral density loci and reveals 14 loci associated with risk of fracture. *Nat Genet* **44**, 491-501 (2012).
4. Zheng, H.F. *et al.* Whole-genome sequencing identifies EN1 as a determinant of bone density and fracture. *Nature* **526**, 112-7 (2015).
5. Arden, N.K., Baker, J., Hogg, C., Baan, K. & Spector, T.D. The heritability of bone mineral density, ultrasound of the calcaneus and hip axis length: a study of postmenopausal twins. *J Bone Miner Res* **11**, 530-4 (1996).
6. Howard, G.M., Nguyen, T.V., Harris, M., Kelly, P.J. & Eisman, J.A. Genetic and environmental contributions to the association between quantitative ultrasound and bone mineral density measurements: a twin study. *J Bone Miner Res* **13**, 1318-27 (1998).
7. Hunter, D.J. *et al.* Genetic variation in bone mineral density and calcaneal ultrasound: a study of the influence of menopause using female twins. *Osteoporos Int* **12**, 406-11 (2001).
8. Lee, M. *et al.* Unique and common genetic effects between bone mineral density and calcaneal quantitative ultrasound measures: the Fels Longitudinal Study. *Osteoporos Int* **17**, 865-71 (2006).
9. Bauer, D.C. *et al.* Broadband ultrasound attenuation predicts fractures strongly and independently of densitometry in older women. A prospective study. Study of Osteoporotic Fractures Research Group. *Arch Intern Med* **157**, 629-34 (1997).
10. Bauer, D.C. *et al.* Quantitative ultrasound predicts hip and non-spine fracture in men: the MrOS study. *Osteoporos Int* **18**, 771-7 (2007).
11. Gonnelli, S. *et al.* Quantitative ultrasound and dual-energy X-ray absorptiometry in the prediction of fragility fracture in men. *Osteoporos Int* **16**, 963-8 (2005).
12. Moayyeri, A. *et al.* Genetic determinants of heel bone properties: genome-wide association meta-analysis and replication in the GEFOS/GENOMOS consortium. *Hum Mol Genet* **23**, 3054-68 (2014).
13. Nelson, M.R. *et al.* The support of human genetic evidence for approved drug indications. *Nat Genet* **47**, 856-60 (2015).
14. Richards, J.B., Zheng, H.F. & Spector, T.D. Genetics of osteoporosis from genome-wide association studies: advances and challenges. *Nat Rev Genet* **13**, 576-88 (2012).
15. Bulik-Sullivan, B.K. *et al.* LD Score regression distinguishes confounding from polygenicity in genome-wide association studies. *Nat Genet* **47**, 291-5 (2015).
16. Duncan, E.L. *et al.* Genome-wide association study using extreme truncate selection identifies novel genes affecting bone mineral density and fracture risk. *PLoS Genet* **7**, e1001372 (2011).
17. Koller, D.L. *et al.* Genome-wide association study of bone mineral density in premenopausal European-American women and replication in African-American women. *J Clin Endocrinol Metab* **95**, 1802-9 (2010).
18. Richards, J.B. *et al.* Bone mineral density, osteoporosis, and osteoporotic fractures: a genome-wide association study. *Lancet* **371**, 1505-12 (2008).
19. Rivadeneira, F. *et al.* Twenty bone-mineral-density loci identified by large-scale meta-analysis of genome-wide association studies. *Nat Genet* **41**, 1199-206 (2009).
20. Styrkarsdottir, U. *et al.* Multiple genetic loci for bone mineral density and fractures. *N Engl J Med* **358**, 2355-65 (2008).
21. Styrkarsdottir, U. *et al.* New sequence variants associated with bone mineral density. *Nat Genet* **41**, 15-7 (2009).

22. Xiong, D.H. *et al.* Genome-wide association and follow-up replication studies identified ADAMTS18 and TGFBR3 as bone mass candidate genes in different ethnic groups. *Am J Hum Genet* **84**, 388-98 (2009).
23. Wood, A.R. *et al.* Defining the role of common variation in the genomic and biological architecture of adult human height. *Nat Genet* **46**, 1173-86 (2014).
24. Mackey, D.C. *et al.* High-trauma fractures and low bone mineral density in older women and men. *JAMA* **298**, 2381-8 (2007).
25. Sanders, K.M. *et al.* The exclusion of high trauma fractures may underestimate the prevalence of bone fragility fractures in the community: the Geelong Osteoporosis Study. *J Bone Miner Res* **13**, 1337-42 (1998).
26. Bulik-Sullivan, B. *et al.* An atlas of genetic correlations across human diseases and traits. *Nat Genet* **47**, 1236-41 (2015).
27. Zheng, J. *et al.* LD Hub: a centralized database and web interface to perform LD score regression that maximizes the potential of summary level GWAS data for SNP heritability and genetic correlation analysis. *Bioinformatics* **33**, 272-279 (2016).
28. Ahmad, O.S. *et al.* A Mendelian Randomization Study of the Effect of Type-2 Diabetes and Glycemic Traits on Bone Mineral Density. *J Bone Miner Res* (2016).
29. Kemp, J.P., Sayers, A., Smith, G.D., Tobias, J.H. & Evans, D.M. Using Mendelian randomization to investigate a possible causal relationship between adiposity and increased bone mineral density at different skeletal sites in children. *Int J Epidemiol* **45**, 1560-1572 (2016).
30. McLaren, W. *et al.* The Ensembl Variant Effect Predictor. *Genome Biol* **17**, 122 (2016).
31. Roadmap Epigenomics, C. *et al.* Integrative analysis of 111 reference human epigenomes. *Nature* **518**, 317-30 (2015).
32. Thurman, R.E. *et al.* The accessible chromatin landscape of the human genome. *Nature* **489**, 75-82 (2012).
33. Grundberg, E. *et al.* Population genomics in a disease targeted primary cell model. *Genome Res* **19**, 1942-52 (2009).
34. Pers, T.H. *et al.* Biological interpretation of genome-wide association studies using predicted gene functions. *Nat Commun* **6**, 5890 (2015).
35. Skarnes, W.C. *et al.* A conditional knockout resource for the genome-wide study of mouse gene function. *Nature* **474**, 337-42 (2011).
36. Bassett, J.H. *et al.* Rapid-throughput skeletal phenotyping of 100 knockout mice identifies 9 new genes that determine bone strength. *PLoS Genet* **8**, e1002858 (2012).
37. Campos-Xavier, A.B. *et al.* Mutations in the heparan-sulfate proteoglycan glypican 6 (GPC6) impair endochondral ossification and cause recessive omodysplasia. *Am J Hum Genet* **84**, 760-70 (2009).
38. Staley, J.R. *et al.* PhenoScanner: a database of human genotype-phenotype associations. *Bioinformatics* **32**, 3207-3209 (2016).
39. Welter, D. *et al.* The NHGRI GWAS Catalog, a curated resource of SNP-trait associations. *Nucleic Acids Res* **42**, D1001-6 (2014).
40. Malinauskas, T. & Jones, E.Y. Extracellular modulators of Wnt signalling. *Curr Opin Struct Biol* **29**, 77-84 (2014).
41. Malinauskas, T., Aricescu, A.R., Lu, W., Siebold, C. & Jones, E.Y. Modular mechanism of Wnt signaling inhibition by Wnt inhibitory factor 1. *Nat Struct Mol Biol* **18**, 886-93 (2011).
42. Sakane, H., Yamamoto, H., Matsumoto, S., Sato, A. & Kikuchi, A. Localization of glypican-4 in different membrane microdomains is involved in the regulation of Wnt signaling. *J Cell Sci* **125**, 449-60 (2012).
43. Moayyeri, A. *et al.* Quantitative ultrasound of the heel and fracture risk assessment: an updated meta-analysis. *Osteoporos Int* **23**, 143-53 (2012).

44. Paternoster, L. *et al.* Multi-ancestry genome-wide association study of 21,000 cases and 95,000 controls identifies new risk loci for atopic dermatitis. *Nat Genet* **47**, 1449-56 (2015).

FIGURE LEGENDS

Figure 1. Effect size in standard deviations for heel eBMD (y-axis) from the current UK Biobank Study plotted against effect size in standard deviations from the previous GEFOS-Seq paper for BMD at the (A) femoral neck, (B) lumbar spine, and (C) forearm (x-axis). Only conditionally independent variants that reach genome-wide significance ($P < 6.6 \times 10^{-9}$) for eBMD in the UK Biobank Study are plotted. Minus $\log_{10}$P-value for the (any) fracture analysis in UK Biobank is represented by the shading of the data points (black for robust evidence of association with fracture and white for poor evidence of association). SNPs that reach Bonferroni corrected significance for fracture ($P < 1.6 \times 10^{-4}$) are labelled in the diagram. The blue dashed trend line shows a strong correlation between estimated effect sizes at the heel and at other sites of the body. SNPs at *SLC8A1* and *AQP1* were significantly related with fracture after correction for multiple testing ($P < 1.6 \times 10^{-4}$) and have not previously been reported associated with BMD or fracture although they both reached nominal significance ($P < 0.05$) in the previous GEFOS-Seq scan.

Figure 2. Relationship between absolute conditional and joint analysis effect size in standard deviations (y-axis) and minor allele frequency (x-axis) for 307 conditionally independent SNPs. Red circles represent SNPs at previously reported BMD loci. Blue circles denote SNPs at novel loci. The black dashed line shows the effect size required for 80% power to detect association at a given minor allele frequency at genome-wide significance ($\alpha = 6.6 \times 10^{-9}$) in the present study. The orange dashed line shows the effect size required for 80% power to detect association at a given minor allele frequency at genome-wide significance ($\alpha = 6.6 \times 10^{-9}$) assuming N = 483,230 individuals when the full UKBiobank Study becomes available.

Figure 3. Genetic correlations between eBMD as measured in the UK Biobank Study (y-axis) and other traits and diseases (x-axis) estimated by LD score regression implemented in LDHub. Genetic correlation (r_G) and corresponding 95% confidence intervals (error bars) between eBMD and traits were estimated using linkage-disequilibrium score regression. The genetic correlation estimates (r_G) are shaded according to their magnitude and direction (red for positive and blue for negative correlation).

Figure 4. Increased bone mass and strength in adult *Glypican 6* knockout mice (*Gpc6*$^{-/-}$) (a) X-ray microradiography images of femur and caudal vertebrae from female wild-type (WT) and *Gpc6*$^{-/-}$ mice at postnatal day 112 (P112). Pseudocolored grey-scale images in which low bone mineral content (BMC) is green and high BMC is pink. Graphs show reference ranges derived from >250 WT mice of identical age, sex and genetic background (*C57BL/6*), mean (solid line), 1.0SD (dotted lines) and 2.0SD (grey box). Values for parameters from individual *Gpc6*$^{-/-}$ mice are shown as red dots and mean values as a black line (n=2 animals). (b) Micro-CT images of proximal femur trabecular bone (left) and mid-diaphysis cortical bone (right) from WT and *Gpc6*$^{-/-}$ mice. Graphs showing trabecular bone volume/tissue volume (BV/TV), trabecular number (Tb.N), trabecular thickness (Tb.Th), trabecular spacing (Tb.Sp), cortical thickness (Ct.Th), internal cortical diameter and cortical bone mineral density (BMD). (c) Representative load displacement curves from destructive 3-point bend testing of WT and *Gpc6*$^{-/-}$ femurs showing yield load, maximum load, fracture load and gradient of the linear elastic phase (stiffness). Graphs showing yield load, maximum load, fracture load, stiffness and energy dissipated prior to fracture (Toughness) (d) Representative load displacement curves from destructive compression testing of WT and *Gpc6*$^{-/-}$ caudal vertebra showing yield load, maximum load and stiffness. *P* values generated by permutation analysis as described in the methods. Scale bars: a,b, 1mm.

TABLES.

Table 1 Genome-wide significant eBMD associated SNPs that show significant association with risk of fracture ($P < 1.6 \times 10^{-4}$)

							ANY FRACTURE				FALL FRACTURE				
RSID	**CHR**	**BP**	**C.GENE**	**EA**	**NEA**	**EAF**	**OR**	**$CI_{95\%-L}$**	**$CI_{95\%-U}$**	**P**	**OR**	**$CI_{95\%-L}$**	**$CI_{95\%-U}$**	**P**	**STATUS**
rs10490046	2	40630678	*SLC8A1*	A	C	0.78	0.94	0.92	0.97	6.8×10^{-6}	0.94	0.91	0.98	1.4×10^{-3}	NOVEL
rs112069922	4	1034997	*IDUA*	C	T	0.95	0.89	0.84	0.93	4.8×10^{-6}	0.90	0.84	0.96	2.2×10^{-3}	KNOWN
rs9491689	6	127398595	*RSPO3*	C	A	0.72	1.05	1.03	1.08	5.0×10^{-5}	1.05	1.02	1.09	2.0×10^{-3}	KNOWN
rs7741021	6	127468274	*RSPO3*	A	C	0.52	1.07	1.04	1.09	1.5×10^{-8}	1.07	1.04	1.10	4.8×10^{-6}	KNOWN
rs4869744	6	151908012	*ESR1*	T	C	0.71	0.95	0.93	0.98	1.3×10^{-4}	0.95	0.92	0.98	8.0×10^{-4}	KNOWN
rs2941741	6	152008982	*ESR1*	G	A	0.58	1.05	1.03	1.08	6.5×10^{-6}	1.07	1.04	1.11	2.4×10^{-6}	KNOWN
rs10276670	7	30956489	*AQP1*	A	G	0.77	0.95	0.92	0.97	4.1×10^{-5}	0.94	0.91	0.97	3.5×10^{-4}	NOVEL
rs2536195	7	120959155	*WNT16*	A	G	0.6	1.10	1.07	1.12	2.6×10^{-15}	1.13	1.10	1.16	1.6×10^{-15}	KNOWN
rs10668066	7	120965464	*WNT16*	G	GCACC	0.75	1.09	1.07	1.12	1.5×10^{-11}	1.13	1.09	1.17	2.5×10^{-12}	KNOWN
rs7099953	10	54426489	*MBL2*	G	T	0.89	0.90	0.87	0.93	4.9×10^{-9}	0.89	0.84	0.93	5.0×10^{-7}	KNOWN
rs7209826	17	41796406	*SOST*	A	G	0.62	1.05	1.03	1.07	3.6×10^{-5}	1.06	1.03	1.10	7.1×10^{-5}	KNOWN
rs188810925	17	41798194	*SOST*	G	A	0.92	1.09	1.04	1.14	9.2×10^{-5}	1.11	1.05	1.17	3.3×10^{-4}	KNOWN

*Beta (β) and standard errors (SE) from BOLT-LMM were transformed using the following formula: (β or SE) / (μ *(1- μ)), where μ = number of cases/number of controls. Approximate odds ratios (OR) and 95% confidence intervals ($CI_{95\%}$) were calculated from the transformed beta and standard error. RSID = Reference SNP cluster ID, CHR = Chromosome, BP = Base pair position of the variant according to human reference sequence (Hg19/GRCh37), C.GENE = closest gene, EA = Effect allele, NEA = Non-effect allele, EAF = Effect allele frequency, and P = Strength of evidence against the null hypothesis of no association between variant and self-reported fracture (i.e. P-value), ANY FRACTURE = any self-reported fracture within the last five years (N = 14,492 cases / 130,563 controls) and FALL FRACTURE = self-reported fracture within the last five years that occurred as the result of a simple fall (N = 8,540 cases / 131,333 controls).

ONLINE METHODS

Measurement of eBMD, fracture and weight in UKBB

In 2006-2010, the UK Biobank recruited 502,647 individuals aged between 37-76 years (99.5% were 40-69 years) from across the country. Each participant provided information regarding their health and lifestyle using touch screen questionnaires, physical measurements and agreement to have their health followed and they also provided blood, urine and saliva samples for future analysis. UK Biobank has ethical approval from the Northwest Multi-centre Research Ethics Committee (MREC) and informed consent was obtained from all participants. Quantitative ultrasound assessment of calcanei was performed in UK Biobank participants using a Sahara Clinical Bone Sonometer [Hologic Corporation (Bedford, Massachusetts, USA)]. Details of the complete protocol employed are publicly available on the UK Biobank website (https://biobank.ctsu.ox.ac.uk/crystal/docs/Ultrasoundbonedensitometry.pdf). Participants were initially measured at baseline (N = 487,428) and had either their left calcaneus (N = 317,815), right calcaneus (N = 4,102) or both calcanei measured (N = 165,511). A subset of these subjects were followed up at two further time points (N = 20,104) and (N = 7,988), during which both heels were measured. A detailed description of the ascertainment procedure is described in the **Supplementary Fig 2**. Prior to quality control, ultrasound data were available for 488,683 individuals at either baseline and/or follow-up assessment. Estimated bone mineral density [eBMD, (g/cm^2)] was derived as a linear combination of speed of sound (SOS) and bone ultrasound attenuation (BUA) (i.e. eBMD = 0.002592 * (BUA + SOS) − 3.687). To reduce the impact of outlying measurements, quality control was applied to male and female subjects separately using the following exclusion thresholds: Speed of sound [SOS; Male: (≤ 1,450 and ≥ 1,700 m/s), Female (≤ 1,455 and ≥ 1,700 m/s)] and broadband ultrasound attenuation [BUA; male: (≤ 27 and ≥ 138 dB/MHz), female (≤ 22 and ≥ 138 dB/MHz)]. Individuals exceeding the following thresholds for eBMD were excluded: [Male: (≤ 0.18 and ≥ 1.06 g/cm^2), Female (≤ 0.12 and ≥ 1.025 g/cm^2)]. Bivariate scatter plots of eBMD, BUA and SOS were visually inspected and any measurements not clustering with the others were removed, leaving a total of 483,230 valid measures (476,618 left and 6,612 right calcaneus) for SOS, BUA and BMD (265,057 females and 218,173 males). Please see **Supplementary Fig. 2** for a detailed description of the QC pipeline and **Supplementary Table 1** for an overview of descriptive statistics of the cohort after quality control.

We defined 14,492 individuals (8,439 female and 6,053 male) as having a fracture, based on answering yes to the question “Have you fractured/broken any bones in the last 5 years?” at either baseline or first follow-up. Individuals were coded as missing if they responded “Do not know” or “Prefer not to answer” at both the baseline and first follow-up, otherwise they were coded as controls (N=130,563). Self-reported fractures have low false positive and false negative rates.[45] Individuals who responded yes to having a fracture were also asked “Did the fracture result from a simple fall (i.e. from standing height)?” We created a second variable using this question, where 8,540 individuals (5,853 female and 2,687 male) had a fracture from a simple fall and 131,333 individuals did not report a fracture. Weight was measured using the Tanita BC418MA body composition analyser.

Preparation, quality control and genetic analysis in UK Biobank samples

Genotype data from the interim May 2015 release of UK Biobank were available for a subset of 152,729 participants. Data was imputed centrally by UK Biobank using IMPUTE2 [46] to a 1000G (Oct 2014) and UK10K reference panel. In addition to the quality control metrics performed centrally by UK Biobank (UK Biobank document #155580 http://biobank.ctsu.ox.ac.uk/crystal/docs/genotyping_qc.pdf), we defined a subset of “white European” ancestry samples using a K-means (K=4) clustering approach based on the first 4 genetically determined principal components. A maximum of 142,487 individuals (76,067 females and 66,420 males) with genotype and valid QUS measures were available for the

present analyses. We tested genetic variants for association with eBMD assuming an additive allelic effect, in a linear mixed non-infinitesimal model implemented in BOLT-LMM [47] to account for cryptic population structure and relatedness. Genotyping array, age and sex were included as covariates in all models. We also included weight as a covariate in a sensitivity analysis to investigate whether power to detect association was increased or if weight mediated the relationship between genotype and eBMD (i.e. some variants may be primarily associated with weight and their effect on eBMD mediated through a causal effect of weight on eBMD [29]). Only SNPs down to a minor allele frequency of 0.1% and with an info-score threshold of > 0.4 were analysed. We additionally analysed the association between eBMD and directly genotyped SNPs on the X chromosome, adjusting for genotyping array, age, sex and the first 4 ancestry principal components, using Plink v1.09 beta 3.38 (7 Jun 2016) software[48] and a nested sample of unrelated subjects (N= 135,729). As the analyses for the X chromosome data were based upon observed genotypes, our quality control was slightly different. We excluded SNPs with evidence of deviation from Hardy-Weinberg Equilibrium (1×10^{-6}), minor allele frequency < 0.1% and overall missing rate > 5%, resulting in 15,552 X chromosome SNPs for analysis. Heterogeneity between sexes in effect size coefficients was tested using EasyStrata [49]. Manhattan and Miami plots of our genome-wide association scans were generated by EasyStrata version 15.3. Regional association plots were generated using LocusZoom (v1.3) [50], using linkage-disequilibrium information estimated from our reference UKBiobank sample, together with the December 2016 release of the NHGRI-EBI Catalog of published genome-wide association studies. SNPs that were associated with eBMD at genome-wide significant levels were additionally tested for association with fracture using BOLT-LMM including age, sex, BMI and the time of reporting the fracture as fixed effects [47].

Estimation of genome-wide significance threshold

Traditional estimates of the genome-wide significance threshold for common variants (MAF >5%) in European populations (i.e. $\alpha = 5 \times 10^{-8}$) are based on a Bonferroni correction of $\alpha = 0.05/10^6$, since there are an estimated 1 million statistically independent SNPs above this MAF threshold. However, in the case of UK Biobank, we have assessed SNPs down to a minor allele frequency of 0.1% in 142,487 individuals and applied an info-score threshold of > 0.4, resulting in 17.17M SNPs. Therefore, we defined a new and more conservative threshold to declare genome-wide significance accounting for the number of independent statistical tests performed in our data. To do so, we applied the method we previously used within the UK10K sequencing consortium [4] which assesses the correlation between nearby test statistics empirically. Analysis of permuted data derived from a small proportion of all tested variants allows assessment of the correlation patterns. Hence, we can estimate, in subsets of the genome of varying size, the relationship between the Bonferroni significance threshold and the empirical significance threshold that corrects for correlations, and thereby extrapolate to the whole genome. Specifically, when assessing all 740,018 variants that met our filtering criteria across chromosome nine (**Supplementary Fig. 9**), we saw a good linear fit between family wise error rate ($\alpha = 0.05$), divided by the number of tests and the empirical significance thresholds. Our estimated genome-wide significance threshold then, accounting for all SNPs MAF ≥ 0.1% and info-score > 0.4 was $\alpha = 6.6 \times 10^{-9}$.

Approximate conditional association analysis

In order to detect multiple independent association signals at each of the genome-wide significant eBMD loci, we applied approximate conditional and joint genome-wide association analysis using the software package GCTA [51]. SNPs with high collinearity (multiple regression $R^2 > 0.9$) were ignored and those situated more than 20 MB away were assumed to be in complete linkage equilibrium. A reference sample of 15,000 unrelated (pairwise relatedness < 0.025) individuals of white British origin, randomly selected from UK Biobank was used to model patterns of linkage disequilibrium (LD) between variants. The reference genotyping dataset consisted of the same 17M variants assessed in our GWAS, but with an additional QC step excluding SNPs that deviated from Hardy-Weinberg

Equilibrium (1×10^{-6}). Conditionally independent variants reaching GWAS significance were annotated to the physically closest gene using bedtools[52] v2.26.0 and the Hg19 Gene range list available from https://www.cog-genomics.org/plink2/.

Estimation of variance explained by significant variants and SNP heritability

We estimated the proportion of phenotypic variance tagged by all SNPs on the genotyping array (i.e. the SNP heritability) using BOLT-REML[53]. In order to calculate the variance explained by all genome-wide significant SNPs we first employed the method of Bigdeli et al. (2016) to shrink the effect sizes of SNPs likely to suffer from "winner's curse"[54]. Briefly the method works by shrinking the effect sizes of SNPs that just pass significance whilst having a negligible effect on SNPs that are more strongly significant (and consequently more accurately and precisely estimated). After calculating the corrected effect sizes we then removed the combined effect of the SNPs on individual's eBMD and recalculated the total expected variance in BOLT-LMM. The difference between this estimate and the total expected variance calculated on the original data without the SNP correction is an estimate of the variance explained by all SNPs.

LD Score regression

To estimate the amount of genomic inflation present in the data that was due to residual population stratification, cryptic relatedness, and other latent sources of bias, we used LD score regression[15]. LD scores were calculated for all high quality SNPs (i.e. INFO score > 0.9 and MAF > 0.1%) from a dataset consisting of 15,000 unrelated individuals from the UK Biobank. To estimate the genetic correlation between eBMD and other complex traits and diseases including those related to osteoporosis, we used a relatively new method based on LD Score regression as implemented in the online web utility LDHub [26,27]. This method uses the cross products of summary test statistics from two GWAS and regresses them against a measure of how much variation each SNP tags (its "LD Score"). Variants with high LD Scores are more likely to contain more true signals and hence provide more chance of overlap with genuine signals between GWAS. The LD score regression method uses summary statistics from the GWAS meta-analysis of eBMD and the other traits of interest, calculates the cross-product of test statistics at each SNP, and then regresses the cross-product on the LD Score. The slope of the regression is a function of the genetic covariance between traits:

$$E(z_{1j}z_{2j}) = \frac{\sqrt{N_1N_2}\rho_g}{M} l_j + \frac{\rho N_s}{\sqrt{N_1N_2}}$$

where N_i is the sample size for study i, ρ_g is the genetic covariance, M is the number of SNPs in the reference panel with MAF between 5% and 50%, l_j is the LD score for SNP j, N_s quantifies the number of individuals that overlap both studies, and ρ is the phenotypic correlation amongst the N_s overlapping samples. Thus, if there is sample overlap (or cryptic relatedness between samples), it will only affect the intercept from the regression (i.e. the term $\frac{\rho N_s}{\sqrt{N_1N_2}}$) and not the slope, and hence estimates of the genetic covariance will not be biased by sample overlap. Likewise, population stratification will affect the intercept but will have minimal impact on the slope (i.e. intuitively since population stratification does not correlate with linkage disequilibrium between nearby markers).

Gene prioritization and pathway analysis

To establish functional connections we conducted three different analyses implemented in the DEPICT v1 tool[34]. First, to prioritize genes with relevant biological roles in the eBMD associated loci functional similarities among genes from different associated regions were tested, where genes with high functional similarity across regions obtained lower prioritization P values. Second, we analysed expression enrichment across particular tissues or cell types, by testing whether genes in the associated eBMD loci were seen highly expressed in any of the 209 Medical Subject Heading (MeSH) annotations using data from

37,427 expression arrays. Third, we performed a gene set enrichment analysis, which tests if the genes in the associated eBMD loci are enriched in reconstituted gene-sets. The 10,968 gene-sets tested have been generated from diverse databases, i.e. Gene Ontology, Kyoto encyclopedia of genes and genomes, REACTOME, InWeb database (high confidence protein-protein interaction), and the Mouse Genetics Initiative (phenotype-genotype relationships). All three analyses used False Discovery Rate (FDR) to adjust for multiple testing, significance was defined at FDR 5%.

The DEPICT analyses were based on independent lead SNPs (r^2<0.1, European populations 1000 genomes reference panel) with P-values below the genome-wide significant threshold ($P < 6.64x10^{-9}$). As many of the Gene-sets tested come from different repositories, they overlap, hence significantly enriched gene-sets were further grouped into '*meta gene sets'* by similarity clustering, as previously described[34]. The visualization of these '*meta gene-sets'* was performed in cytoscape [55], filtering for '*meta gene sets'* at FDR <1%.

We also compared the DEPICT gene set enrichment results to analyses using the Meta-analysis gene-set enrichment of variant associations (MAGENTA) software[56]. Briefly, MAGENTA maps each gene in the genome to a single index SNP with the lowest p value within a 110 kb upstream and 40 kb downstream window (excluding genes in the HLA region due to complex patterns of linkage disequilibrium). This P value is then corrected for confounding factors (e.g. SNP density, gene size etc.) in a linear regression model and each gene is ranked by its adjusted gene score. The observed number of gene scores in a given pathway, with a ranked score above a specified threshold (i.e. 95th and 75th percentiles of all gene scores) is then calculated. This observed statistic is then compared to 1,000,000 randomly permuted pathways of identical size. This generates an empirical GSEA *P* value for each gene set. A gene set was declared significant when an individual pathway reached a FDR < 0.05 in either analysis. We tested 3217 pre-specified gene sets from Gene Ontology, Ingenuity, Kyoto Encyclopedia of Genes and Genomes (KEGG), Protein Analysis Through Evolutionary Relationships (PANTHER), BioCarta and Reactome databases.

Prioritising candidate genes and possible causal variants at each eBMD locus
We combined a number of approaches to identify possible causal SNPs at each eBMD signal (defined here as all SNPs within 500 kb of conditionally independent lead SNP that met genome-wide significance). First, we annotated all SNPs within a locus (defined as +/- 500 kb from a conditionally independent lead SNP) for deleterious coding variation annotation using the Variant Effect Predictor (VEP)[30] if they were significantly associated with eBMD ($P < 6.6x10^{-9}$). Deleterious SNPs were classified as such if they had one of the following sequence ontology terms: frameshift_variant, inframe_deletion, inframe_insertion, initator_codon_variant, missense_variant, splice_acceptor_variant, splice_donor_variant, stop_gained, or stop_lost.

Next, we identified 305 autosomal lead SNPs and further defined sets of plausible causal SNPs within each locus using FINEMAP[57]. For each locus, FINEMAP implements a shotgun stochastic search algorithm to test multiple causal configurations of SNPs, calculating within a Bayesian framework the posterior probabilities of each configuration to identify the number of likely causal SNPs. We note that this approach assumes that the true causal variant(s) have been included in the analysis and have been well imputed. We also emphasize that approaches such as this that are based solely on association test statistics and linkage disequilibrium are unlikely to be definitive with respect to the identification of causal variants/genes. Thus, we regard these fine mapping analyses as one of several approaches that can be used to implicate specific variants/genes in osteoporosis aetiology. When the same variant/gene is implicated using multiple independent approaches (e.g. mouse knockout, human knockout, gene expression and eQTL studies etc.) then we can be increasingly confident of the identity of the gene/variant(s) underlying the statistical association.

For a given number of plausible causal SNPs, FINEMAP will calculate for each SNP their Bayes factor which quantifies the evidence that the particular SNP is causal. We retained only SNPs with Bayes factors greater than 100, or $\log_{10}$ Bayes factors greater than 2, as our plausible causal SNPs for each locus.

Each set of plausible causal SNPs was then annotated for overlap with DNase I hypersensitive sites (DHS) using a master list derived from 115 cell types[4]. DHS are focal sites of open chromatin comprising the collective transcription factor (TF) binding sites in a given cell type. We further annotated each SNP inhabiting a DHS using Contextual Analysis of Transcription Factor Occupancy (CATO) scores. CATO, previously described by Maurano et al. [4], scores the likelihood of a variant causing allelic imbalance of a DHS by modelling both local sequence context and direct effects on the TF recognition sequences for 44 TF motif families. CATO scores range between 0 and 1 and we considered SNPs with CATO scores greater than 0.1 as having very strong functional evidence (corresponding to a 51% positive predictive rate in the initial training set [4]).

Genetically modified animals used for functional validation: The International Mouse Phenotyping Consortium (IMPC) [58] together with the International Knockout Mouse Consortium (IKMC) are generating null alleles for all protein coding genes on a C57BL/6 genetic background [59]. These mice are phenotyped through a broad-based phenotyping screen [60]. This approach can be used for functional investigation of candidate genes identified by GWAS analysis of human disease traits, and studies have already ascribed novel functions for poorly annotated or previously unpublished genes. The Origins of Bone and Cartilage Disease (OBCD) study (http://www.boneandcartilage.com) is undertaking a validated multi-parameter skeletal phenotype screen [36] of mutant mouse lines generated by Wellcome Trust Sanger Institute as part of the IKMC and IMPC effort.

OBCD methods: Samples from 16 week-old female wild-type and knockout mice are stored in 70% ethanol, anonymised and randomly assigned to batches for rapid throughput analysis in an unselected fashion. The relative bone mineral content and length of the femur and caudal vertebrae are determined at 10μm pixel resolution by digital X-ray microradiography (Faxitron MX20) . Micro-CT (Scanco uCT50, 70kV, 200μA, 0.5mm aluminium filter) is used to determine cortical bone parameters (thickness Ct.Th, BMD, medullary diameter) at 10μm voxel resolution in a 1.5mm region centred in the mid-shaft region 56% along the length of the femur distal to the femoral head, and trabecular parameters (bone volume BV/TV, trabecular number Tb.N, thickness Tb.Th, spacing Tb.Sp) at 5μm voxel resolution in a 1mm region beginning 100μm proximal to the distal growth plate. Biomechanical variables of bone strength and toughness (yield load, maximum load, fracture load, % energy dissipated prior to fracture) are derived from destructive 3-point bend testing of the femur and compression testing of caudal vertebra 6 and 7 (Instron 5543 load frame, 100N load cell) [36]. Overall, 19 skeletal parameters are reported for each individual mouse studied and compared to reference data obtained from >250 16 week-old wild-type C57BL/6 female mice. Coefficients of Variation (CV) for each skeletal parameter were as follows:
femur BMC (2.0%) and length (2.1%); vertebra BMC (2.1%) and length (2.3%); trabecular bone BV/TV (18.5%), Tb.N (7.3%), Tb.Th (7.9%) and Tb.Sp (8.3%); cortical bone Ct.Th (4.3%), Int.Diam (6.0%) and BMD (4.0%); femur yield load (13.2%), maximum load (10.0%), fracture load (29.0%), stiffness (13.7%) and energy dissipated prior to fracture (26.7%); and vertebra yield load (13.0%), maximum load (10.3%) and stiffness (13.3%).

In **Supplementary Table 15**, we have highlighted knockout mice with phenotypes greater than 2 SDs away from the mean of wild type mice. We generated P-values for the reported *Gpc6*$^{-/-}$ mouse phenotypes through permutation. To do so we first identified the least extreme phenotype for the *Gpc6*$^{-/-}$ mice tested. We then permuted the knockout labels 100,000 times

to observe the number of times we observed two knockout animals with both phenotypes as extreme as the least extreme *Gpc6*$^{-/-}$ mouse phenotype. The P-value was then calculated as the number of extreme permutations divided by 100,000. All mouse studies were undertaken by Wellcome Trust Sanger Institute Mouse Genetics Project as part of the International Knockout Mouse Consortium and licensed by the UK Home Office in accordance with the Animals (Scientific Procedures) Act 1986 and the recommendations of the Weatherall report.

Gene expression in primary human and murine osteoblasts: To study human osteoblasts, we undertook cis-eQTL analyses of plausible causal regulatory SNPs in 95 primary human osteoblasts as previously described by Grundberg et al[33], performed with an updated imputation panel, the combined UK10K and 1000 Genomes Phase 1 v3 reference panel[61]. We used an alpha level of α=0.05 to identify possible gene targets of plausible causal SNPs.

We investigated the possibility that heel eBMD associations and cis-eQTL effects in osteoblasts may represent different signals (i.e. as opposed to a causal effect of osteoblast expression on eBMD) by performing two sample summary Mendelian randomization analysis on osteoblast eQTL and heel eBMD GWAS results[62,63]. A HEIDI (heterogeneity in dependent instruments) test was used to identify situations in which the lead cis-eQTL was likely to be in linkage disequilibrium with two distinct causal variants (i.e. one affecting gene expression and the other affecting eBMD variation), as opposed to expression of the relevant gene mediating the relationship between the SNP and eBMD. Intuitively the test works by comparing estimates of the putative causal effect of gene expression on eBMD obtained by Mendelian randomization analysis of each variant whilst taking into account dependencies between the SNPs. Under a causal model, different SNPs should produce the same causal estimate (subject to sampling error), whereas under a model of linkage (i.e. two separate signals in the region, one affecting gene expression in osteoblasts and the other affecting eBMD), the estimates from the Mendelian randomization analysis may significantly differ. In the context of our study, a significant HEIDI test suggests that expression of the relevant gene in osteoblasts does not mediate the SNP – eBMD association. We therefore performed HEIDI tests for all the probes listed in **Supplementary Table 10** that were implicated in our gene expression analyses. In order to avoid weak SNP instruments potentially affecting our results we only included SNPs in the eQTL analysis that exhibited strong evidence of association (i.e. F statistic > 10)[63].

Gene expression profiles of candidate genes were examined in primary mouse osteoblasts undergoing differentiation. These data have been described in detail previously [64] and are publicly available from the Gene Expression Omnibus (GSE54461). To study murine osteoblasts, pre-osteoblast-like cells were obtained from neonatal calvaria collected from C57BL/6J carrying a transgene expressing Cyan Florescent Protein (CFP) under the control of the Col 3.6Kb promoter. The cells were placed into culture for 4 days in growth media, removed from culture and cells not expressing CFP were removed by FACS sorting. The remaining pre-osteoblast cells were re-plated, were subjected to an osteoblast differentiation cocktail and RNA was collected every two days from day 2 to 18 days post differentiation. Next Generation RNA sequencing (RNAseq) was used to evaluate the transcriptome at each time point using an Illumina HiSeq 2000. Three technical replicates per samples were sequenced. The alignments for abundance estimation of transcripts was conducted using Bowtie version 0.12.9, using the NCBIm37 reference genome. Expression level per gene was calculated using RSEM version 1.2.0 with the parameters of --fragment-length-mean 280 and --fragment-length-sd 50, and the expression level for each sample was normalized relative to the per sample upper quartile.

Gene expression in murine osteocytes: Osteocyte expression was determined through an analysis of whole transcriptome sequencing derived from four different bone types from throughout the mouse skeleton – the tibia, femur, humerus and calvaria (marrow removed,

n=8 per bone). A threshold of expression was determined based on the distribution of normalised gene expression for each sample modifying a statistical approach by Hart et al. (2013) [65]. “Expressed” genes were above this threshold for 8 of 8 replicates in any bone type. The specificity of these genes expression in the skeleton was determined by comparing transcriptome-sequencing data from bone-samples with osteocytes isolated to those with the marrow left intact (n=5 per group) (S.E.Y, J.H.D.B, G.R.W, P.I.C manuscript in preparation).

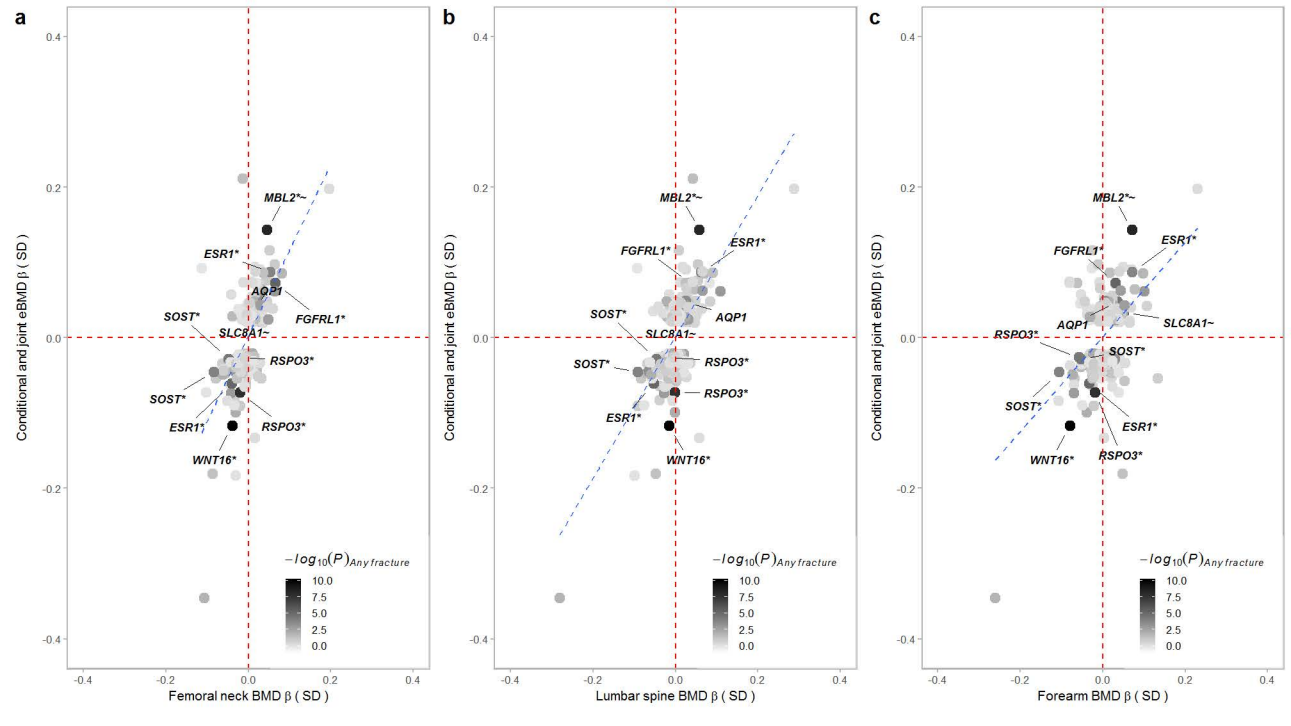
Gene expression in mouse osteoclasts: Expression of genes in murine osteoclasts was determined using publically available data obtained using Next-Gen RNA-sequencing applied to bone marrow derived osteoclasts obtained from 6-8 week old C57BL/6 mice (GEO Accession Number: GSM1873361).

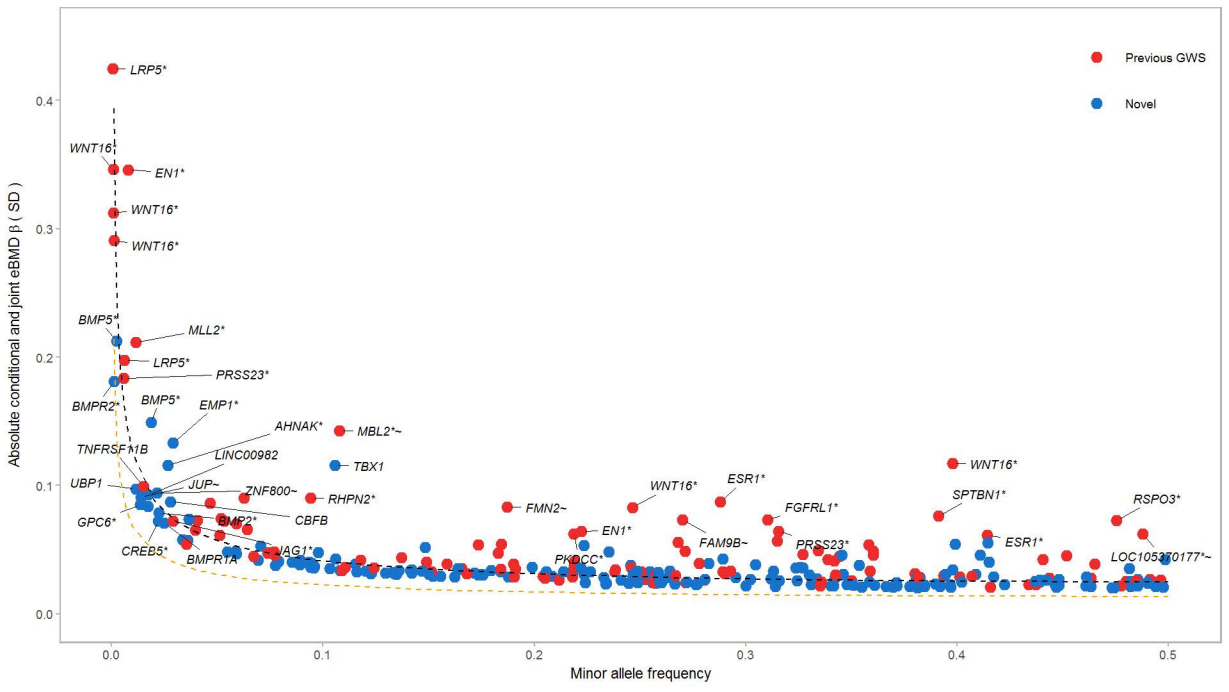
DATA AVAILABILITY AND ACCESSION CODE AVAILABILITY STATEMENTS:

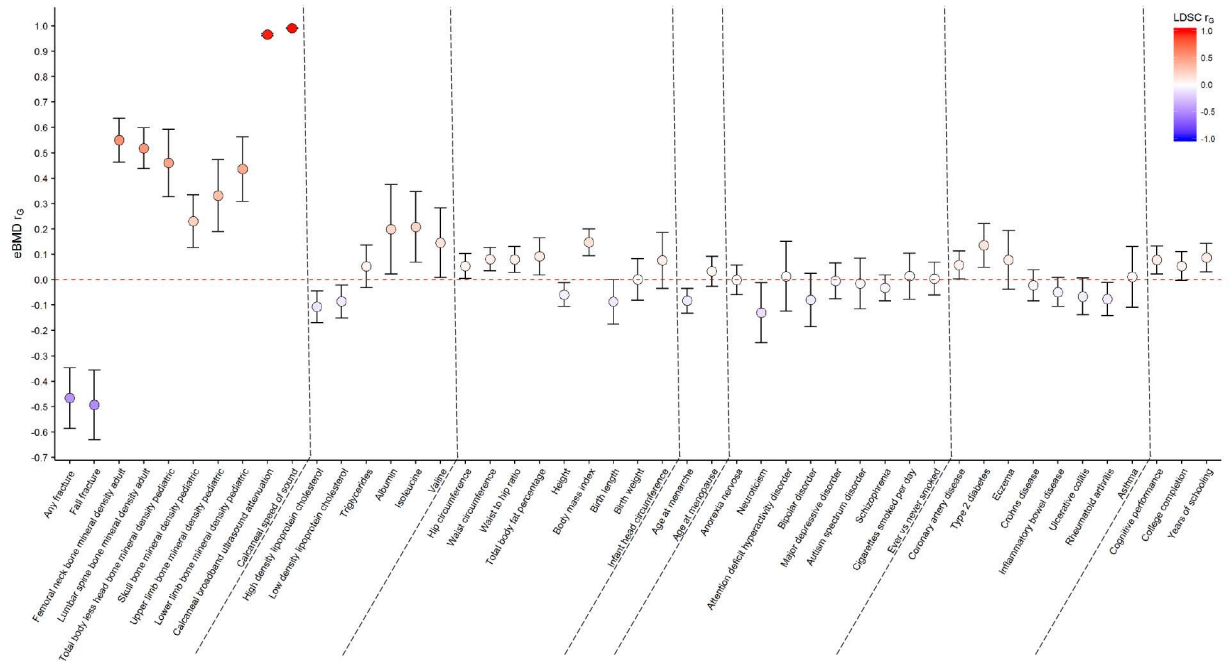
The human genotype and phenotype data on which the results of this study are based are available upon application from the UK Biobank Study (http://www.ukbiobank.ac.uk/). GWAS summary statistics from this study available via the GEnetic Factors for OSteoporosis Consortium website (http://www.gefos.org/). No new datasets or related accession codes were generated as part of this study. Mouse phenotype data are available online at the IMPC (http://www.mousephenotype.org) and OBCD (http://www.boneandcartilage.com).

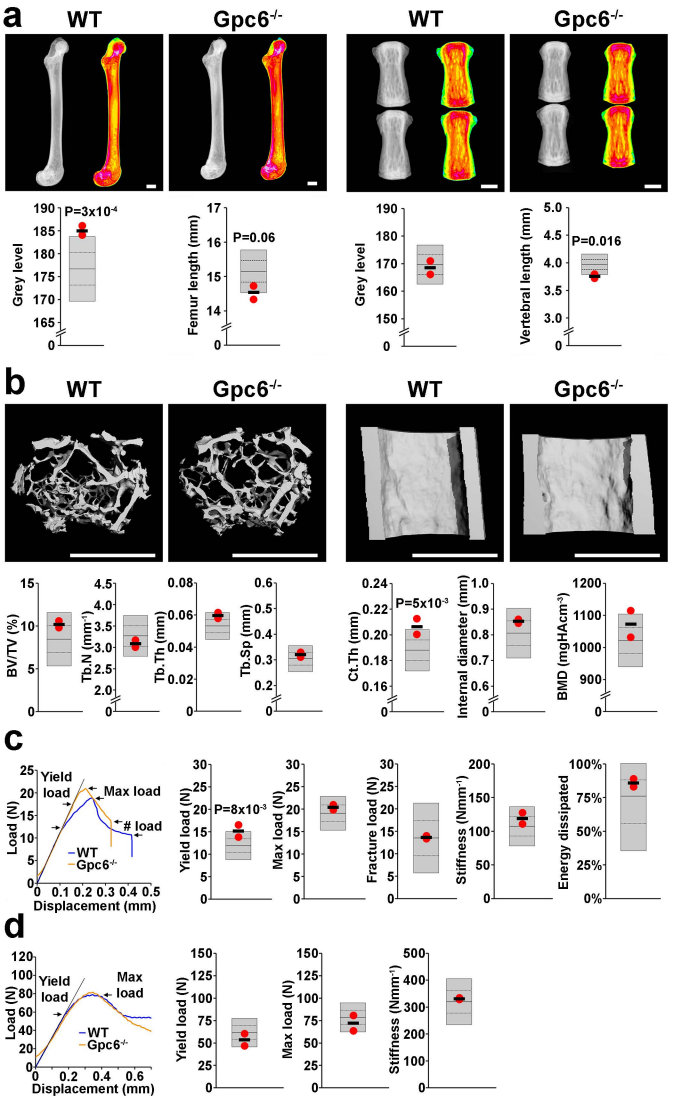
REFERENCES:

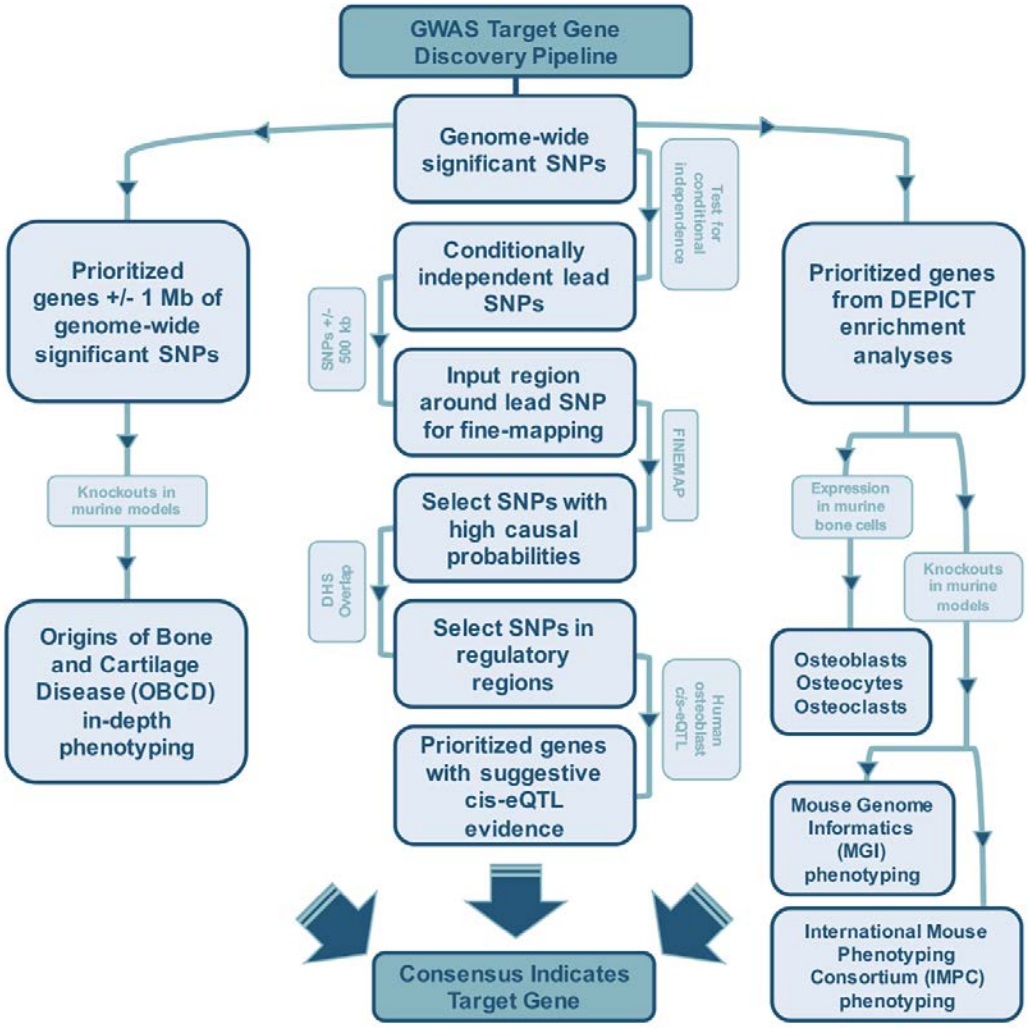
45. Ismail, A.A. *et al.* Validity of self-report of fractures: results from a prospective study in men and women across Europe. EPOS Study Group. European Prospective Osteoporosis Study Group. *Osteoporos Int* **11**, 248-54 (2000).
46. Howie, B., Marchini, J. & Stephens, M. Genotype imputation with thousands of genomes. *G3 (Bethesda)* **1**, 457-70 (2011).
47. Loh, P.R. *et al.* Efficient Bayesian mixed-model analysis increases association power in large cohorts. *Nat Genet* **47**, 284-90 (2015).
48. Chang, C.C. *et al.* Second-generation PLINK: rising to the challenge of larger and richer datasets. *Gigascience* **4**, 7 (2015).
49. Winkler, T.W. *et al.* EasyStrata: evaluation and visualization of stratified genome-wide association meta-analysis data. *Bioinformatics* **31**, 259-61 (2015).
50. Pruim, R.J. *et al.* LocusZoom: regional visualization of genome-wide association scan results. *Bioinformatics* **26**, 2336-7 (2010).
51. Yang, J. *et al.* Conditional and joint multiple-SNP analysis of GWAS summary statistics identifies additional variants influencing complex traits. *Nat Genet* **44**, 369-75, S1-3 (2012).
52. Quinlan, A.R. & Hall, I.M. BEDTools: a flexible suite of utilities for comparing genomic features. *Bioinformatics* **26**, 841-2 (2010).
53. Loh, P.R. *et al.* Contrasting genetic architectures of schizophrenia and other complex diseases using fast variance-components analysis. *Nat Genet* **47**, 1385-92 (2015).
54. Bigdeli, T.B. *et al.* A simple yet accurate correction for winner's curse can predict signals discovered in much larger genome scans. *Bioinformatics* **32**, 2598-603 (2016).
55. Saito, R. *et al.* A travel guide to Cytoscape plugins. *Nat Methods* **9**, 1069-76 (2012).
56. Segre, A.V. *et al.* Common inherited variation in mitochondrial genes is not enriched for associations with type 2 diabetes or related glycemic traits. *PLoS Genet* **6**(2010).
57. Benner, C. *et al.* FINEMAP: efficient variable selection using summary data from genome-wide association studies. *Bioinformatics* **32**, 1493-501 (2016).
58. Consortium, E.P. An integrated encyclopedia of DNA elements in the human genome. *Nature* **489**, 57-74 (2012).
59. Bernstein, B.E. *et al.* The NIH Roadmap Epigenomics Mapping Consortium. *Nat Biotechnol* **28**, 1045-8 (2010).
60. Koscielny, G. *et al.* The International Mouse Phenotyping Consortium Web Portal, a unified point of access for knockout mice and related phenotyping data. *Nucleic Acids Res* **42**, D802-9 (2014).
61. International Mouse Knockout, C., Collins, F.S., Rossant, J. & Wurst, W. A mouse for all reasons. *Cell* **128**, 9-13 (2007).
62. Hrabe de Angelis, M. *et al.* Analysis of mammalian gene function through broad-based phenotypic screens across a consortium of mouse clinics. *Nat Genet* **47**, 969-78 (2015).
63. Huang, J. *et al.* Improved imputation of low-frequency and rare variants using the UK10K haplotype reference panel. *Nat Commun* **6**, 8111 (2015).
64. Evans, D.M. & Davey Smith, G. Mendelian Randomization: New Applications in the Coming Age of Hypothesis-Free Causality. *Annu Rev Genomics Hum Genet* **16**, 327-50 (2015).
65. Zhu, Z. *et al.* Integration of summary data from GWAS and eQTL studies predicts complex trait gene targets. *Nat Genet* **48**, 481-7 (2016).
66. Kemp, J.P. *et al.* Phenotypic dissection of bone mineral density reveals skeletal site specificity and facilitates the identification of novel loci in the genetic regulation of bone mass attainment. *PLoS Genet* **10**, e1004423 (2014).
67. Hart, T., Komori, H.K., LaMere, S., Podshivalova, K. & Salomon, D.R. Finding the active genes in deep RNA-seq gene expression studies. *BMC Genomics* **14**, 778 (2013).


a
b
c
Conditional and joint eBMD β (SD)
Femoral neck BMD β (SD)
Lumbar spine BMD β (SD)
Forearm BMD β (SD)
0.4
0.2
0.0
-0.2
-0.4
MBL2*~
ESR1*
AQP1
FGFRL1*
SOST*
SLC8A1~
RSPO3*
SOST*
ESR1*
RSPO3*
WNT16*
FGFRL1*
ESR1*
AQP1
SOST*
SLC8A1~
RSPO3*
SOST*
RSPO3*
ESR1*
WNT16*
AQP1
SLC8A1~
RSPO3*
SOST*
SOST*
ESR1*
WNT16*
RSPO3*
$-log_{10}(P)_{Any\ fracture}$
10.0
7.5
5.0
2.5
0.0


Previous GWS
Novel
LRP5*
WNT16
EN1*
WNT16*
WNT16*
BMP5*
MLL2*
LRP5*
PRSS23*
BMPR2*
BMP5*
EMP1*
AHNAK*
MBL2*~
TNFRSF11B
LINC00982
TBX1
UBP1
JUP~
ZNF800~
RHPN2*
GPC6*
BMP2*
CBFB
CREB5*
BMPR1A
JAG1*
FMN2~
WNT16*
ESR1*
EN1*
FAM9B~
PKDCC*
FGFRL1*
PRSS23*
WNT16*
SPTBN1*
ESR1*
RSPO3*
LOC105370177*~
Absolute conditional and joint eBMD β (SD)
Minor allele frequency
0.0
0.1
0.2
0.3
0.4
0.5


eBMD rG
LDSC rG
1.0
0.5
0.0
-0.5
-1.0
Any fracture
Fall fracture
Femoral neck bone mineral density adult
Lumbar spine bone mineral density adult
Total body less head bone mineral density adult
Skull bone mineral density pediatric
Upper limb bone mineral density pediatric
Lower limb bone mineral density pediatric
Calcaneal broadband ultrasonic attenuation
Calcaneal speed of sound
High density lipoprotein cholesterol
Low density lipoprotein cholesterol
Triglycerides
Albumin
Isoleucine
Valine
Hip circumference
Waist circumference
Waist to hip ratio
Total body fat percentage
Height
Body mass index
Birth length
Birth weight
Infant head circumference
Age at menarche
Age at menopause
Anorexia nervosa
Neuroticism
Attention deficit hyperactivity disorder
Bipolar disorder
Major depressive disorder
Autism spectrum disorder
Schizophrenia
Cigarettes smoked per day
Ever vs never smoked
Coronary artery disease
Type 2 diabetes
Eczema
Crohns disease
Inflammatory bowel disease
Ulcerative colitis
Rheumatoid arthritis
Asthma
Cognitive performance
College completion
Years of schooling

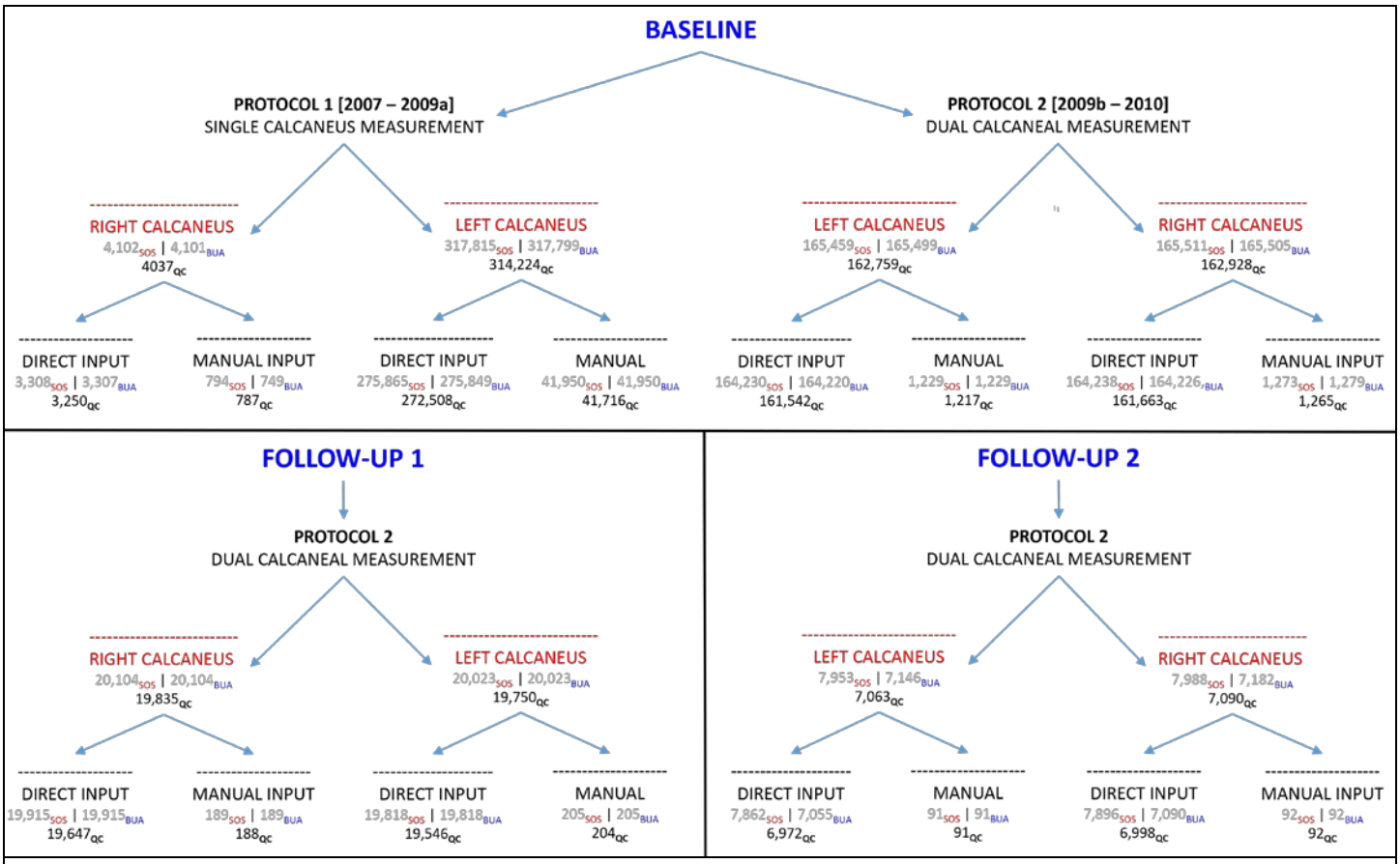

a
WT
Gpc6-/-
WT
Gpc6-/-
Grey level
P=3x10-4
Femur length (mm)
P=0.06
Grey level
Vertebral length (mm)
P=0.016
b
WT
Gpc6-/-
WT
Gpc6-/-
BV/TV (%)
Tb.N (mm-1)
Tb.Th (mm)
Tb.Sp (mm)
Ct.Th (mm)
P=5x10-3
Internal diameter (mm)
BMD (mgHAcm-3)
c
Yield load
Max load
load
WT
Gpc6-/-
Load (N)
Displacement (mm)
Yield load (N)
P=8x10-3
Max load (N)
Fracture load (N)
Stiffness (Nmm-1)
Energy dissipated
d
Yield load
Max load
WT
Gpc6-/-
Load (N)
Displacement (mm)
Yield load (N)
Max load (N)
Stiffness (Nmm-1)



Supplementary Figure 1

Flowchart illustrating the three complementary strategies for gene prioritization employed in this study.

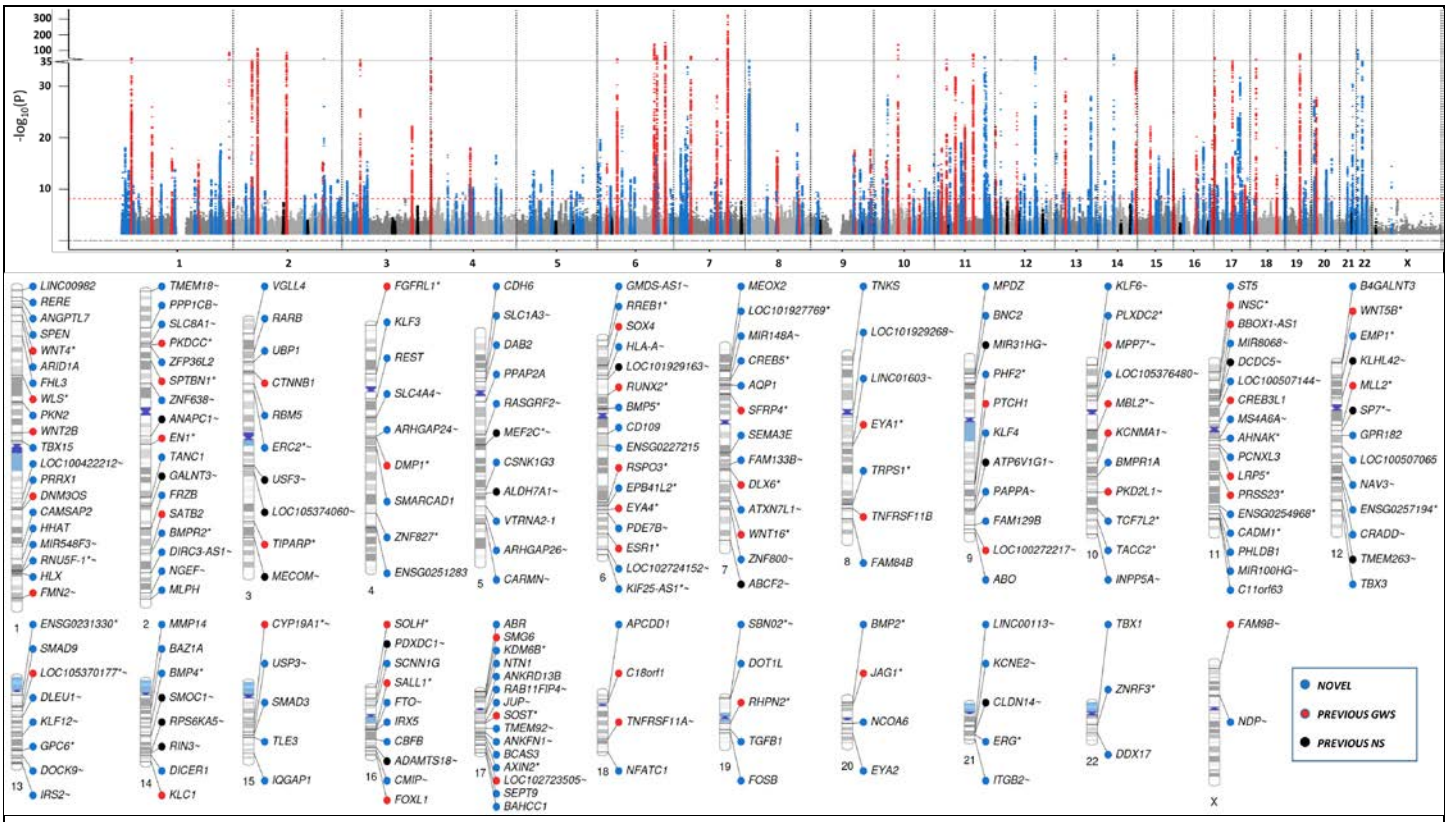
.



Supplementary Figure 2

Flow diagram illustrating calcaneal quantitative ultrasound (QUS) data collection by the UK Biobank.

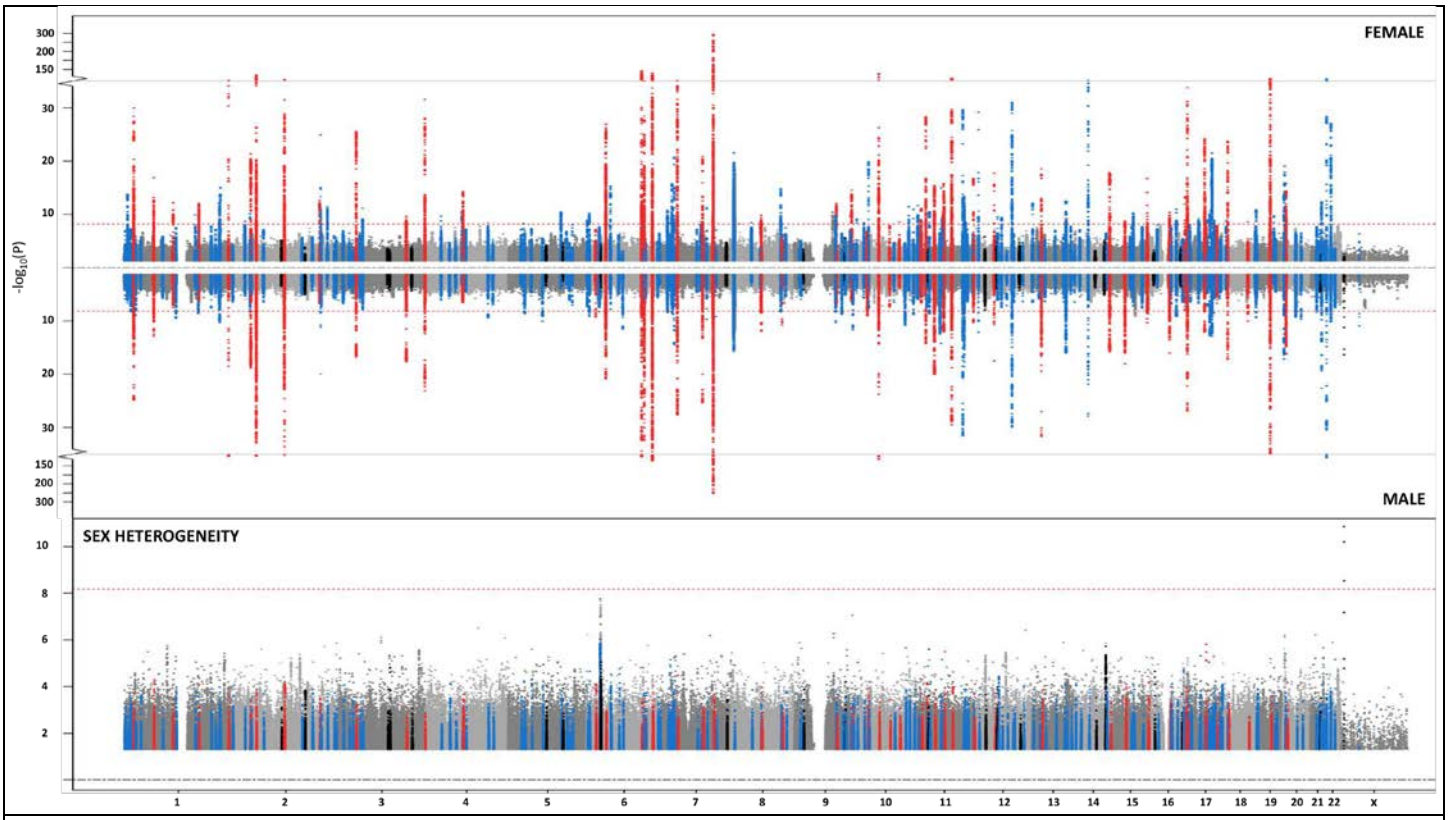
QUS data was collected at three time points: Baseline (2007 - 2010), Follow-up 1 (2012 - 2013) and Follow-up 2 (2014 - 2016). At baseline, QUS was performed using two protocols (denoted protocol 1 and 2). Protocol 1 was implemented from 2007 to mid-2009 and involved measuring the left calcaneus. Only in cases where the left was missing or deemed unsuitable was the right calcaneus measured. Protocol 2 was introduced from mid-2009, (replacing protocol 1) and differed only in that it involved measuring both the left and right calcanei. Protocol 2 was further used for both follow up assessments. For all three time points, calcaneal QUS was performed with the Sahara Clinical Bone Sonometer [Hologic Corporation (Bedford, Massachusetts, USA)]. Vox software was used to automatically collect data from the sonometer (denoted direct input). In cases where direct input failed, QUS outcomes were manually keyed into Vox by the attending healthcare technician or nurse (i.e. manual input). The number of individuals with non-missing measures for speed of sound (SOS) and broadband ultrasound attenuation (BUA) recorded at each assessment period are indicated in light grey. Further details on these methods are publicly available on the UK Biobank website (UK Biobank document #100248 https://biobank.ctsu.ox.ac.uk/crystal/docs/Ultrasoundbonedensitometry.pdf). To reduce the impact of outlying measurements, quality control was applied to male and female subjects separately using the following exclusion thresholds: SOS [Male: (≤ 1,450 and ≥ 1,700 m/s), Female (≤ 1,455 and ≥ 1,700 m/s)] and BUA [Male: (≤ 27 and ≥ 138 dB/MHz), Female (≤ 22 and ≥ 138 dB/MHz)]. Individuals exceeding the threshold for SOS or BUA or both were removed from the analysis. Estimated bone mineral density [eBMD, (g/cm2)] was derived as a linear combination of SOS and BUA (i.e. eBMD = 0.002592 * (BUA + SOS) − 3.687). Individuals exceeding the following thresholds for eBMD were further excluded: [Male: (≤ 0.18 and ≥ 1.06 g/cm2), Female (≤ 0.12 and ≥ 1.025 g/cm2)]. The number of individuals with non-missing measures for SOS, BUA and eBMD after QC are indicated in black. A unique list of individuals with a valid measure for the left calcaneus (N=477,380) and/or right (N=183,824) were identified separately across all three time points. Individuals with a valid right calcaneus measure were included in the final data set when no left measures were available, giving a preliminary working dataset of N=483,992 unique individuals. Bivariate scatter plots of eBMD, BUA and SOS were visually inspected and 762 additional outliers were removed, leaving a total of 483,230 valid QUS measures (left=476,618 and right=6,612) for SOS, BUA and BMD (265,057 females and 218,173 males).



Supplementary Figure 3

Manhattan plot and phenogram showing genome-wide association study results for eBMD in the UKBiobank Study.

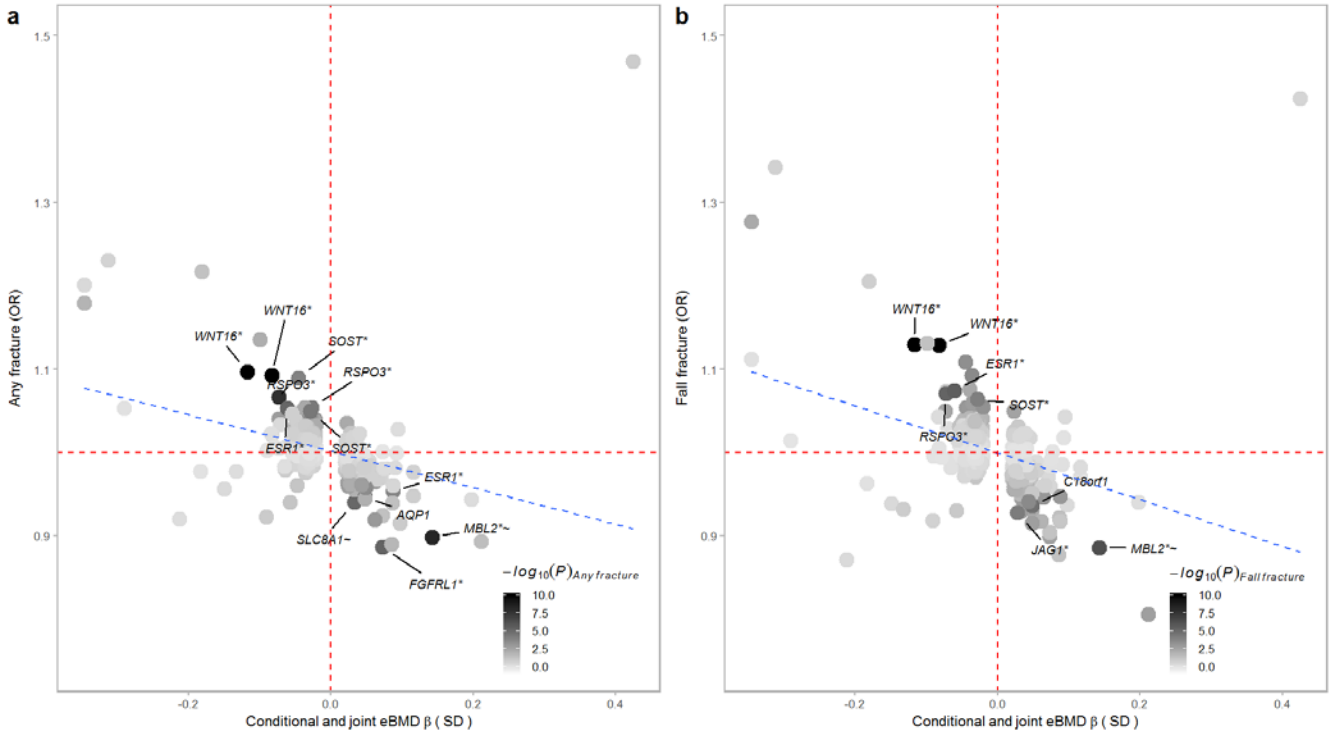
The dashed red line denotes the threshold for declaring genome-wide significance ($\alpha = 6.6 \times 10^{-9}$). In total, 307 conditionally independent SNPs at 203 loci passed the criteria for genome-wide significance. 153 novel loci (i.e. defined as >1MB from previously reported genome-wide significant BMD variant) reaching genome-wide significance are displayed in blue. Previously reported loci that reached genome-wide significance are displayed in red, and previously reported loci failing to reach genome-wide significance in our study are shown in black. Loci that contain more than one conditionally independent signal are marked with an asterisk. Each locus was annotated using the gene contained within the closest gene region identified by DEPICT. In situations where multiple genes were present in a single DEPICT region, priority was given to the gene that displayed a bone phenotype in knockout mouse model, followed by the gene expressed in the most murine bone cell types (3>2>1), followed by the gene with the lowest depict gene p-value. Asterisks denote multiple conditionally independent variants present at the locus, and the "~" symbol denotes the gene closest to the locus (in the case of no genes prioritized by DEPICT at that locus). The *FAM9B* locus was not genome-wide significant in the analysis of all individuals, but was significant in the analysis of males only.



Supplementary Figure 4

Analysis of sex heterogeneity in eBMD.

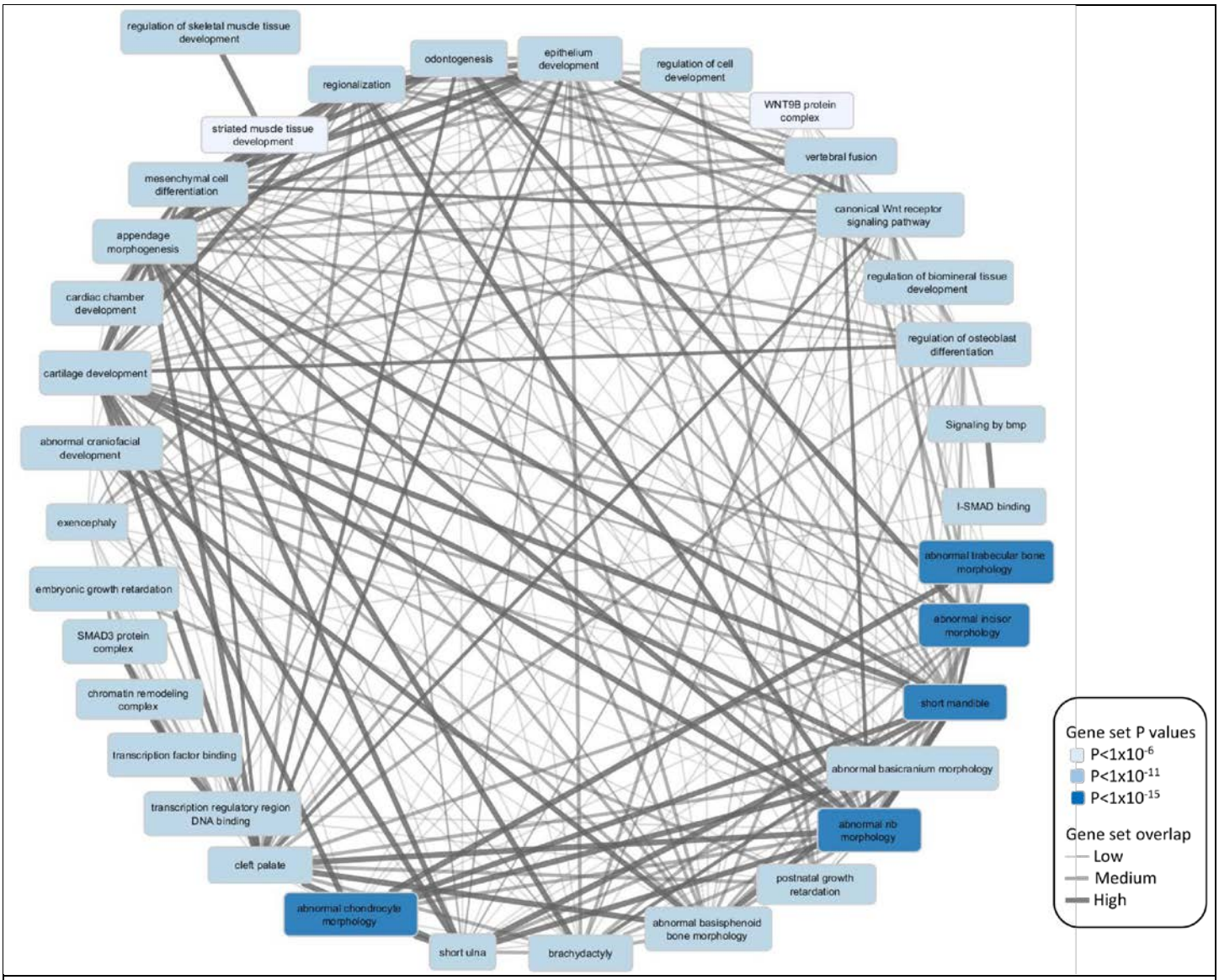
The top graph is a Miami plot of genome-wide association results for males (top panel) and females (bottom panel). The bottom graph is a Manhattan plot for the test for sex heterogeneity in eBMD regression coefficients between males and females. Previously reported loci that reached genome-wide significance are displayed in red, and previously reported loci failing to reach genome-wide significance in our study are shown in black.



Supplementary Figure 5

Plot of the relationship between estimated conditional effect sizes in standard deviations for eBMD (x-axis) and odds of fracture (y-axis) for genome-wide significant eBMD variants.

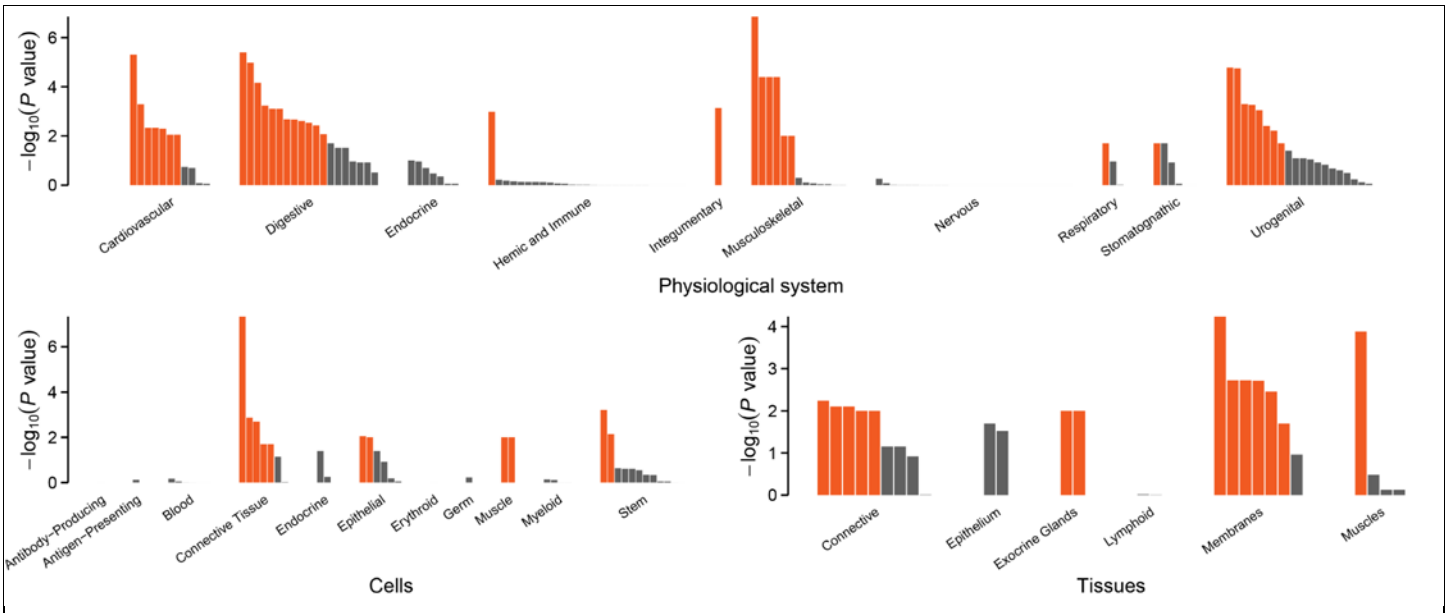
The plot on the left is for any fracture, and the plot on the right is for fracture from a simple fall. The shading of the data points represents the P-value for the test of association with fracture (black for robust evidence of association with fracture and white for poor evidence of an association). Variants that meet Bonferroni significance ($P < 1.6 \times 10^{-4}$) are labelled in the plots.



Supplementary Figure 6

***Meta gene-sets* enriched for genes in eBMD associated loci.**

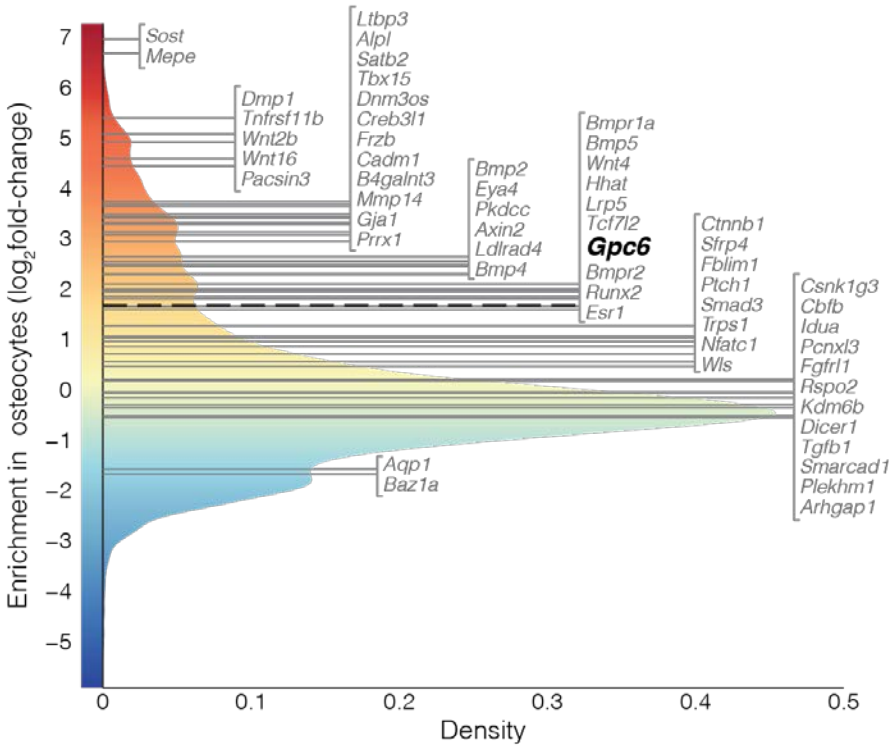
35 *Meta gene-sets* were defined from similarity clustering of significantly enriched gene sets (FDR<1%). Each *Meta gene-set* was named after one of its member gene sets. The color of the *Meta gene-sets* represents the P value of the member set. Interconnection line width represents the Pearson correlation ρ between the gene membership scores for each *Meta gene-set* ($\rho < 0.3$, no line; $0.3 \leq \rho < 0.5$,narrow width; $0.5 \leq \rho < 0.7$, medium width; $\rho \geq 0.7$, thick width)..



Supplementary Figure 7

Tissue/cell type enrichment analysis for genes in eBMD associated loci.

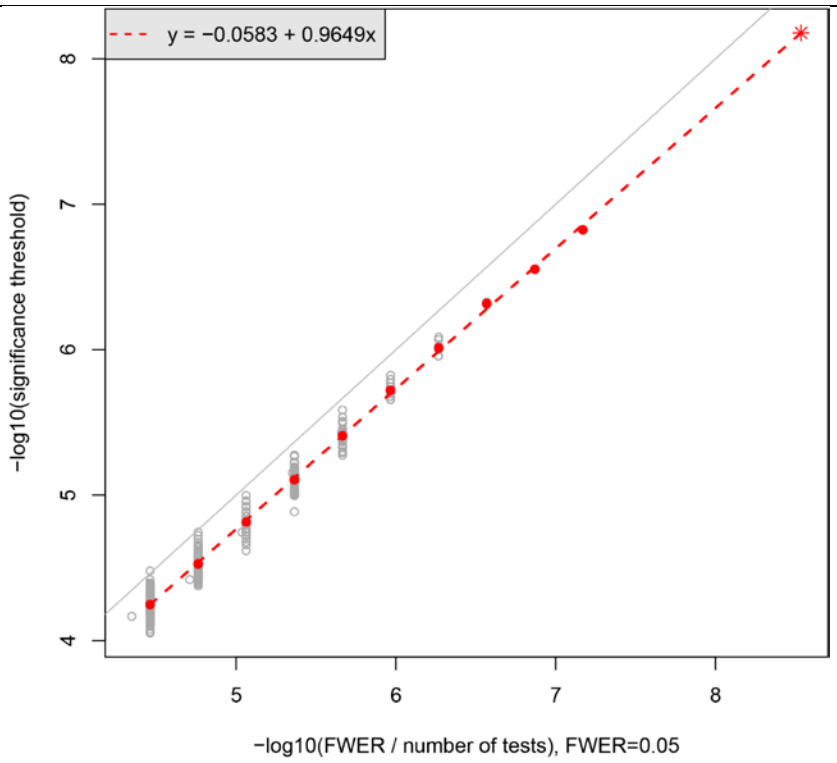
Columns represent the level of evidence for genes in the associated loci to be highly expressed in any of the 209 Medical Subject Heading (MeSH) tissue and cell type annotations. Highlighted in orange are these tissue/cell types significantly (FDR<5%) enriched for the expression of genes in the associated loci. Results are summarized in **Supplementary Table 12**



Supplementary Figure 8

Osteocyte enrichment of DEPICT genes with skeletal phenotypes in knockout mice.

A density plot of the log_2 fold-change of gene expression in osteocyte-isolated bone samples relative to marrow containing bone samples, highlighting all genes expressed in osteocytes that produce a skeletal phenotype when knocked out in mice.



Supplementary Figure 9

Calculation of genome-wide significance threshold.

After permuting phenotypes and reanalysing the associations against genetic variation on chromosome 9, empirical significance thresholds required to control the family-wise error rate at 0.05 are plotted against Bonferroni thresholds, both on the $-\log_{10}$ scale, for subregions of the chromosome of varying size (see also **Online Methods**).

Supplementary Note

Strategy One: Bioinformatic, Statistical and Functional Genomics in Humans
First, we annotated all variants within +/- 500 kb from each conditionally independent lead SNP for deleterious coding variation using the Variant Effect Predictor (VEP)[33] if they were significantly associated with eBMD ($P < 6.6x10^{-9}$). SNPs were classified as deleterious if they had one of the following sequence ontology terms: "frameshift variant", "inframe deletion", "inframe insertion", "initiator codon variant", "missense variant", "splice acceptor variant", "splice donor variant", "stop gained", or "stop lost". We identified 136 deleterious SNPs across 103 loci, mapping to 86 unique genes, from a total of 61,430 genome-wide significant SNPs across 307 loci (**Supplementary Table 8**). These included variants in genes with defined roles in bone biology including *WLS*, *WNT16*, *LRP5*, and *TNFSF11* (which encodes RANKL), as well as other genes that have not previously been implicated in bone.

We next used a shotgun stochastic approach, as applied in FINEMAP, to create configurations of plausible causal SNPs from +/- 500kb around each conditionally independent lead SNP (**Supplementary Table 9**, **Supplementary Fig. 6**). For each region, FINEMAP estimates the posterior probability of there being a particular number of causal SNPs contributing to trait variation, and then ranks all SNPs in the region by their probability of being causal. We designated SNPs meeting a $\log_{10}$ Bayes Factor > 2 as "plausible causal SNPs" (**Supplementary Table 9**). We then explored whether any of these SNPs were at DNase I hypersensitivity sites (DHS) and perturbed transcription factor binding sites by using ENCODE DNase I maps [34,35] and applying contextual analysis of transcription factor occupancy (CATO) scores[4]. Importantly these latter two approaches provide potential functional information that cannot be confounded by LD to another functional variant.

We identified plausible causal SNPs around 300 of the 305 conditionally independent autosomal variants (**Supplementary Table 9**). Five signals from the *WNT16* locus (locus index 133 to 137) had highly significant association statistics from the GWAS that were censored at $P = 2.3x10^{-324}$ rendering statistical fine mapping at this locus inconclusive. Of the 300 remaining signals, 75% were predicted to have three or fewer plausible causal SNPs. Statistical fine-mapping reduced the average physical extent of a locus from 1 Mb to a mean of 344 kb and the number of SNPs per locus from a mean of 6395 per locus (i.e. based on a physical distance metric of 1MB either side of the conditionally independent lead SNP) to a mean of 21 plausible causal SNPs (**Supplementary Table 9**).

Of the 136 deleterious SNPs identified by the VEP software, 28 variants mapping to 24 unique genes, were predicted to be plausibly causal from our analyses using FINEMAP ($\log_{10}$ Bayes factor > 2), and we have annotated these SNPs in bold in **Supplementary Table 8**. Interestingly, this list included *MMP14*, a potentially novel osteoporosis gene. *Mmp14*$^{-/-}$ mice exhibit a decreased BMD phenotype through diminished collagen turnover[36] (also see mouse phenotyping section below). In humans, Winchester syndrome, a very rare disease characterized by severe osteolysis in the hands and feet and generalized osteoporosis and bone thinning is caused by homozygous mutations in *MMP14*[37].

Next, we assessed the intersection of plausible causal SNPs with DHS to identify SNPs that may be functional, and to identify potential target genes we tested the association of plausible causal SNPs with *cis*-eQTL expression of genes in human osteoblasts from 95 donors[38] who had also had their DNA genome-wide genotyped and imputed to a combined UK10K and 1000 Genomes reference panel[39]. Of the 300 loci, we identified 1,339 plausible causal SNPs within DHS and 385 potential target genes ($P < 0.05$) based on *cis*-eQTL evidence in human osteoblasts (**Supplementary Table 10**).

We investigated whether the eQTL results were consistent with osteoblast expression mediating the association between SNPs and eBMD using two sample Mendelian randomization analyses[40,41]. HEIDI (heterogeneity in dependent instruments) tests were conducted to identify situations in which cis-eQTLs were likely to reflect two or more distinct causal variants (i.e. one set affecting gene expression and the others affecting eBMD variation), as opposed to situations consistent with expression of the relevant gene potentially mediating the relationship between the SNP and eBMD in osteoblasts (**Supplementary Table 10**). Although our cis eQTL sample was small (i.e. 95 individuals), several probes demonstrated large Mendelian randomization estimates of the association between gene expression and eBMD. However significant HEIDI tests at these genes suggested that differences in osteoblast expression, at least at these more strongly associated loci, were unlikely to mediate the association between SNPs and eBMD.

Supplementary Table 1. UK Biobank Study descriptives.

ENTIRE COHORT		FEMALES (N = 265,057)						MALES (N = 218,173)					
TRAIT	UNIT	MIN	MAX	RANGE	MEDIAN	MEAN	SD	MIN	MAX	RANGE	MEDIAN	MEAN	SD
AGE	years	39.0	74.1	35.1	57.0	56.4	8.0	38.0	75.8	37.8	58.0	56.8	8.2
WEIGHT	kg	30.1	196.0	165.9	69.0	71.4	14.0	38.8	197.7	158.9	84.1	85.6	14.1
HEIGHT	cm	121.0	199.0	78.0	162.0	162.4	6.3	122.0	209.0	87.0	176.0	175.6	6.8
SOS	m/s^{-}	1455.0	1698.6	243.5	1546.2	1549.1	30.4	1460.2	1700.0	239.7	1555.1	1558.1	31.6
BUA	dB/MHz	22.1	138.0	115.9	71.6	72.7	16.3	27.1	138.0	110.9	81.6	82.6	17.2
eBMD	g/cm^{-}	0.15	1.02	0.87	0.51	0.52	0.12	0.18	1.03	0.85	0.56	0.57	0.12

GWAS COHORT		FEMALES (N = 76,067)						MALES (N = 66,420)					
TRAIT	UNIT	MIN	MAX	RANGE	MEDIAN	MEAN	SD	MIN	MAX	RANGE	MEDIAN	MEAN	SD
AGE	years	39.0	74.1	35.1	58.0	56.5	7.9	40.0	74.4	34.4	59.0	57.1	8.1
WEIGHT	kg	32.1	196.0	163.9	69.2	71.6	14.1	40.8	197.1	156.3	84.4	86.0	14.2
HEIGHT	cm	126.0	192.0	66.0	162.0	162.5	6.2	122.0	205.0	83.0	175.5	175.6	6.8
SOS	m/s^{-}	1455.8	1693.9	238.2	1545.2	1548.1	30.1	1460.8	1693.2	232.4	1554.5	1557.5	31.6
BUA	dB/MHz	22.6	138.0	115.4	71.3	72.3	16.2	27.6	138.0	110.4	81.4	82.4	17.2
eBMD	g/cm2	0.15	0.98	0.82	0.50	0.51	0.12	0.18	1.00	0.82	0.55	0.56	0.12

SOS	Speed of sound
BUA	Broadband ultrasound attenuation
eBMD	Estimated bone mineral density
N	Sample size
MIN	Minimum recorded value of trait
MAX	Maximum recorded value of trait
RANGE	Difference between maximum trait and minimum trait value
MEDIAN	Median value of trait
MEAN	Mean value of trait
SD	Standard deviation

Supplementary Table 2. Association results for 307 conditionally independent SNPs that reach genome-wide significance in the UKBiobank eMIM GWAS

| All European UNCONDITIONALLY INDEPENDENT eMIM LINKAGE DISEQUILIBRIA | | | | | | | | | | | | GCTA-COJO | | | | | | | ALTERN DATASET | | | | | | | | | | | |

Supplementary Table 3. Look up of 307 conditionally independent genome-wide significant SNPs for eBMD in the previous GEFOS-Seq Study and association results for fracture in the UKBB Study.

| | AT BIOBANK CONDITIONALLY INDEPENDENT eBMD ASSOCIATED VARIANTS | | | | | | | | | | EBMD GWAS | | | | | | | | | |

Supplementary Table 4. Look-up of published genome-wide significant BMD variants in the UK Biobank GWAS (eBMD, fracture), and the GEFOS-Seq Study (FN-BMD, LS-BMD, FA-BMD)

PUBLISHED VARIANTS PREVIOUSLY ASSOCIATED WITH OSTEOPOROSIS AND OTHER BONE RELATED TRAI									eBMD				FEMORAL NECK BMD				LUMBAR SPINE BMD				FOREARM BMD				ANY FRACTURE				FALL FRACTURE			
LOCUS BIN	CHR	BP	RSID	C.GENE	EA	NEA	EAF	PMID	AUTHOR	TRAIT	EAF	β	SE	P	EAF	β	SE	P	EAF	β	SE	P	EAF	β	SE	P	EAF	OR	95%-CLL	95%-CLU	P	EAF	OR	95%-CLL	95%-CLU	P
1		22643718	rs3753353	WNT4	A	T	0.18	24945404	KEMP_JP	TBLH-BMD/LL-BMD	0.79	0.04	0.05	0.4	0.84	0.06	0.06	0.3	0.79	0.02	0.06	0.7	0.82	0.11	0.06	0.07	0.19	0.01E-01	0.19	0.04	0.998	1.043	0.38	0.01	0.999	0.995	1.003	4.20E-01
1		22450487	rs2235529	WNT4	C	T	0.84	24945404	KEMP_JP	LL-BMD	0.85	0.05	0.05	0.305	4.70E-24	0.82	0.03	0.010	2.81E-03	0.82	0.03	0.012	2.38E-02	0.82	0.01	0.022	7.77E-01	0.85	0.987	0.957	1.017	3.90E-01	0.85	0.987	0.957	1.017	8.30E-01
1		22403724	rs2572932	WNT4	C	A	0.69	22504420	ESTRADA,K	LS-BMD/FN-BMD	0.76	0.04	0.04	9.30E-27	-	-	-	-	-	-	-	-	-	-	-	-	-	0.76	0.972	0.947	0.997	3.10E-02	0.76	0.972	0.947	0.997	1.30E-01
1		22452887	rs3820498	WNT4	G	C	0.79	24945404	KEMP_JP	SK-BMD	0.80	0.05	0.04	3.70E-31	0.78	0.04	0.010	1.07E-05	0.78	0.05	0.011	2.91E-06	0.78	0.02	0.020	3.25E-01	0.82	0.975	0.948	1.003	7.80E-02	0.83	0.975	0.948	1.003	9.70E-02
1		22636447	rs7524102	ZBTB40	G	A	0.17	18445771/19070	STYRKARSDOTTIR,U/RIVADENEIRA/LS-BMD/FN-BMD		0.18	0.06	0.04	1.50E-46	0.20	0.08	0.010	7.36E-17	0.20	0.09	0.011	2.41E-14	0.20	0.07	0.021	6.38E-04	0.18	0.973	0.945	1.001	6.00E-02	0.18	0.973	0.945	1.001	5.70E-01
1		22703351	rs12402465	ZBTB40	G	A	0.77	24924962	ZHANG,Y.H	LS-BMD/FN-BMD/TH-BMC	0.18	0.00	0.03	0.903	0.22	0.08	0.011	1.81E-12	0.22	0.08	0.014	1.57E-09	0.22	0.07	0.027	1.18E-02	0.18	0.974	0.946	1.003	7.80E-02	0.18	0.974	0.946	1.003	6.40E-01
1		22702858	rs6696981	ZBTB40	T	G	0.14	18445771/19070	STYRKARSDOTTIR,U	LS-BMD/FN-BMD	0.12	0.05	0.05	6.30E-25	0.14	0.07	0.012	4.78E-08	0.14	0.08	0.014	9.02E-09	0.14	0.06	0.024	1.74E-02	0.12	0.967	0.934	1.000	5.10E-02	0.12	0.967	0.934	1.000	3.80E-01
1		22711473	rs6427849	ZBTB40	T	G	0.17	19091982/22504	RIVADENEIRA,F/ESTRADA,K	LS-BMD/FN-BMD	0.18	0.06	0.04	6.02E-50	0.19	0.08	0.010	5.90E-16	0.19	0.09	0.012	1.15E-13	0.19	0.07	0.021	4.66E-04	0.19	0.978	0.950	1.007	1.30E-01	0.18	0.978	0.950	1.007	8.30E-01
1		22772339	rs7543980	ZBTB40	A	C	0.19	19070252	STYRKARSDOTTIR,U	FN-BMD	0.22	0.05	0.04	1.20E-34	0.20	0.06	0.011	4.61E-10	0.20	0.06	0.013	3.92E-07	0.22	0.05	0.021	1.57E-02	0.19	0.983	0.937	1.010	2.20E-01	0.22	0.983	0.937	1.010	8.10E-02
2		68635075	rs143074Z	GNG12-AS1/LS-C	T	C	0.21	19891982	RIVADENEIRA,F	LS-BMD/FN-BMD	0.22	0.03	0.04	1.70E-10	0.21	0.06	0.009	1.13E-10	0.21	0.08	0.011	6.30E-14	0.21	0.01	0.019	7.51E-01	0.22	0.958	0.971	1.024	8.60E-01	0.22	0.958	0.971	1.024	3.50E-01
2		68635390	rs7482952	GNG12-AS1/LS-C	A	G	0.21	19070252	STYRKARSDOTTIR,U	FN-BMD	0.22	0.03	0.04	1.60E-10	0.21	0.06	0.009	1.13E-10	0.21	0.08	0.011	6.30E-14	0.21	0.01	0.019	7.95E-01	0.22	0.958	0.971	1.025	8.60E-01	0.22	0.958	0.971	1.025	3.50E-01
2		68635385	rs74825952	GNG12-AS1/LS-A	G	T	0.07	22504420	ESTRADA,K	LS-BMD/FN-BMD	0.92	0.02	0.06	6.40E-03	0.93	0.04	0.014	3.04E-03	0.93	0.04	0.016	7.85E-03	0.93	-0.01	0.029	6.48E-01	0.92	0.970	0.930	1.012	1.60E-01	0.92	0.970	0.930	1.012	2.50E-01
2		68647716	rs12407328	GNG12-AS1/LS-T	C	G	0.06	22504420	ESTRADA,K	LS-BMD/FN-BMD	0.60	0.03	0.03	3.50E-16	0.65	0.05	0.009	5.07E-09	0.65	0.06	0.009	4.33E-12	0.65	0.00	0.016	8.85E-01	0.60	0.992	0.970	1.015	4.90E-01	0.60	0.992	0.970	1.015	7.60E-01
2		68648697	rs2568752	GNG12-AS1/LS-T	C	T	0.38	22504420	ESTRADA,K	LS-BMD	0.38	0.02	0.03	4.20E-10	0.38	0.03	0.007	1.46E-06	0.38	0.04	0.008	1.76E-06	0.38	0.00	0.013	1.85E-01	0.39	1.000	0.977	1.023	9.70E-01	0.39	1.000	0.977	1.023	5.30E-01
2		68637510	rs7430740	GNG12-AS1/LS-T	C	G	0.45	24249748	ZHANG,L	LS-BMD	0.38	0.02	0.03	4.90E-10	0.41	0.04	0.006	3.50E-09	0.41	0.06	0.009	2.98E-11	0.41	-0.02	0.016	2.85E-01	0.38	0.988	0.966	1.011	3.00E-01	0.38	0.988	0.966	1.011	6.30E-01
2		112102122	rs4954453	AAF/LS-A	C	T	0.43	24945404	KEMP_JP	NW	0.56	0.00	0.03	0.903	0.57	0.03	0.007	1.52E-07	0.59	-0.02	0.008	5.05E-02	0.59	-0.02	0.016	1.58E-01	0.55	1.005	0.982	1.029	6.50E-01	0.55	1.005	0.982	1.029	9.20E-01
4		172199573	rs479336	DMK3	G	T	0.26	22504420	ESTRADA,K	FN-BMD	0.25	0.02	0.04	1.70E-10	0.30	0.04	0.009	9.08E-07	0.30	0.03	0.011	9.74E-04	0.30	0.01	0.018	5.61E-01	0.25	0.996	0.971	1.022	7.50E-01	0.25	0.996	0.971	1.022	6.60E-01
5		24059724	rs9287237	FAT2	T	G	0.16	23437003	PATERNOSTER,L	T-sBMD	0.18	0.08	0.04	3.20E-78	0.20	0.04	0.010	1.47E-04	0.20	0.04	0.012	1.86E-03	0.20	0.05	0.021	1.82E-02	0.18	0.967	0.929	1.017	4.00E-01	0.18	0.967	0.929	1.017	7.90E-01
6		42250549	rs2235482	ZBTB46	A	C	0.23	22504420	ESTRADA,K	FN-BMD	0.22	0.05	0.04	1.20E-32	0.22	0.04	0.009	1.94E-06	0.22	0.01	0.010	3.92E-01	0.22	0.07	0.019	4.58E-04	0.23	0.950	0.984	1.017	4.10E-01	0.23	0.950	0.984	1.017	8.10E-02
7		54569707	rs4233949	SPTBN2	C	G	0.38	22504420	ESTRADA,K	LS-BMD/FN-BMD	0.39	0.07	0.003	2.40E-110	-	-	-	-	0.39	0.07	0.003	1.20E-101	0.39	0.07	0.006	1.31E-32	0.39	0.980	0.958	1.003	8.60E-02	0.39	0.980	0.958	1.003	9.50E-01
7		54569457	rs1858930	SPTBN2	A	G	0.34	19891982/24439	RIVADENEIRA,F/MOAYYERI,A	LS-BMD/FN-BMD	0.36	0.08	0.003	1.30E-111	0.28	0.02	0.008	4.32E-03	0.28	0.05	0.009	1.70E-07	0.28	0.01	0.016	7.23E-01	0.34	0.988	0.963	1.009	2.20E-01	0.34	0.988	0.963	1.009	7.20E-01
8		112500305	rs17040775	ANAPC2	A	C	0.76	22504420	ESTRADA,K	FN-BMD	0.76	0.01	0.04	3.10E-02	0.81	0.02	0.009	1.25E-02	0.81	0.00	0.011	7.14E-01	0.81	0.04	0.019	4.03E-02	0.76	0.991	0.965	1.017	4.90E-01	0.76	0.991	0.965	1.017	1.10E-01
9		21903589	rs18785281	LOC105035797	A	G	0.22	22504420	ESTRADA,K	LS-BMD/FN-BMD	0.22	0.03	0.04	6.20E-14	0.24	0.04	0.009	5.20E-07	0.24	0.04	0.011	4.20E-05	0.24	0.03	0.019	1.86E-01	0.22	1.002	0.976	1.030	1.30E-01	0.22	1.002	0.976	1.030	4.30E-01
9		119154972	rs4742437	LOC105037709	C	T	0.06	24924962	ZHENG,HF	LS-BMD/FN-BMD	0.06	0.10	0.06	0.116	0.06	0.10	0.016	7.51E-01	0.10	0.08	0.018	8.53E-06	0.10	0.05	0.032	1.25E-01	0.06	0.979	0.934	1.026	3.70E-01	0.06	0.979	0.934	1.026	4.30E-01
9		119507607	rs115423648	ENG	T	C	0.01	26733130	STYRKARSDOTTIR,U	LS-BMD/FN-BMD	0.01	0.38	0.020	6.20E-86	0.01	0.11	0.045	2.13E-02	0.01	0.28	0.052	1.76E-07	0.01	0.26	0.093	6.22E-03	0.01	0.848	0.746	0.964	1.20E-02	0.01	0.848	0.746	0.964	4.50E-03
9		119529929	rs34181397	ENG	A	G	0.04	24945404	KEMP_JP	FN-BMD	0.04	0.05	0.03	0.103	0.10	0.10	0.019	2.52E-07	0.10	0.03	0.022	0.203	0.10	0.03	0.039	3.52E-01	0.04	0.956	0.937	1.057	8.80E-01	0.04	0.956	0.937	1.057	7.90E-02
9		119545994	rs11892564	ENG	T	C	0.02	26387764	ZHENG,HF	LS-BMD/FRACTURE*	0.02	0.23	0.013	9.90E-67	0.01	0.12	0.034	7.23E-04	0.01	0.24	0.039	4.10E-09	0.01	0.17	0.069	1.77E-02	0.02	0.960	0.880	1.049	3.60E-01	0.02	0.960	0.880	1.049	2.10E-01
9		119613444	rs1883539669	ENG	T	C	0.01	26387764	ZHENG,HF	LS-BMD	0.02	0.19	0.018	7.50E-27	0.02	0.15	0.032	2.31E-03	0.02	0.18	0.036	1.76E-06	0.02	0.09	0.065	1.85E-01	0.02	1.006	0.930	1.087	8.80E-01	0.02	1.006	0.930	1.087	9.80E-01
10		76537268	rs10178530	C3orf43	A	C	0.51	26387764	ZHENG,HF	FN-BMD	0.51	0.01	0.03	2.70E-04	0.57	0.06	0.008	1.20E-14	0.57	0.05	0.009	4.97E-09	0.57	0.04	0.016	1.37E-02	0.51	1.000	0.997	1.042	8.40E-02	0.51	1.020	0.997	1.042	1.10E-01
11		19657814	rs6726821	GALNT3	T	G	0.51	24945404	KEMP_JP	TBLH-BMD/LL-BMD	0.51	0.01	0.03	5.50E-04	0.57	0.06	0.008	4.74E-14	0.57	0.05	0.009	1.07E-08	0.57	0.04	0.016	2.09E-02	0.51	1.023	1.001	1.046	4.20E-02	0.51	1.023	1.001	1.046	4.80E-02
11		19658344	rs7941518	GALNT3	C	T	0.49	25733022	DUNCAN,EL	LS-BMD	0.49	0.01	0.03	5.50E-04	0.43	0.06	0.008	2.73E-14	0.58	0.05	0.009	1.60E-08	0.43	0.04	0.016	1.88E-02	0.49	1.023	1.001	1.046	3.70E-02	0.49	1.023	1.001	1.046	5.40E-02
12		106601046	rs1346004	GALNT3	G	A	0.5	22504420	ESTRADA,K	LS-BMD/FN-BMD	0.51	0.01	0.03	1.90E-04	0.57	0.06	0.008	7.15E-14	0.57	0.05	0.009	8.71E-09	0.57	0.03	0.016	3.98E-02	0.51	1.020	0.998	1.043	7.20E-02	0.51	1.020	0.998	1.043	9.10E-02
12		106603281	rs11985286	GALNT3	A	G	0.49	22504420	ESTRADA,K	LS-BMD	0.49	0.01	0.03	1.90E-04	0.43	0.06	0.008	2.73E-14	0.58	0.05	0.009	1.60E-08	0.43	0.04	0.016	1.88E-02	0.49	1.023	1.001	1.046	3.70E-02	0.49	1.023	1.001	1.046	5.40E-02
12		200676326	rs905378	FTCD/NL1	A	G	0.83	21573128	KOLI,J	LS-BMD/FN-BMD	0.31	0.01	0.04	1.10E-02	0.33	0.00	0.009	9.76E-01	0.33	0.00	0.017	9.88E-01	0.31	0.019	0.955	0.944	1.027	2.70E-01	0.85	0.953	0.924	0.984	2.70E-03	0.85	0.953	0.924	0.984	2.30E-03
12		99944S	rs8027815	IDUA	G	A	0.77	24249748	ZHANG,L	FN-BMD	0.85	0.07	0.05	4.50E-49	0.81	0.05	0.011	4.55E-05	0.81	0.05	0.013	8.32E-05	0.81	0.08	0.021	4.56E-04	0.85	0.955	0.925	0.985	4.00E-03	0.85	0.955	0.925	0.985	2.90E-03
12		99773840	rs4762033	MEPE	T	C	0.43	22504420	ESTRADA,K	LS-BMD/FN-BMD	0.34	0.03	0.03	3.50E-17	0.34	0.03	0.008	2.79E-05	0.34	0.03	0.010	1.52E-03	0.34	0.03	0.018	3.40E-03	0.34	0.984	0.959	1.031	7.40E-01	0.34	0.984	0.959	1.031	8.40E-01
12		88775243	rs4714403	MEPE	T	C	0.34	19891982	RIVADENEIRA,F	LS-BMD	0.34	0.03	0.04	3.60E-17	0.34	0.03	0.008	2.38E-05	0.34	0.05	0.009	1.80E-07	0.34	0.00	0.017	7.73E-01	0.34	1.009	0.985	1.033	4.70E-01	0.34	1.009	0.985	1.033	2.10E-01
12		88739710	rs4633104	MEPE	T	C	0.34	24249748	ZHANG,L	LS-BMD	0.35	0.03	0.04	4.60E-17	0.34	0.03	0.008	1.54E-02	0.33	0.04	0.009	3.31E-05	0.33	0.02	0.016	1.21E-01	0.34	1.034	1.002	1.067	3.20E-02	0.34	1.034	1.002	1.067	3.20E-02
13		88138731	rs11951031	MEF2C	C	T	0.94	23572188	ZHENG,HF	FA-BMD	0.94	0.00	0.07	9.70E-01	-	-	-	-	-	-	-	-	-	-	-	-	-	0.94	0.977	0.933	1.023	3.20E-01	0.94	0.977	0.933	1.023	1.10E-01
13		88337782	rs8004139	MEF2C-AS2	T	G	0.41	24249748	ZHANG,L	FN-BMD	0.53	0.00	0.03	3.00E-01	0.49	0.08	0.008	1.43E-23	0.49	0.11	0.009	4.68E-01	0.49	0.09	0.016	2.52E-08	0.53	0.989	0.967	1.011	3.30E-01	0.53	0.989	0.967	1.011	4.30E-01
13		88376581	rs9584944	MEF2C-AS3	G	A	0.41	26733130	STYRKARSDOTTIR,U	LS-BMD/FN-BMD	0.53	0.00	0.03	3.00E-01	0.48	0.08	0.008	1.43E-23	0.48	0.11	0.009	4.68E-01	0.48	0.09	0.016	2.52E-08	0.53	0.989	0.967	1.011	3.10E-01	0.53	0.989	0.967	1.011	4.30E-01
20		125918148	rs13182402	ALDH7A1	A	G	0.86	20072603	GLIOY	FRACTURE*	0.90	0.00	0.06	5.90E-01	0.89	0.02	0.012	5.57E-02	0.89	0.01	0.014	6.34E-01	0.89	0.01	0.026	7.28E-01	0.90	1.004	0.968	1.042	8.30E-01	0.90	1.004	0.968	1.042	9.40E-01
21		21394613	rs466456	LINC00362	A	G	0.49	22504420	ESTRADA,K	LS-BMD/FN-BMD	0.51	0.01	0.03	1.70E-04	0.57	0.06	0.008	1.20E-14	0.57	0.05	0.009	4.97E-09	0.57	0.04	0.016	1.37E-02	0.51	1.000	0.997	1.042	8.40E-02	0.51	1.020	0.997	1.042	1.10E-01
22		32244627	rs3130340	LOC105370163	C	T	0.21	19070252	STYRKARSDOTTIR,U	LS-BMD	0.24	0.00	0.04	7.10E-01	0.24	0.03	0.010	1.13E-02	0.24	0.03	0.012	1.27E-02	0.24	0.02	0.022	4.98E-01	0.24	0.969	0.944	0.994	1.70E-02	0.24	0.969	0.944	0.994	1.30E-02
23		44639184	rs11156764	LOC105370575	C	T	0.6	22504420	ESTRADA,K	LS-BMD	0.58	0.02	0.03	7.40E-11	0.61	0.05	0.008	1.08E-01	0.61	0.02	0.009	9.78E-03	0.61	0.00	0.016	9.66E-01	0.58	0.985	0.963	1.007	1.80E-01	0.58	0.985	0.963	1.007	3.70E-01
24		126510848	rs4148178	CLEC19A	T	G	0.39	24945404	KEMP_JP	SK-BMD	0.34	0.04	0.04	3.40E-24	0.36	0.02	0.009	1.45E-02	0.36	0.03	0.011	1.50E-03	0.36	0.04	0.019	4.55E-02	0.34	0.966	0.946	1.012	2.20E-01	0.34	0.966	0.946	1.012	2.30E-01
24		126820598	rs2130804	MIR588	T	G	0.24	24945404	KEMP_JP	SK-BMD	0.23	0.02	0.04	3.00E-04	0.21	0.00	0.009	7.55E-01	0.21	0.01	0.010	4.48E-01	0.21	0.00	0.019	9.45E-01	0.23	0.999	0.973	1.026	9.50E-01	0.23	0.999	0.973	1.026	9.80E-01
24		126868996	rs2042475	RSPO3	C	T	0.24	24945404	KEMP_JP	SK-BMD	0.24	0.02	0.04	1.30E-07	0.24	0.00	0.009	7.55E-01	0.21	0.01	0.010	4.48E-01	0.21	0.00	0.019	9.45E-01	0.23	0.999	0.973	1.026	9.50E-01	0.23	0.999	0.973	1.026	9.80E-01
6		127167072	rs13240985	RSPO3	A	C	0.76	21533022/22504	DUNCAN,EL/ESTRADA,K	LS-BMD/FN-BMD	0.75	-0.02	0.04	7.50E-08	0.81	0.05	0.009	1.35E-08	0.81	0.04	0.010	2.81E-04	0.81	0.07	0.018	8.54E-05	0.75	0.958	0.973	1.024	8.80E-01	0.75	0.958	0.973	1.024	7.00E-01
7		124402347	rs3731298	RSPO3	T	G	0.07	26733130	STYRKARSDOTTIR,U	LS-BMD	0.07	0.05	0.05	2.00E-24	0.07	0.04	0.009	4.00E-06	0.07	0.04	0.011	1.50E-04	0.07	0.04	0.020	0.073	0.969	1.022	0.945	1.102	0.05	0.020	0.873	0.969	1.022	0.945	1.102	0.05
7		124748274	rs741021	CALCA/B	A	G	0.47	24249748	ZHANG,L	BJ/AOS/sBMD	0.48	0.08	0.003	8.60E-140	0.45	0.02	0.007	9.49E-03	0.45	0.00	0.009	0.45	0.02	0.016	2.51E-01	0.48	0.988	0.967	1.010	2.80E-01	0.48	0.988	0.967	1.010	4.80E-01
25		133335804	rs271170	LINC00326	T	C	0.67	23437003	PATERNOSTER,L	C-sBMD	0.67	-0.04	0.04	3.00E-27	0.73	-0.02	0.006	2.05E-03	0.73	-0.02	0.009	3.34E-02	0.73	0.06	0.017	8.13E-04	0.67	1.022	0.998	1.047	7.30E-02	0.67	1.022	0.998	1.047	6.60E-02
25		133360896	rs4144636	CDCD7P	A	G	0.65	23437003	PATERNOSTER,L	BA-BMD	0.65	-0.04	0.04	3.20E-29	0.71	-0.02	0.006	1.05E-03	0.71	-0.02	0.009	3.15E-02	0.71	0.06	0.017	3.55E-04	0.67	1.022	0.998	1.046	7.30E-02	0.67	1.022	0.998	1.046	6.60E-02
26		51847901	rs84795S5	CCDC270	A	C	0.65	18445771/19070	STYRKARSDOTTIR,U	FN-BMD	0.60	0.07	0.003	3.00E-95	0.50	0.04	0.008	3.56E-28	0.50	0.05	0.009	2.39E-07	0.50	0.05	0.016	2.15E-03	0.60	0.976	0.954	0.998	3.50E-02	0.60	0.976	0.954	0.998	8.40E-02
26		51918472	rs84795217	CCDC270	C	G	0.6	24437003	PATERNOSTER,L	C-sBMD	0.60	0.08	0.003	1.40E-120	0.48	0.05	0.008	1.23E-32	0.48	0.06	0.009	8.03E-10	0.48	0.07	0.016	3.34E-05	0.60	0.976	0.947	0.995	4.10E-03	0.60	0.976	0.947	0.995	3.40E-02
26		51858456	rs6930279	CCDC270	G	C	0.6	23437003	PATERNOSTER,L	C-sBMD	0.60	0.08	0.003	7.60E-125	0.49	0.05	0.008	8.07E-11	0.49	0.06	0.009	1.27E-09	0.49	0.06	0.016	5.65E-05	0.60	0.969	0.947	0.991	5.70E-03	0.60	0.969	0.947	0.991	2.90E-02
26		51858506	rs8178159	CCDC270	C	T	0.72	24249748	ZHANG,L	LS-BMD	0.88	0.10	0.005	8.00E-96	0.81	0.06	0.011	2.26E-08	0.81	0.08	0.013	2.04E-09	0.81	0.09	0.024	8.68E-05	0.88	0.953	0.921	0.985	5.00E-03	0.88	0.953	0.921	0.985	3.20E-03
26		51851408	rs84795244	CCDC270	C	T	0.31	18445771/19070	STYRKARSDOTTIR,U	LS-BMD/FN-BMD	0.71	0.07	0.003	1.00E-92	0.49	0.05	0.008	1.45E-32	0.49	0.06	0.009	1.00E-09	0.49	0.06	0.016	2.68E-05	0.71	0.954	0.931	0.977	1.50E-04	0.71	0.954	0.931	0.977	1.50E-04
26		51910182	rs4880739	CCDC270	A	T	0.69	24439505	MOAYYERI,A	BUA,SOS	0.71	0.09	0.004	9.40E-158	0.59	0.05	0.009	1.47E-09	0.59	0.06	0.010	5.65E-09	0.59	0.07	0.017	2.64E-05	0.71	0.954	0.931	0.977	1.50E-04	0.71	0.954	0.931	0.977	1.50E-04
26		51919778	rs10403042	CCDC270	C	T	0.69	24439505	MOAYYERI,A	BUA,SOS	0.71	0.09	0.004	5.20E-157	-	-	-	-	-	-	-	-	-	-	-	-	-	0.71	0.954	0.931	0.977	1.50E-04	0.71	0.953	0.930	0.976	1.30E-04
26		51932778	rs1023940	CCDC270	A	G	0.51	26733130	STYRKARSDOTTIR,U	LS-BMD/FN-BMD	0.49	0.06	0.003	2.20E-87	0.47	0.05	0.008	3.64E-09	0.47	0.06	0.009	6.47E-13	0.47	0.04	0.016	1.84E-02	0.49	0.972	0.950	0.994	1.10E-02	0.49	0.972	0.950	0.994	7.80E-04
26		51933175	rs1083004	CCDC270	A	G	0.53	18445771/19070	STYRKARSDOTTIR,U	LS-BMD/FN-BMD	0.49	0.06	0.003	2.10E-87	0.46	0.04	0.007	8.66E-09	0.46	0.06	0.009	1.05E-12	0.46	0.03	0.016	3.32E-02	0.49	0.970	0.949	0.992	7.40E-03	0.49	0.970	0.949	0.992	3.10E-04
26		51933677	rs7159137	CCDC270	G	A	0.51	18445771/19070	STYRKARSDOTTIR,U	LS-BMD/FN-BMD	0.67	0.05	0.004	1.00E-44	-	-	-	-	-	-	-	-	-	-	-	-	-	0.67	0.954	0.932	0.977	1.70E-05	0.67	0.954	0.932	0.977	8.70E-06
26		51934668	rs7751841	CCDC270	G	A	0.77	18445771/19070	STYRKARSDOTTIR,U/ESTRADA,	LS-BMD/FN-BMD	0.78	0.05	0.004	1.90E-32	-	-	-	-	-	-	-	-	-	-	-	-	-	0.81	-0.01	0.919	5.71E-01	0.78	0.962	0.937	0.988	4.70E-03	0.78	0.962	0.937	0.988	8.00E-03
26		51934127	rs6859157	CCDC270	T	C	0.34	19070252	STYRKARSDOTTIR,U	FN-BMD	0.65	0.05	0.003	2.50E-82	0.63	0.03	0.008	2.53E-04	0.63	0.05	0.009	1.98E-08	0.63	0.03	0.016	0.059	0.982	0.957	0.994	0.005	0.982	0.957	0.994	0.005	0.982	0.957	0.994	0.005
26		52008780	rs3020331	ESR1	T	C	0.43	24439505	MOAYYERI,A	BUA,SOS	0.42	0.08	0.003	8.80E-116	0.36	0.04	0.008	4.51E-07	0.36	0.05	0.009	1.45E-08	0.36	0.03	0.016	4.86E-02	0.42	0.949	0.928	0.971	6.00E-06	0.42	0.949	0.928	0.971	1.40E-06

Supplementary Table 5. Results of GWAS for genome-wide significant variants corrected for weight

JOINT/CONDITIONAL ANALYSIS (GWAS SIGNIFICANT VARIANTS)																					
SNP	rsID	CHR	BP	C.GENO	OTHER	EA	MAF	EAF	OBS	β	SE	P	N	β	SE	P	N	β	SE	P	LOCUS NAME (adjusted for weight)
1	rs2977670	1	72757853	FUT9	C	T	0.39	0.39	1.00	-0.03	0.00	1.25E-16	143287	-0.03	0.00	1.25E-16	143287	-0.03	0.00	1.25E-16	FUT9
2	rs6426301	1	72757853	FUT9	C	T	0.39	0.39	1.00	-0.03	0.00	1.25E-16	143287	-0.03	0.00	1.25E-16	143287	-0.03	0.00	1.25E-16	FUT9
3	rs6426301	1	72757853	FUT9	C	T	0.39	0.39	1.00	-0.03	0.00	1.25E-16	143287	-0.03	0.00	1.25E-16	143287	-0.03	0.00	1.25E-16	FUT9
4	rs6426301	1	72757853	FUT9	C	T	0.39	0.39	1.00	-0.03	0.00	1.25E-16	143287	-0.03	0.00	1.25E-16	143287	-0.03	0.00	1.25E-16	FUT9
5	rs6426301	1	72757853	FUT9	C	T	0.39	0.39	1.00	-0.03	0.00	1.25E-16	143287	-0.03	0.00	1.25E-16	143287	-0.03	0.00	1.25E-16	FUT9
6	rs6426301	1	72757853	FUT9	C	T	0.39	0.39	1.00	-0.03	0.00	1.25E-16	143287	-0.03	0.00	1.25E-16	143287	-0.03	0.00	1.25E-16	FUT9
7	rs6426301	1	72757853	FUT9	C	T	0.39	0.39	1.00	-0.03	0.00	1.25E-16	143287	-0.03	0.00	1.25E-16	143287	-0.03	0.00	1.25E-16	FUT9
8	rs6426301	1	72757853	FUT9	C	T	0.39	0.39	1.00	-0.03	0.00	1.25E-16	143287	-0.03	0.00	1.25E-16	143287	-0.03	0.00	1.25E-16	FUT9
9	rs6426301	1	72757853	FUT9	C	T	0.39	0.39	1.00	-0.03	0.00	1.25E-16	143287	-0.03	0.00	1.25E-16	143287	-0.03	0.00	1.25E-16	FUT9
10	rs6426301	1	72757853	FUT9	C	T	0.39	0.39	1.00	-0.03	0.00	1.25E-16	143287	-0.03	0.00	1.25E-16	143287	-0.03	0.00	1.25E-16	FUT9
11	rs6426301	1	72757853	FUT9	C	T	0.39	0.39	1.00	-0.03	0.00	1.25E-16	143287	-0.03	0.00	1.25E-16	143287	-0.03	0.00	1.25E-16	FUT9
12	rs6426301	1	72757853	FUT9	C	T	0.39	0.39	1.00	-0.03	0.00	1.25E-16	143287	-0.03	0.00	1.25E-16	143287	-0.03	0.00	1.25E-16	FUT9
13	rs6426301	1	72757853	FUT9	C	T	0.39	0.39	1.00	-0.03	0.00	1.25E-16	143287	-0.03	0.00	1.25E-16	143287	-0.03	0.00	1.25E-16	FUT9
14	rs6426301	1	72757853	FUT9	C	T	0.39	0.39	1.00	-0.03	0.00	1.25E-16	143287	-0.03	0.00	1.25E-16	143287	-0.03	0.00	1.25E-16	FUT9
15	rs6426301	1	72757853	FUT9	C	T	0.39	0.39	1.00	-0.03	0.00	1.25E-16	143287	-0.03	0.00	1.25E-16	143287	-0.03	0.00	1.25E-16	FUT9
16	rs6426301	1	72757853	FUT9	C	T	0.39	0.39	1.00	-0.03	0.00	1.25E-16	143287	-0.03	0.00	1.25E-16	143287	-0.03	0.00	1.25E-16	FUT9
17	rs6426301	1	72757853	FUT9	C	T	0.39	0.39	1.00	-0.03	0.00	1.25E-16	143287	-0.03	0.00	1.25E-16	143287	-0.03	0.00	1.25E-16	FUT9
18	rs6426301	1	72757853	FUT9	C	T	0.39	0.39	1.00	-0.03	0.00	1.25E-16	143287	-0.03	0.00	1.25E-16	143287	-0.03	0.00	1.25E-16	FUT9
19	rs6426301	1	72757853	FUT9	C	T	0.39	0.39	1.00	-0.03	0.00	1.25E-16	143287	-0.03	0.00	1.25E-16	143287	-0.03	0.00	1.25E-16	FUT9
20	rs6426301	1	72757853	FUT9	C	T	0.39	0.39	1.00	-0.03	0.00	1.25E-16	143287	-0.03	0.00	1.25E-16	143287	-0.03	0.00	1.25E-16	FUT9
21	rs6426301	1	72757853	FUT9	C	T	0.39	0.39	1.00	-0.03	0.00	1.25E-16	143287	-0.03	0.00	1.25E-16	143287	-0.03	0.00	1.25E-16	FUT9
22	rs6426301	1	72757853	FUT9	C	T	0.39	0.39	1.00	-0.03	0.00	1.25E-16	143287	-0.03	0.00	1.25E-16	143287	-0.03	0.00	1.25E-16	FUT9
23	rs6426301	1	72757853	FUT9	C	T	0.39	0.39	1.00	-0.03	0.00	1.25E-16	143287	-0.03	0.00	1.25E-16	143287	-0.03	0.00	1.25E-16	FUT9
24	rs6426301	1	72757853	FUT9	C	T	0.39	0.39	1.00	-0.03	0.00	1.25E-16	143287	-0.03	0.00	1.25E-16	143287	-0.03	0.00	1.25E-16	FUT9
25	rs6426301	1	72757853	FUT9	C	T	0.39	0.39	1.00	-0.03	0.00	1.25E-16	143287	-0.03	0.00	1.25E-16	143287	-0.03	0.00	1.25E-16	FUT9
26	rs6426301	1	72757853	FUT9	C	T	0.39	0.39	1.00	-0.03	0.00	1.25E-16	143287	-0.03	0.00	1.25E-16	143287	-0.03	0.00	1.25E-16	FUT9
27	rs6426301	1	72757853	FUT9	C	T	0.39	0.39	1.00	-0.03	0.00	1.25E-16	143287	-0.03	0.00	1.25E-16	143287	-0.03	0.00	1.25E-16	FUT9
28	rs6426301	1	72757853	FUT9	C	T	0.39	0.39	1.00	-0.03	0.00	1.25E-16	143287	-0.03	0.00	1.25E-16	143287	-0.03	0.00	1.25E-16	FUT9
29	rs6426301	1	72757853	FUT9	C	T	0.39	0.39	1.00	-0.03	0.00	1.25E-16	143287	-0.03	0.00	1.25E-16	143287	-0.03	0.00	1.25E-16	FUT9
30	rs6426301	1	72757853	FUT9	C	T	0.39	0.39	1.00	-0.03	0.00	1.25E-16	143287	-0.03	0.00	1.25E-16	143287	-0.03	0.00	1.25E-16	FUT9
31	rs6426301	1	72757853	FUT9	C	T	0.39	0.39	1.00	-0.03	0.00	1.25E-16	143287	-0.03	0.00	1.25E-16	143287	-0.03	0.00	1.25E-16	FUT9
32	rs6426301	1	72757853	FUT9	C	T	0.39	0.39	1.00	-0.03	0.00	1.25E-16	143287	-0.03	0.00	1.25E-16	143287	-0.03	0.00	1.25E-16	FUT9
33	rs6426301	1	72757853	FUT9	C	T	0.39	0.39	1.00	-0.03	0.00	1.25E-16	143287	-0.03	0.00	1.25E-16	143287	-0.03	0.00	1.25E-16	FUT9
34	rs6426301	1	72757853	FUT9	C	T	0.39	0.39	1.00	-0.03	0.00	1.25E-16	143287	-0.03	0.00	1.25E-16	143287	-0.03	0.00	1.25E-16	FUT9
35	rs6426301	1	72757853	FUT9	C	T	0.39	0.39	1.00	-0.03	0.00	1.25E-16	143287	-0.03	0.00	1.25E-16	143287	-0.03	0.00	1.25E-16	FUT9
36	rs6426301	1	72757853	FUT9	C	T	0.39	0.39	1.00	-0.03	0.00	1.25E-16	143287	-0.03	0.00	1.25E-16	143287	-0.03	0.00	1.25E-16	FUT9
37	rs6426301	1	72757853	FUT9	C	T	0.39	0.39	1.00	-0.03	0.00	1.25E-16	143287	-0.03	0.00	1.25E-16	143287	-0.03	0.00	1.25E-16	FUT9
38	rs6426301	1	72757853	FUT9	C	T	0.39	0.39	1.00	-0.03	0.00	1.25E-16	143287	-0.03	0.00	1.25E-16	143287	-0.03	0.00	1.25E-16	FUT9
39	rs6426301	1	72757853	FUT9	C	T	0.39	0.39	1.00	-0.03	0.00	1.25E-16	143287	-0.03	0.00	1.25E-16	143287	-0.03	0.00	1.25E-16	FUT9
40	rs6426301	1	72757853	FUT9	C	T	0.39	0.39	1.00	-0.03	0.00	1.25E-16	143287	-0.03	0.00	1.25E-16	143287	-0.03	0.00	1.25E-16	FUT9
41	rs6426301	1	72757853	FUT9	C	T	0.39	0.39	1.00	-0.03	0.00	1.25E-16	143287	-0.03	0.00	1.25E-16	143287	-0.03	0.00	1.25E-16	FUT9
42	rs6426301	1	72757853	FUT9	C	T	0.39	0.39	1.00	-0.03	0.00	1.25E-16	143287	-0.03	0.00	1.25E-16	143287	-0.03	0.00	1.25E-16	FUT9
43	rs6426301	1	72757853	FUT9	C	T	0.39	0.39	1.00	-0.03	0.00	1.25E-16	143287	-0.03	0.00	1.25E-16	143287	-0.03	0.00	1.25E-16	FUT9
44	rs6426301	1	72757853	FUT9	C	T	0.39	0.39	1.00	-0.03	0.00	1.25E-16	143287	-0.03	0.00	1.25E-16	143287	-0.03	0.00	1.25E-16	FUT9
45	rs6426301	1	72757853	FUT9	C	T	0.39	0.39	1.00	-0.03	0.00	1.25E-16	143287	-0.03	0.00	1.25E-16	143287	-0.03	0.00	1.25E-16	FUT9
46	rs6426301	1	72757853	FUT9	C	T	0.39	0.39	1.00	-0.03	0.00	1.25E-16	143287	-0.03	0.00	1.25E-16	143287	-0.03	0.00	1.25E-16	FUT9
47	rs6426301	1	72757853	FUT9	C	T	0.39	0.39	1.00	-0.03	0.00	1.25E-16	143287	-0.03	0.00	1.25E-16	143287	-0.03	0.00	1.25E-16	FUT9
48	rs6426301	1	72757853	FUT9	C	T	0.39	0.39	1.00	-0.03	0.00	1.25E-16	143287	-0.03	0.00	1.25E-16	143287	-0.03	0.00	1.25E-16	FUT9
49	rs6426301	1	72757853	FUT9	C	T	0.39	0.39	1.00	-0.03	0.00	1.25E-16	143287	-0.03	0.00	1.25E-16	143287	-0.03	0.00	1.25E-16	FUT9
50	rs6426301	1	72757853	FUT9	C	T	0.39	0.39	1.00	-0.03	0.00	1.25E-16	143287	-0.03	0.00	1.25E-16	143287	-0.03	0.00	1.25E-16	FUT9
51	rs6426301	1	72757853	FUT9	C	T	0.39	0.39	1.00	-0.03	0.00	1.25E-16	143287	-0.03	0.00	1.25E-16	143287	-0.03	0.00	1.25E-16	FUT9
52	rs6426301	1	72757853	FUT9	C	T	0.39	0.39	1.00	-0.03	0.00	1.25E-16	143287	-0.03	0.00	1.25E-16	143287	-0.03	0.00	1.25E-16	FUT9
53	rs6426301	1	72757853	FUT9	C	T	0.39	0.39	1.00	-0.03	0.00	1.25E-16	143287	-0.03	0.00	1.25E-16	143287	-0.03	0.00	1.25E-16	FUT9
54	rs6426301	1	72757853	FUT9	C	T	0.39	0.39	1.00	-0.03	0.00	1.25E-16	143287	-0.03	0.00	1.25E-16	143287	-0.03	0.00	1.25E-16	FUT9
55	rs6426301	1	72757853	FUT9	C	T	0.39	0.39	1.00	-0.03	0.00	1.25E-16	143287	-0.03	0.00	1.25E-16	143287	-0.03	0.00	1.25E-16	FUT9
56	rs6426301	1	72757853	FUT9	C	T	0.39	0.39	1.00	-0.03	0.00	1.25E-16	143287	-0.03	0.00	1.25E-16	143287	-0.03	0.00	1.25E-16	FUT9
57	rs6426301	1	72757853	FUT9	C	T	0.39	0.39	1.00	-0.03	0.00	1.25E-16	143287	-0.03	0.00	1.25E-16	143287	-0.03	0.00	1.25E-16	FUT9
58	rs6426301	1	72757853	FUT9	C	T	0.39	0.39	1.00	-0.03	0.00	1.25E-16	143287	-0.03	0.00	1.25E-16	143287	-0.03	0.00	1.25E-16	FUT9
59	rs6426301	1	72757853	FUT9	C	T	0.39	0.39	1.00	-0.03	0.00	1.25E-16	143287	-0.03	0.00	1.25E-16	143287	-0.03	0.00	1.25E-16	FUT9
60	rs6426301	1	72757853	FUT9	C	T	0.39	0.39	1.00	-0.03	0.00	1.25E-16	143287	-0.03	0.00	1.25E-16	143287	-0.03	0.00	1.25E-16	FUT9
61	rs6426301	1	72757853	FUT9	C	T	0.39	0.39	1.00	-0.03	0.00	1.25E-16	143287	-0.03	0.00	1.25E-16	143287	-0.03	0.00	1.25E-16	FUT9
62	rs6426301	1	72757853	FUT9	C	T	0.39	0.39	1.00	-0.03	0.00	1.25E-16	143287	-0.03	0.00	1.25E-16	143287	-0.03	0.00	1.25E-16	FUT9
63	rs6426301	1	72757853	FUT9	C	T	0.39	0.39	1.00	-0.03	0.00	1.25E-16	143287	-0.03	0.00	1.25E-16	143287	-0.03	0.00	1.25E-16	FUT9
64	rs6426301	1	72757853	FUT9	C	T	0.39	0.39	1.00	-0.03	0.00	1.25E-16	143287	-0.03	0.00	1.25E-16	143287	-0.03	0.00	1.25E-16	FUT9
65	rs6426301	1	72757853	FUT9	C	T	0.39	0.39	1.00	-0.03	0.00	1.25E-16	143287	-0.03	0.00	1.25E-16	143287	-0.03	0.00	1.25E-16	FUT9
66	rs6426301	1	72757853	FUT9	C	T	0.39	0.39	1.00	-0.03	0.00	1.25E-16	143287	-0.03	0.00	1.25E-16	143287	-0.03	0.00	1.25E-16	FUT9
67	rs6426301	1	72757853	FUT9	C	T	0.39	0.39	1.00	-0.03	0.00	1.25E-16	143287	-0.03	0.00	1.25E-16	143287	-0.03	0.00	1.25E-16	FUT9
68	rs6426301	1	72757853	FUT9	C	T	0.39	0.39	1.00	-0.03	0.00	1.25E-16	143287	-0.03	0.00	1.25E-16	143287	-0.03	0.00	1.25E-16	FUT9
69	rs6426301	1	72757853	FUT9	C	T	0.39	0.39	1.00	-0.03	0.00	1.25E-16	143287	-0.03	0.00	1.25E-16	143287	-0.03	0.00	1.25E-16	FUT9
70	rs6426301	1	72757853	FUT9	C	T	0.39	0.39	1.00	-0.03	0.00	1.25E-16	143287	-0.03	0.00	1.25E-16	143287	-0.03	0.00	1.25E-16	FUT9
71	rs6426301	1	72757853	FUT9	C	T	0.39	0.39	1.00	-0.03	0.00	1.25E-16	143287	-0.03	0.00	1.25E-16	143287	-0.03	0.00	1.25E-16	FUT9
72	rs6426301	1	72757853	FUT9	C	T	0.39	0.39	1.00	-0.03	0.00	1.25E-16	143287	-0.03	0.00	1.25E-16	143287	-0.03	0.00	1.25E-16	FUT9
73	rs6426301	1	72757853	FUT9	C	T	0.39	0.39	1.00	-0.03	0.00	1.25E-16	143287	-0.03	0.00	1.25E-16	143287	-0.03	0.00	1.25E-16	FUT9
74	rs6426301	1	72757853	FUT9	C	T	0.39	0.39	1.00	-0.03	0.00	1.25E-16	143287	-0.03	0.00	1.25E-16	143287	-0.03	0.00	1.25E-16	FUT9
75	rs6426301	1	72757853	FUT9	C	T	0.39	0.39	1.00	-0.03	0.00	1.25E-16	143287	-0.03	0.00	1.25E-16	143287	-0.03	0.00	1.25E-16	FUT9
76	rs6426301	1	72757853	FUT9	C	T	0.39	0.39	1.00	-0.03	0.00	1.25E-16	143287	-0.03	0.00	1.25E-16	143287	-0.03	0.00	1.25E-16	FUT9
77	rs6426301	1	72757853	FUT9	C	T	0.39	0.39	1.00	-0.03	0.00	1.25E-16	143287	-0.03	0.00	1.25E-16	143287	-0.03	0.00	1.25E-16	FUT9
78	rs6426301	1	72757853	FUT9	C	T	0.39	0.39	1.00	-0.03	0.00	1.25E-16	143287	-0.03	0.00	1.25E-16	143287	-0.03	0.00	1.25E-16	FUT9
79	rs6426301	1	72757853	FUT9	C	T	0.39	0.39	1.00	-0.03	0.00	1.25E-16	143287	-0.03	0.00	1.25E-16	143287	-0.03	0.00	1.25E-16	FUT9
80	rs6426301	1	72757853	FUT9	C	T	0.39	0.39	1.00	-0.03	0.00	1.25E-16	143287	-0.03	0.00	1.25E-16	143287	-0.03	0.00	1.25E-16	FUT9
81	rs6426301	1	72757853	FUT9	C	T	0.39	0.39	1.00	-0.03	0.00	1.25E-16	143287	-0.03	0.00	1.25E-16	143287	-0.03	0.00	1.25E-16	FUT9
82	rs6426301	1	72757853	FUT9	C	T	0.39	0.39	1.00	-0.03	0.00	1.25E-16	143287	-0.03	0.00	1.25E-16	143287	-0.03	0.00	1.25E-16	FUT9
83	rs6426301	1	72757853	FUT9	C	T	0.39	0.39	1.00	-0.03	0.00	1.25E-16	143287	-0.03	0.00	1.25E-16	143287	-0.03	0.00	1.25E-16	FUT9
84	rs6426301	1	72757853	FUT9	C	T	0.39	0.39	1.00	-0.03	0.00	1.25E-16	143287	-0.03	0.00	1.25E-16	143287	-0.03	0.00	1.25E-16	FUT9
85	rs6426301	1	72757853	FUT9	C	T	0.39	0.39	1.00	-0.03	0.00	1.25E-16	143287	-0.03	0.00	1.25E-16	143287	-0.03	0.00	1.25E-16	FUT9
86	rs6426301	1	72757853	FUT9	C	T	0.39	0.39	1.00	-0.03	0.00	1.25E-16	143287	-0.03	0.00	1.25E-16	143287	-0.03	0.00	1.25E-16	FUT9
87	rs6426301	1	72757853	FUT9	C	T	0.39	0.39	1.00	-0.03	0.00	1.25E-16	143287	-0.03	0.00	1.25E-16	143287	-0.03	0.00	1.25E-16	FUT9
88	rs6426301	1	72757853	FUT9	C	T	0.39	0.39	1.00	-0.03	0.00	1.25E-16	143287	-0.03	0.00	1.25E-16	143287	-0.03	0.00	1.25E-16	FUT9
89	rs6426301	1	72757853	FUT9	C	T	0.39	0.39	1.00	-0.03	0.00	1.25E-16	143287	-0.03	0.00	1.25E-16	143287	-0.03	0.00	1.25E-16	FUT9
90	rs6426301	1	72757853	FUT9	C	T	0.39	0.39	1.00	-0.03	0.00	1.25E-16	143287	-0.03	0.00	1.25E-16	143287	-0.03	0.00	1.25E-16	FUT9
91	rs6426301	1	72757853	FUT9	C	T	0.39	0.39	1.00	-0.03	0.00	1.25E-16	143287	-0.03	0.00	1.25E-16	143287	-0.03	0.00	1.25E-16	FUT9
92	rs6426301	1	72757853	FUT9	C	T	0.39	0.39	1.00	-0.03	0.00	1.25E-16	143287	-0.03	0.00	1.25E-16	143287	-0.03	0.00	1.25E-16	FUT9
93	rs6426301	1	72757853	FUT9	C	T	0.39	0.39	1.00	-0.03	0.00	1.25E-16	143287	-0.03	0.00	1.25E-16	143287	-0.03	0.00	1.25E-16	FUT9
94	rs6426301	1	72757853	FUT9	C	T	0.39	0.39	1.00	-0.03	0.00	1.25E-16	143287	-0.03	0.00	1.25E-16	143287	-0.03	0.00	1.25E-16	FUT9
95	rs6426301	1	72757853	FUT9	C	T	0.39	0.39	1.00	-0.03	0.00	1.25E-16	143287	-0.03	0.00	1.25E-16	143287	-0.03	0.00	1.25E-16	FUT9
96	rs6426301	1	72757853	FUT9	C	T	0.39	0.39	1.00	-0.03	0.00	1.25E-16	143287	-0.03	0.00	1.25E-16	143287	-0.03	0.00	1.25E-16	FUT9
97	rs6426301	1	72757853	FUT9	C	T	0.39	0.39	1.00	-0.03	0.00	1.25E-16	143287	-0.03	0.00	1.25E-16	143287	-0.03	0.00	1.25E-16	FUT9
98	rs6426301	1	72757853	FUT9	C	T	0.39	0.39	1.00	-0.03	0.00	1.25E-16	143287	-0.03	0.00	1.25E-16	143287	-0.03	0.00	1.25E-16	FUT9
99	rs6426301	1	72757853	FUT9	C	T	0.39	0.39	1.00	-0.03	0.00	1.25E-16	143287	-0.03	0.00	1.25E-16	143287	-0.03	0.00	1.25E-16	FUT9
100	rs6426301	1	72757853	FUT9	C	T	0.39	0.39	1.00	-0.03	0.00	1.25E-16	143287	-0.03	0.00	1.25E-16	143287	-0.03	0.00	1.25E-16	FUT9

INDEX Unique index assigned to each conditionally independent eGWAS associated variant. * denotes that the results reported for this variant are derived from analysis of males only (i.e. SNPIC 3
CHR Chromosome
BP Base pair position of the variant according to human reference sequence (GRCh37), Hg2
C.GENO Closest gene to reported variant
OTHER Other base pair between conditionally independent eGWAS associated variant and the closest gn
EA Effect allele
MAF Minor allele frequency
INFO Imputed information score
β Per allele effect in standard deviations of rank-based inverse normally transformed eBDI
SE Standard error of the β
P Strength of evidence against the null hypothesis of no association between variant and eBMD (i.e. P-valu
N Sample size
EAF.J Frequency of the effect allele in the reference sample used for conditional and joint genome-wide association analy
OBS.J Number of observations of each variant in reference dataset used for conditional and joint genome-wide association analysis
B.J Per allele effect size estimate from joint and joint conditional) associated snps in standard deviations of rank-based inverse-normally transformed eBI
SE.J Standard error of β.J
P.J Strength of evidence against the null hypothesis of no association between the variant and eBDI as estimated by conditional and joint genome-wide association analysis. (i.e. P-v
N.J Estimated effective sample size
LOCUS NAME Locus name as per NCBI and SNP+/-1
β.W Per allele effect in standard deviations of rank-based inverse normally transformed eBMD adjusted for weig
SE.W Standard error of the β.W
P.W Strength of evidence against the null hypothesis of no association between variant and eBMD adjusted for weight (i.e. P-valu

Each locus was annotated using the gene contained within the closest gene region identified by DEPICT analysis. In situations where multiple genes were present in a single DEPICT region, priority was given to the gene that displayed a bone phenotype in the corresponding knockout mouse model, followed by the gene expressed in the most murine bone cell types (OsX>O), followed by the gene with the lowest DEPICT P value. * denotes multiple conditionally independent variants present at the locus and ** denotes the closest gene to the locus (i.e. no region detected through DEPICT that lies within 1Mb).

Supplementary Table 6. Results of the test for sex heterogeneity at 307 genome-wide significant SNPs.

SNP_ID	CHROM	LOWER POSITION	UPPER POSITION	RSID	ANCESTRAL ALLELE	DERIVED ALLELE	GENE	DISTANCE	TYPE	SNP_ID	CHROM	POSITION	RSID	ANCESTRAL ALLELE	DERIVED ALLELE	GENE	DISTANCE	TYPE	SNP_ID	CHROM	POSITION	RSID	ANCESTRAL ALLELE	DERIVED ALLELE	GENE	DISTANCE	TYPE
1	1	1868233	1868233	rs1189326	C	T	LEPR	0	intron	1	1	1868233	rs1189326	C	T	LEPR	0	intron	1	1	1868233	rs1189326	C	T	LEPR	0	intron
2	1	19868609	19868609	rs6677604	G	A	CR1	0	intron	2	1	19868609	rs6677604	G	A	CR1	0	intron	2	1	19868609	rs6677604	G	A	CR1	0	intron
3	1	19868609	19868609	rs6691369	T	C	CR1	0	intron	3	1	19868609	rs6691369	T	C	CR1	0	intron	3	1	19868609	rs6691369	T	C	CR1	0	intron
4	1	19868609	19868609	rs6691377	T	C	CR1	0	intron	4	1	19868609	rs6691377	T	C	CR1	0	intron	4	1	19868609	rs6691377	T	C	CR1	0	intron
5	1	19868609	19868609	rs6691378	T	C	CR1	0	intron	5	1	19868609	rs6691378	T	C	CR1	0	intron	5	1	19868609	rs6691378	T	C	CR1	0	intron
6	1	19868609	19868609	rs6691379	T	C	CR1	0	intron	6	1	19868609	rs6691379	T	C	CR1	0	intron	6	1	19868609	rs6691379	T	C	CR1	0	intron
7	1	19868609	19868609	rs6691380	T	C	CR1	0	intron	7	1	19868609	rs6691380	T	C	CR1	0	intron	7	1	19868609	rs6691380	T	C	CR1	0	intron
8	1	19868609	19868609	rs6691381	T	C	CR1	0	intron	8	1	19868609	rs6691381	T	C	CR1	0	intron	8	1	19868609	rs6691381	T	C	CR1	0	intron
9	1	19868609	19868609	rs6691382	T	C	CR1	0	intron	9	1	19868609	rs6691382	T	C	CR1	0	intron	9	1	19868609	rs6691382	T	C	CR1	0	intron
10	1	19868609	19868609	rs6691383	T	C	CR1	0	intron	10	1	19868609	rs6691383	T	C	CR1	0	intron	10	1	19868609	rs6691383	T	C	CR1	0	intron
11	1	19868609	19868609	rs6691384	T	C	CR1	0	intron	11	1	19868609	rs6691384	T	C	CR1	0	intron	11	1	19868609	rs6691384	T	C	CR1	0	intron
12	1	19868609	19868609	rs6691385	T	C	CR1	0	intron	12	1	19868609	rs6691385	T	C	CR1	0	intron	12	1	19868609	rs6691385	T	C	CR1	0	intron
13	1	19868609	19868609	rs6691386	T	C	CR1	0	intron	13	1	19868609	rs6691386	T	C	CR1	0	intron	13	1	19868609	rs6691386	T	C	CR1	0	intron
14	1	19868609	19868609	rs6691387	T	C	CR1	0	intron	14	1	19868609	rs6691387	T	C	CR1	0	intron	14	1	19868609	rs6691387	T	C	CR1	0	intron
15	1	19868609	19868609	rs6691388	T	C	CR1	0	intron	15	1	19868609	rs6691388	T	C	CR1	0	intron	15	1	19868609	rs6691388	T	C	CR1	0	intron
16	1	19868609	19868609	rs6691389	T	C	CR1	0	intron	16	1	19868609	rs6691389	T	C	CR1	0	intron	16	1	19868609	rs6691389	T	C	CR1	0	intron
17	1	19868609	19868609	rs6691390	T	C	CR1	0	intron	17	1	19868609	rs6691390	T	C	CR1	0	intron	17	1	19868609	rs6691390	T	C	CR1	0	intron
18	1	19868609	19868609	rs6691391	T	C	CR1	0	intron	18	1	19868609	rs6691391	T	C	CR1	0	intron	18	1	19868609	rs6691391	T	C	CR1	0	intron
19	1	19868609	19868609	rs6691392	T	C	CR1	0	intron	19	1	19868609	rs6691392	T	C	CR1	0	intron	19	1	19868609	rs6691392	T	C	CR1	0	intron
20	1	19868609	19868609	rs6691393	T	C	CR1	0	intron	20	1	19868609	rs6691393	T	C	CR1	0	intron	20	1	19868609	rs6691393	T	C	CR1	0	intron
21	1	19868609	19868609	rs6691394	T	C	CR1	0	intron	21	1	19868609	rs6691394	T	C	CR1	0	intron	21	1	19868609	rs6691394	T	C	CR1	0	intron
22	1	19868609	19868609	rs6691395	T	C	CR1	0	intron	22	1	19868609	rs6691395	T	C	CR1	0	intron	22	1	19868609	rs6691395	T	C	CR1	0	intron
23	1	19868609	19868609	rs6691396	T	C	CR1	0	intron	23	1	19868609	rs6691396	T	C	CR1	0	intron	23	1	19868609	rs6691396	T	C	CR1	0	intron
24	1	19868609	19868609	rs6691397	T	C	CR1	0	intron	24	1	19868609	rs6691397	T	C	CR1	0	intron	24	1	19868609	rs6691397	T	C	CR1	0	intron
25	1	19868609	19868609	rs6691398	T	C	CR1	0	intron	25	1	19868609	rs6691398	T	C	CR1	0	intron	25	1	19868609	rs6691398	T	C	CR1	0	intron
26	1	19868609	19868609	rs6691399	T	C	CR1	0	intron	26	1	19868609	rs6691399	T	C	CR1	0	intron	26	1	19868609	rs6691399	T	C	CR1	0	intron
27	1	19868609	19868609	rs6691400	T	C	CR1	0	intron	27	1	19868609	rs6691400	T	C	CR1	0	intron	27	1	19868609	rs6691400	T	C	CR1	0	intron
28	1	19868609	19868609	rs6691401	T	C	CR1	0	intron	28	1	19868609	rs6691401	T	C	CR1	0	intron	28	1	19868609	rs6691401	T	C	CR1	0	intron
29	1	19868609	19868609	rs6691402	T	C	CR1	0	intron	29	1	19868609	rs6691402	T	C	CR1	0	intron	29	1	19868609	rs6691402	T	C	CR1	0	intron
30	1	19868609	19868609	rs6691403	T	C	CR1	0	intron	30	1	19868609	rs6691403	T	C	CR1	0	intron	30	1	19868609	rs6691403	T	C	CR1	0	intron
31	1	19868609	19868609	rs6691404	T	C	CR1	0	intron	31	1	19868609	rs6691404	T	C	CR1	0	intron	31	1	19868609	rs6691404	T	C	CR1	0	intron
32	1	19868609	19868609	rs6691405	T	C	CR1	0	intron	32	1	19868609	rs6691405	T	C	CR1	0	intron	32	1	19868609	rs6691405	T	C	CR1	0	intron
33	1	19868609	19868609	rs6691406	T	C	CR1	0	intron	33	1	19868609	rs6691406	T	C	CR1	0	intron	33	1	19868609	rs6691406	T	C	CR1	0	intron
34	1	19868609	19868609	rs6691407	T	C	CR1	0	intron	34	1	19868609	rs6691407	T	C	CR1	0	intron	34	1	19868609	rs6691407	T	C	CR1	0	intron
35	1	19868609	19868609	rs6691408	T	C	CR1	0	intron	35	1	19868609	rs6691408	T	C	CR1	0	intron	35	1	19868609	rs6691408	T	C	CR1	0	intron
36	1	19868609	19868609	rs6691409	T	C	CR1	0	intron	36	1	19868609	rs6691409	T	C	CR1	0	intron	36	1	19868609	rs6691409	T	C	CR1	0	intron
37	1	19868609	19868609	rs6691410	T	C	CR1	0	intron	37	1	19868609	rs6691410	T	C	CR1	0	intron	37	1	19868609	rs6691410	T	C	CR1	0	intron
38	1	19868609	19868609	rs6691411	T	C	CR1	0	intron	38	1	19868609	rs6691411	T	C	CR1	0	intron	38	1	19868609	rs6691411	T	C	CR1	0	intron
39	1	19868609	19868609	rs6691412	T	C	CR1	0	intron	39	1	19868609	rs6691412	T	C	CR1	0	intron	39	1	19868609	rs6691412	T	C	CR1	0	intron
40	1	19868609	19868609	rs6691413	T	C	CR1	0	intron	40	1	19868609	rs6691413	T	C	CR1	0	intron	40	1	19868609	rs6691413	T	C	CR1	0	intron
41	1	19868609	19868609	rs6691414	T	C	CR1	0	intron	41	1	19868609	rs6691414	T	C	CR1	0	intron	41	1	19868609	rs6691414	T	C	CR1	0	intron
42	1	19868609	19868609	rs6691415	T	C	CR1	0	intron	42	1	19868609	rs6691415	T	C	CR1	0	intron	42	1	19868609	rs6691415	T	C	CR1	0	intron
43	1	19868609	19868609	rs6691416	T	C	CR1	0	intron	43	1	19868609	rs6691416	T	C	CR1	0	intron	43	1	19868609	rs6691416	T	C	CR1	0	intron
44	1	19868609	19868609	rs6691417	T	C	CR1	0	intron	44	1	19868609	rs6691417	T	C	CR1	0	intron	44	1	19868609	rs6691417	T	C	CR1	0	intron
45	1	19868609	19868609	rs6691418	T	C	CR1	0	intron	45	1	19868609	rs6691418	T	C	CR1	0	intron	45	1	19868609	rs6691418	T	C	CR1	0	intron
46	1	19868609	19868609	rs6691419	T	C	CR1	0	intron	46	1	19868609	rs6691419	T	C	CR1	0	intron	46	1	19868609	rs6691419	T	C	CR1	0	intron
47	1	19868609	19868609	rs6691420	T	C	CR1	0	intron	47	1	19868609	rs6691420	T	C	CR1	0	intron	47	1	19868609	rs6691420	T	C	CR1	0	intron
48	1	19868609	19868609	rs6691421	T	C	CR1	0	intron	48	1	19868609	rs6691421	T	C	CR1	0	intron	48	1	19868609	rs6691421	T	C	CR1	0	intron
49	1	19868609	19868609	rs6691422	T	C	CR1	0	intron	49	1	19868609	rs6691422	T	C	CR1	0	intron	49	1	19868609	rs6691422	T	C	CR1	0	intron
50	1	19868609	19868609	rs6691423	T	C	CR1	0	intron	50	1	19868609	rs6691423	T	C	CR1	0	intron	50	1	19868609	rs6691423	T	C	CR1	0	intron
51	1	19868609	19868609	rs6691424	T	C	CR1	0	intron	51	1	19868609	rs6691424	T	C	CR1	0	intron	51	1	19868609	rs6691424	T	C	CR1	0	intron
52	1	19868609	19868609	rs6691425	T	C	CR1	0	intron	52	1	19868609	rs6691425	T	C	CR1	0	intron	52	1	19868609	rs6691425	T	C	CR1	0	intron
53	1	19868609	19868609	rs6691426	T	C	CR1	0	intron	53	1	19868609	rs6691426	T	C	CR1	0	intron	53	1	19868609	rs6691426	T	C	CR1	0	intron
54	1	19868609	19868609	rs6691427	T	C	CR1	0	intron	54	1	19868609	rs6691427	T	C	CR1	0	intron	54	1	19868609	rs6691427	T	C	CR1	0	intron
55	1	19868609	19868609	rs6691428	T	C	CR1	0	intron	55	1	19868609	rs6691428	T	C	CR1	0	intron	55	1	19868609	rs6691428	T	C	CR1	0	intron
56	1	19868609	19868609	rs6691429	T	C	CR1	0	intron	56	1	19868609	rs6691429	T	C	CR1	0	intron	56	1	19868609	rs6691429	T	C	CR1	0	intron
57	1	19868609	19868609	rs6691430	T	C	CR1	0	intron	57	1	19868609	rs6691430	T	C	CR1	0	intron	57	1	19868609	rs6691430	T	C	CR1	0	intron
58	1	19868609	19868609	rs6691431	T	C	CR1	0	intron	58	1	19868609	rs6691431	T	C	CR1	0	intron	58	1	19868609	rs6691431	T	C	CR1	0	intron
59	1	19868609	19868609	rs6691432	T	C	CR1	0	intron	59	1	19868609	rs6691432	T	C	CR1	0	intron	59	1	19868609	rs6691432	T	C	CR1	0	intron
60	1	19868609	19868609	rs6691433	T	C	CR1	0	intron	60	1	19868609	rs6691433	T	C	CR1	0	intron	60	1	19868609	rs6691433	T	C	CR1	0	intron
61	1	19868609	19868609	rs6691434	T	C	CR1	0	intron	61	1	19868609	rs6691434	T	C	CR1	0	intron	61	1	19868609	rs6691434	T	C	CR1	0	intron
62	1	19868609	19868609	rs6691435	T	C	CR1	0	intron	62	1	19868609	rs6691435	T	C	CR1	0	intron	62	1	19868609	rs6691435	T	C	CR1	0	intron
63	1	19868609	19868609	rs6691436	T	C	CR1	0	intron	63	1	19868609	rs6691436	T	C	CR1	0	intron	63	1	19868609	rs6691436	T	C	CR1	0	intron
64	1	19868609	19868609	rs6691437	T	C	CR1	0	intron	64	1	19868609	rs6691437	T	C	CR1	0	intron	64	1	19868609	rs6691437	T	C	CR1	0	intron
65	1	19868609	19868609	rs6691438	T	C	CR1	0	intron	65	1	19868609	rs6691438	T	C	CR1	0	intron	65	1	19868609	rs6691438	T	C	CR1	0	intron
66	1	19868609	19868609	rs6691439	T	C	CR1	0	intron	66	1	19868609	rs6691439	T	C	CR1	0	intron	66	1	19868609	rs6691439	T	C	CR1	0	intron
67	1	19868609	19868609	rs6691440	T	C	CR1	0	intron	67	1	19868609	rs6691440	T	C	CR1	0	intron	67	1	19868609	rs6691440	T	C	CR1	0	intron
68	1	19868609	19868609	rs6691441	T	C	CR1	0	intron	68	1	19868609	rs6691441	T	C	CR1	0	intron	68	1	19868609	rs6691441	T	C	CR1	0	intron
69	1	19868609	19868609	rs6691442	T	C	CR1	0	intron	69	1	19868609	rs6691442	T	C	CR1	0	intron	69	1	19868609	rs6691442	T	C	CR1	0	intron
70	1	19868609	19868609	rs6691443	T	C	CR1	0	intron	70	1	19868609	rs6691443	T	C	CR1	0	intron	70	1	19868609	rs6691443	T	C	CR1	0	intron
71	1	19868609	19868609	rs6691444	T	C	CR1	0	intron	71	1	19868609	rs6691444	T	C	CR1	0	intron	71	1	19868609	rs6691444	T	C	CR1	0	intron
72	1	19868609	19868609	rs6691445	T	C	CR1	0	intron	72	1	19868609	rs6691445	T	C	CR1	0	intron	72	1	19868609	rs6691445	T	C	CR1	0	intron
73	1	19868609	19868609	rs6691446	T	C	CR1	0	intron	73	1	19868609	rs6691446	T	C	CR1	0	intron	73	1	19868609	rs6691446	T	C	CR1	0	intron
74	1	19868609	19868609	rs6691447	T	C	CR1	0	intron	74	1	19868609	rs6691447	T	C	CR1	0	intron	74	1	19868609	rs6691447	T	C	CR1	0	intron
75	1	19868609	19868609	rs6691448	T	C	CR1	0	intron	75	1	19868609	rs6691448	T	C	CR1	0	intron	75	1	19868609	rs6691448	T	C	CR1	0	intron
76	1	19868609	19868609	rs6691449	T	C	CR1	0	intron	76	1	19868609	rs6691449	T	C	CR1	0	intron	76	1	19868609	rs6691449	T	C	CR1	0	intron
77	1	19868609	19868609	rs6691450	T	C	CR1	0	intron	77	1	19868609	rs6691450	T	C	CR1	0	intron	77	1	19868609	rs6691450	T	C	CR1	0	intron
78	1	19868609	19868609	rs6691451	T	C	CR1	0	intron	78	1	19868609	rs6691451	T	C	CR1	0	intron	78	1	19868609	rs6691451	T	C	CR1	0	intron
79	1	19868609	19868609	rs6691452	T	C	CR1	0	intron	79	1	19868609	rs6691452	T	C	CR1	0	intron	79	1	19868609	rs6691452	T	C	CR1	0	intron
80	1	19868609	19868609	rs6691453	T	C	CR1	0	intron	80	1	19868609	rs6691453	T	C	CR1	0	intron	80	1	19868609	rs6691453	T	C	CR1	0	intron
81	1	19868609	19868609	rs6691454	T	C	CR1	0	intron	81	1	19868609	rs6691454	T	C	CR1	0	intron	81	1	19868609	rs6691454	T	C	CR1	0	intron
82	1	19868609	19868609	rs6691455	T	C	CR1	0	intron	82	1	19868609	rs6691455	T	C	CR1	0	intron	82	1	19868609	rs6691455	T	C	CR1	0	intron
83	1	19868609	19868609	rs6691456	T	C	CR1	0	intron	83	1	19868609	rs6691456	T	C	CR1	0	intron	83	1	19868609	rs6691456	T	C	CR1	0	intron
84	1	19868609	19868609	rs6691457	T	C	CR1	0	intron	84	1	19868609	rs6691457	T	C	CR1	0	intron	84	1	19868609	rs6691457	T	C	CR1	0	intron
85	1	19868609	19868609	rs6691458	T	C	CR1	0	intron	85	1	19868609	rs6691458	T	C	CR1	0	intron	85	1	19868609	rs6691458	T	C	CR1	0	intron
86	1	19868609	19868609	rs6691459	T	C	CR1	0	intron	86	1	19868609	rs6691459	T	C	CR1	0	intron	86	1	19868609	rs6691459	T	C	CR1	0	intron
87	1	19868609	19868609	rs6691460	T	C	CR1	0	intron	87	1	19868609	rs6691460	T	C	CR1	0	intron	87	1	19868609	rs6691460	T	C	CR1	0	intron
88	1	19868609	19868609	rs6691461	T	C	CR1	0	intron	88	1	19868609	rs6691461	T	C	CR1	0	intron	88	1	19868609	rs6691461	T	C	CR1	0	intron
89	1	19868609	19868609	rs6691462	T	C	CR1	0	intron	89	1	19868609	rs6691462	T	C	CR1	0	intron	89	1	19868609	rs6691462	T	C	CR1	0	intron
90	1	19868609	19868609	rs6691463	T	C	CR1	0	intron	90	1	19868609	rs6691463	T	C	CR1	0	intron	90	1	19868609	rs6691463	T	C	CR1	0	intron
91	1	19868609	19868609	rs6691464	T	C	CR1	0	intron	91	1	19868609	rs6691464	T	C	CR1	0	intron	91	1	19868609	rs6691464	T	C	CR1	0	intron
92	1	19868609	19868609	rs6691465	T	C	CR1	0	intron	92	1	19868609	rs6691465	T	C	CR1	0	intron	92	1	19868609	rs6691465	T	C	CR1	0	intron
93	1	19868609	19868609	rs6691466	T	C	CR1	0	intron	93	1	19868609	rs6691466	T	C	CR1	0	intron	93	1	19868609	rs6691466	T	C	CR1	0	intron
94	1	19868609	19868609	rs6691467	T	C	CR1	0	intron	94	1	19868609	rs6691467	T	C	CR1	0	intron	94	1	19868609	rs6691467	T	C	CR1	0	intron
95	1	19868609	19868609	rs6691468	T	C	CR1	0	intron	95	1	19868609	rs6691468	T	C	CR1	0	intron	95	1	19868609	rs6691468	T	C	CR1	0	intron
96	1	19868609	19868609	rs6691469	T	C	CR1	0	intron	96	1	19868609	rs6691469	T	C	CR1	0	intron	96	1	19868609	rs6691469	T	C	CR1	0	intron
97	1	19868609	19868609	rs6691470	T	C	CR1	0	intron	97	1	19868609	rs6691470	T	C	CR1	0	intron	97	1	19868609	rs6691470	T	C	CR1	0	intron
98	1	19868609	19868609	rs6691471	T	C	CR1	0	intron	98	1	19868609	rs6691471	T	C	CR1	0	intron	98	1	19868609	rs6691471	T	C	CR1	0	intron
99	1	19868609	19868609	rs6691472	T	C	CR1	0	intron	99	1	19868609	rs6691472	T	C	CR1	0	intron	99	1	19868609	rs6691472	T	C	CR1	0	intron
100	1	19868609	19868609	rs6691473	T	C	CR1	0	intron	100	1	19868609	rs6691473	T	C	CR1	0	intron	100	1	19868609	rs6691473	T	C	CR1	0	intron

HSID1 Unique index assigned to each conditionally independent rsRNS3 association variant. * denotes that the results reported for this variant are derived from analyses of males only (i.e. rsRNS 39)
RNPID Unique variant identifier denoted by chromosome position effect allele non-effect allele, used to differentiate multi-allelic variants that have the same rsid and share the same pp
CHR Chromosome
POS Base pair position of the variant according to human reference sequence (GRCh37), hg19
C.I.95/95 Closest gene to reported variant
CLOST Distance in base pairs between conditionally independent rsRNS associated variant and the closest gen
TYPE Variant type
NEA Non-effect allele
EAF Effect allele frequency
MAF Minor allele frequency
INFO Imputation information
BETA Effect size estimate (standard deviations of rank-based inverse normally transformed rsRNS
SE Standard error of Beta
P Strength of evidence against the null hypothesis of no association between variant and rsRNS (i.e. P-value
N Sample size
Pcov.int Strength of evidence against the null hypothesis of no sex heterogeneity in rsRNS regression coefficients (i.e. P-value
LOCUS_ID Each locus was annotated using the gene contained within the closest gene region identified by GWTCT analysis. In situations where multiple genes were present in a single GWTCT region, priority was given to the gene that displayed a bone phenotype in the corresponding knockout mouse model, followed by the gene expressed in the most murine bone cell types (GWTCT), followed by the gene with the lowest GWTCT P value. * denotes multiple conditionally independent variants present at the locus and ~ denotes the closest gene to the locus (i.e. no region detected through GWTCT that lies within 1Mb)

Supplementary Table 7. Genetic correlation analyses using LD Hub.

					ANMD				ANY FRACTURE				HALL FRACTURE			
TRAIT	CONSORTIUM/AUTHOR	N	PMID	YEAR	rg	SE	Z	P	rg	SE	Z	P	rg	SE	Z	P
Total cholesterol	GLGC	99900	20686565	2010	0.038	0.029	-0.71	7.05E-03	0.11	0.060	1.68	9.40E-02	0.08	0.075	0.99	3.22E-01
HDL cholesterol	GLGC	100184	20686565	2010	-0.13	0.032	-3.37	1.00E-03	0.09	0.063	1.47	1.41E-01	0.10	0.073	1.46	1.52E-01
LDL cholesterol	GLGC	95454	20686565	2010	0.09	0.033	-2.60	9.05E-03	0.11	0.076	1.53	1.34E-01	0.13	0.094	1.50	1.34E-01
Triglycerides	GLGC	96598	20686565	2010	0.05	0.043	1.23	2.19E-01	-0.02	0.051	-0.46	6.44E-01	-0.09	0.065	-1.37	1.71E-01
Insulin-like growth factor 1	CHARGE consortium (CHARGE+)	17535	27329300	2016	0.06	0.045	1.37	1.71E-01	-0.15	0.108	-2.33	2.00E-02	-0.14	0.121	-1.16	2.47E-01
Insulin like growth factor binding protein 3	CHARGE consortium (CHARGE+)	18995	27329300	2016	0.01	0.047	0.29	7.74E-01	-0.15	0.129	-1.90	5.80E-02	-0.19	0.130	-1.42	1.56E-01
Leptin adjusted for body mass index	Kilpeläinen	32161	26833966	2016	0.06	0.059	0.97	3.33E-01	0.17	0.125	1.35	1.79E-01	0.24	0.131	1.80	7.20E-02
Leptin	Kilpeläinen	32161	26833966	2016	0.10	0.051	1.90	5.75E-02	0.07	0.106	0.65	5.15E-01	0.17	0.119	1.41	1.59E-01
Mean diameter for VLDL particles	MAGNETIC	19273	27555778	2016	0.05	0.050	1.01	3.11E-01	0.07	0.122	0.55	5.81E-01	0.05	0.140	0.39	6.98E-01
Mean diameter for LDL particles	MAGNETIC	19273	27555778	2016	0.03	0.050	0.59	5.53E-01	0.08	0.134	0.57	5.68E-01	0.10	0.149	0.67	5.05E-01
Mean diameter for HDL particles	MAGNETIC	19273	27555778	2016	0.07	0.050	-1.31	1.91E-01	0.12	0.129	0.93	3.53E-01	0.06	0.142	-0.39	6.96E-01
Concentration of chylomicrons and largest VLDL particles	MAGNETIC	18993	27555778	2016	0.04	0.062	0.72	4.73E-01	0.12	0.159	0.86	3.90E-01	0.13	0.158	0.80	4.22E-01
Concentration of very large VLDL particles	MAGNETIC	18968	27555778	2016	0.04	0.054	0.77	4.41E-01	0.16	0.127	0.77	4.39E-01	0.08	0.151	0.53	5.96E-01
Concentration of large VLDL particles	MAGNETIC	18993	27555778	2016	0.04	0.045	0.81	4.18E-01	0.00	0.121	-0.03	9.78E-01	-0.01	0.138	-0.08	9.35E-01
Concentration of medium VLDL particles	MAGNETIC	19273	27555778	2016	0.03	0.048	0.63	5.49E-01	0.09	0.125	0.68	4.94E-01	0.12	0.140	0.83	4.08E-01
Concentration of small VLDL particles	MAGNETIC	19273	27555778	2016	0.05	0.051	-1.02	3.06E-01	0.15	0.127	1.23	2.18E-01	0.09	0.145	0.57	5.65E-01
Concentration of very small VLDL particles	MAGNETIC	19273	27555778	2016	-0.07	0.061	-1.22	2.23E-01	0.14	0.157	0.93	3.66E-01	0.12	0.179	0.69	4.88E-01
Concentration of large LDL particles	MAGNETIC	19273	27555778	2016	0.13	0.068	-1.84	6.65E-02	0.20	0.166	1.32	1.88E-01	0.23	0.190	1.22	2.22E-01
Concentration of medium LDL particles	MAGNETIC	19273	27555778	2016	0.11	0.063	-1.69	9.20E-02	0.16	0.158	0.98	3.26E-01	0.23	0.181	1.27	2.06E-01
Concentration of small LDL particles	MAGNETIC	19273	27555778	2016	0.12	0.065	-1.74	8.20E-02	0.25	0.165	1.53	1.26E-01	0.24	0.191	1.28	2.02E-01
Concentration of IDL particles	MAGNETIC	19273	27555778	2016	-0.10	0.069	-1.47	1.43E-01	0.20	0.163	1.25	2.11E-01	0.13	0.188	0.71	4.78E-01
Concentration of very large HDL particles	MAGNETIC	19273	27555778	2016	0.10	0.065	-1.57	1.16E-01	-0.14	0.151	-0.91	3.63E-01	0.03	0.159	-0.21	8.35E-01
Concentration of large HDL particles	MAGNETIC	19273	27555778	2016	-0.07	0.059	-1.21	2.28E-01	-0.06	0.125	-0.50	6.18E-01	0.04	0.143	0.27	7.89E-01
Concentration of medium HDL particles	MAGNETIC	19273	27555778	2016	-0.02	0.058	-0.23	8.18E-01	0.21	0.143	1.50	1.34E-01	0.15	0.168	0.87	3.85E-01
Concentration of small HDL particles	MAGNETIC	19282	27555778	2016	-	-	-	-	-	-	-	-	-	-	-	-
Total lipids in chylomicrons and largest VLDL particles	MAGNETIC	18993	27555778	2016	0.06	0.058	1.02	3.10E-01	0.00	0.127	-0.02	9.85E-01	0.05	0.145	0.35	7.26E-01
Total lipids in very large VLDL	MAGNETIC	19273	27555778	2016	0.06	0.051	1.18	2.40E-01	-0.02	0.119	-0.17	8.65E-01	0.04	0.135	0.29	7.66E-01
Total lipids in large VLDL	MAGNETIC	18968	27555778	2016	0.12	0.068	-1.76	8.10E-02	0.22	0.167	1.33	1.85E-01	0.23	0.191	1.19	2.34E-01
Total lipids in medium VLDL	MAGNETIC	19273	27555778	2016	0.02	0.051	0.29	7.71E-01	0.10	0.133	0.76	4.47E-01	0.05	0.152	0.30	7.65E-01
Total lipids in small VLDL	MAGNETIC	19273	27555778	2016	0.08	0.053	-1.50	1.34E-01	0.16	0.137	1.18	2.40E-01	0.08	0.162	0.46	6.51E-01
Total lipids in very small VLDL	MAGNETIC	19273	27555778	2016	-0.07	0.053	-1.23	2.19E-01	0.10	0.141	0.74	4.61E-01	0.11	0.161	0.70	4.82E-01
Total lipids in large LDL	MAGNETIC	19273	27555778	2016	0.05	0.054	-0.98	3.82E-01	0.14	0.134	1.11	2.66E-01	0.02	0.135	0.13	8.93E-01
Total lipids in medium LDL	MAGNETIC	19273	27555778	2016	-0.12	0.066	-1.80	7.10E-02	0.23	0.164	1.38	1.67E-01	0.23	0.187	1.25	2.13E-01
Total lipids in small LDL	MAGNETIC	19273	27555778	2016	0.01	0.064	0.17	8.65E-01	0.22	0.178	1.23	2.18E-01	0.09	0.197	0.46	6.45E-01
Total lipids in IDL	MAGNETIC	19273	27555778	2016	-0.11	0.067	-1.62	1.05E-01	0.20	0.165	1.68	2.81E-01	0.22	0.191	1.24	2.02E-01
Total lipids in very large HDL	MAGNETIC	19273	27555778	2016	-0.15	0.064	-1.78	7.65E-02	-0.18	0.194	-0.91	3.61E-01	0.03	0.195	0.16	8.73E-01
Total lipids in large HDL	MAGNETIC	19273	27555778	2016	-0.08	0.060	-1.29	1.96E-01	0.15	0.140	1.04	2.96E-01	0.16	0.167	0.92	3.55E-01
Total lipids in medium HDL	MAGNETIC	19273	27555778	2016	-0.03	0.058	-0.48	6.29E-01	0.12	0.142	0.82	4.09E-01	0.14	0.167	0.82	4.09E-01
Total lipids in small HDL	MAGNETIC	19273	27555778	2016	-0.03	0.073	0.40	6.91E-01	0.23	0.154	1.52	1.28E-01	0.14	0.181	0.76	4.46E-01
Phospholipids in small HDL	MAGNETIC	18965	27555778	2016	-	-	-	-	-	-	-	-	-	-	-	-
Phospholipids in serum	MAGNETIC	20697	27555778	2016	-	-	-	-	-	-	-	-	-	-	-	-
Triglycerides in chylomicrons and largest VLDL particles	MAGNETIC	21546	27555778	2016	0.04	0.060	0.69	4.89E-01	0.05	0.139	0.46	6.44E-01	0.10	0.163	0.60	5.48E-01
Triglycerides in very large VLDL	MAGNETIC	21548	27555778	2016	0.04	0.050	0.87	3.84E-01	0.03	0.118	0.24	8.14E-01	0.02	0.136	0.16	8.73E-01
Triglycerides in large VLDL	MAGNETIC	21239	27555778	2016	0.03	0.049	0.62	5.39E-01	0.05	0.122	0.44	6.57E-01	0.01	0.143	0.04	9.20E-01
Triglycerides in medium VLDL	MAGNETIC	21241	27555778	2016	0.05	0.048	0.97	3.31E-01	0.03	0.119	0.25	8.01E-01	0.03	0.136	0.19	8.47E-01
Triglycerides in small VLDL	MAGNETIC	21558	27555778	2016	0.05	0.049	-1.11	2.65E-01	0.12	0.125	0.97	3.33E-01	0.04	0.150	0.27	7.88E-01
Triglycerides in very small VLDL	MAGNETIC	19273	27555778	2016	-0.03	0.049	-0.57	5.68E-01	0.13	0.128	1.02	3.08E-01	0.12	0.147	0.83	4.08E-01
Triglycerides in large LDL	MAGNETIC	20898	27555778	2016	-	-	-	-	-	-	-	-	-	-	-	-
Triglycerides in medium LDL	MAGNETIC	13524	27555778	2016	-	-	-	-	-	-	-	-	-	-	-	-
Triglycerides in small LDL	MAGNETIC	13171	27555778	2016	-	-	-	-	-	-	-	-	-	-	-	-
Triglycerides in IDL	MAGNETIC	19273	27555778	2016	-0.07	0.054	-1.29	1.96E-01	0.15	0.140	1.04	2.99E-01	0.15	0.162	0.92	3.56E-01
Triglycerides in very large HDL	MAGNETIC	21536	27555778	2016	-0.06	0.058	-1.09	2.75E-01	0.06	0.151	0.43	6.63E-01	0.14	0.167	0.85	3.97E-01
Triglycerides in large HDL	MAGNETIC	13532	27555778	2016	-	-	-	-	-	-	-	-	-	-	-	-
Triglycerides in medium HDL	MAGNETIC	24778	27555778	2016	-	-	-	-	-	-	-	-	-	-	-	-
Triglycerides in small HDL	MAGNETIC	21558	27555778	2016	-0.01	0.049	-0.13	8.98E-01	0.15	0.125	1.18	2.37E-01	0.13	0.145	0.90	3.70E-01
Triglycerides in serum	MAGNETIC	21545	27555778	2016	-0.01	0.051	-0.27	7.90E-01	0.15	0.127	1.16	2.44E-01	0.10	0.147	0.69	4.91E-01
Total cholesterol in chylomicrons and largest VLDL particles	MAGNETIC	24810	27555778	2016	-	-	-	-	-	-	-	-	-	-	-	-
Total cholesterol in very large VLDL	MAGNETIC	19238	27555778	2016	-	-	-	-	-	-	-	-	-	-	-	-
Total cholesterol in large VLDL	MAGNETIC	21235	27555778	2016	-0.13	0.072	-1.85	6.43E-02	0.16	0.162	0.96	3.37E-01	0.18	0.185	0.95	3.45E-01
Total cholesterol in medium VLDL	MAGNETIC	21251	27555778	2016	-0.02	0.071	-0.29	7.74E-01	0.03	0.150	0.23	8.20E-01	0.12	0.172	0.69	4.91E-01
Total cholesterol in small VLDL	MAGNETIC	21557	27555778	2016	-0.12	0.063	-1.91	5.60E-02	0.24	0.158	1.51	1.32E-01	0.22	0.179	1.23	2.17E-01
Total cholesterol in large LDL	MAGNETIC	21552	27555778	2016	-0.10	0.058	-1.68	9.20E-02	-0.02	0.130	-0.19	8.53E-01	0.03	0.143	0.18	8.58E-01
Total cholesterol in medium LDL	MAGNETIC	21559	27555778	2016	-0.12	0.065	-1.88	6.05E-02	0.22	0.163	1.34	1.81E-01	0.21	0.185	1.16	2.50E-01
Total cholesterol in small LDL	MAGNETIC	21556	27555778	2016	-0.04	0.072	-0.56	5.74E-01	0.26	0.187	1.62	5.50E-02	0.23	0.195	1.17	2.41E-01
Total cholesterol in IDL	MAGNETIC	19273	27555778	2016	-0.12	0.070	-1.73	8.36E-02	0.18	0.168	1.04	2.99E-01	0.23	0.195	1.20	2.31E-01
Total cholesterol in very large HDL	MAGNETIC	21540	27555778	2016	-0.25	0.126	-1.94	5.23E-02	-0.09	0.243	-0.38	7.04E-01	0.30	0.249	1.20	2.32E-01
Total cholesterol in large HDL	MAGNETIC	21558	27555778	2016	-0.05	0.060	-0.91	3.62E-01	0.16	0.146	1.01	3.12E-01	0.20	0.167	1.20	2.30E-01
Total cholesterol in medium HDL	MAGNETIC	21558	27555778	2016	0.02	0.060	0.23	8.21E-01	0.22	0.167	1.32	1.88E-01	0.15	0.183	0.80	4.25E-01
Total cholesterol in small HDL	MAGNETIC	13499	27555778	2016	-	-	-	-	-	-	-	-	-	-	-	-
Total cholesterol in serum	MAGNETIC	21491	27555778	2016	-0.01	0.046	-0.31	7.54E-01	0.11	0.121	0.93	3.51E-01	0.09	0.139	0.63	5.31E-01
Total cholesterol in IDL	MAGNETIC	21559	27555778	2016	0.01	0.053	0.22	8.29E-01	0.09	0.129	0.69	4.88E-01	0.06	0.150	0.43	6.71E-01
Total cholesterol in HDL	MAGNETIC	21555	27555778	2016	-0.11	0.063	-1.70	9.00E-02	0.07	0.128	0.53	5.93E-01	0.14	0.144	0.98	3.30E-01
Total cholesterol in chylomicrons and largest VLDL particles	MAGNETIC	13697	27555778	2016	-	-	-	-	-	-	-	-	-	-	-	-
Free cholesterol in very large VLDL	MAGNETIC	13476	27555778	2016	-	-	-	-	-	-	-	-	-	-	-	-
Free cholesterol in large VLDL	MAGNETIC	21238	27555778	2016	-0.12	0.069	-1.78	7.40E-02	0.19	0.162	1.19	2.34E-01	0.20	0.186	1.06	2.89E-01
Free cholesterol in medium VLDL	MAGNETIC	21240	27555778	2016	-0.01	0.047	-0.28	7.77E-01	0.11	0.122	0.93	3.53E-01	0.08	0.142	0.59	5.57E-01
Free cholesterol in small VLDL	MAGNETIC	21559	27555778	2016	-0.13	0.061	-2.11	3.50E-02	0.21	0.150	1.39	1.64E-01	0.22	0.171	1.30	1.94E-01
Free cholesterol in large LDL	MAGNETIC	21555	27555778	2016	-0.06	0.055	-0.94	3.48E-01	0.02	0.116	0.17	8.67E-01	0.02	0.137	0.15	8.80E-01
Free cholesterol in medium LDL	MAGNETIC	13544	27555778	2016	-	-	-	-	-	-	-	-	-	-	-	-
Free cholesterol in small LDL	MAGNETIC	13506	27555778	2016	-	-	-	-	-	-	-	-	-	-	-	-
Free cholesterol in IDL	MAGNETIC	21559	27555778	2016	-0.10	0.063	-1.56	1.19E-01	0.14	0.150	0.94	3.47E-01	0.10	0.170	0.61	5.41E-01
Free cholesterol in very large HDL	MAGNETIC	21543	27555778	2016	-0.17	0.087	-1.99	4.65E-02	-0.06	0.164	-0.31	7.54E-01	0.24	0.185	1.24	2.15E-01
Free cholesterol in large HDL	MAGNETIC	21559	27555778	2016	0.13	0.063	1.16	1.74E-01	-0.12	0.154	-0.54	5.88E-01	-0.13	0.244	-0.55	5.86E-01
Free cholesterol in medium HDL	MAGNETIC	21559	27555778	2016	-0.03	0.055	-0.49	6.23E-01	0.25	0.145	1.61	1.08E-01	0.17	0.163	1.06	2.90E-01
Free cholesterol in small HDL	MAGNETIC	13497	27555778	2016	-	-	-	-	-	-	-	-	-	-	-	-
Free cholesterol in serum	MAGNETIC	13497	27555778	2016	-0.21	0.103	-2.01	4.43E-02	0.41	0.227	1.79	7.45E-02	0.51	0.260	1.95	5.10E-02
Free cholesterol to esterified cholesterol ratio	MAGNETIC	13497	27555778	2016	-0.30	0.108	-1.81	7.00E-02	0.27	0.226	1.20	2.31E-01	0.27	0.242	1.11	2.68E-01
Cholesterol esters in chylomicrons and largest VLDL particles	MAGNETIC	24478	27555778	2016	-	-	-	-	-	-	-	-	-	-	-	-
Cholesterol esters in very large VLDL	MAGNETIC	24482	27555778	2016	-	-	-	-	-	-	-	-	-	-	-	-
Cholesterol esters in large VLDL	MAGNETIC	18968	27555778	2016	-0.12	0.069	-1.78	7.53E-02	0.22	0.168	1.33	1.83E-01	0.23	0.192	1.21	2.25E-01
Cholesterol esters in medium VLDL	MAGNETIC	19273	27555778	2016	-0.02	0.045	-0.46	6.44E-01	0.11	0.117	0.91	3.65E-01	0.10	0.130	0.75	4.54E-01
Cholesterol esters in small VLDL	MAGNETIC	19278	27555778	2016	-	-	-	-	-	-	-	-	-	-	-	-
Cholesterol esters in large LDL (Previously - VLDL)	MAGNETIC	19273	27555778	2016	-0.06	0.056	-1.03	3.04E-01	-0.02	0.117	-0.19	8.49E-01	0.02	0.137	0.12	9.02E-01
Cholesterol esters in medium LDL	MAGNETIC	19273	27555778	2016	-0.12	0.068	-1.82	6.85E-02	0.15	0.166	0.87	3.82E-01	0.19	0.190	1.01	3.14E-01
Cholesterol esters in small LDL	MAGNETIC	21555	27555778	2016	-	-	-	-	-	-	-	-	-	-	-	-
Cholesterol esters in IDL	MAGNETIC	19273	27555778	2016	-	-	-	-	-	-	-	-	-	-	-	-
Cholesterol esters in very large HDL	MAGNETIC	13506	27555778	2016	-	-	-	-	-	-	-	-	-	-	-	-
Cholesterol esters in large HDL	MAGNETIC	19273	27555778	2016	-0.11	0.066	-1.69	9.00E-02	0.19	0.162	1.12	2.63E-01	0.21	0.186	1.10	2.70E-01
Cholesterol esters in medium HDL	MAGNETIC	19273	27555778	2016	-0.01	0.076	-0.17	8.67E-01	0.20	0.168	1.28	2.02E-01	0.15	0.184	0.79	4.30E-01
Cholesterol esters in small HDL	MAGNETIC	13497	27555778	2016	-	-	-	-	-	-	-	-	-	-	-	-
Cholesterol esters in serum	MAGNETIC	24479	27555778	2016	-	-	-	-	-	-	-	-	-	-	-	-
Apolipoprotein AI	MAGNETIC	20687	27555778	2016	-0.13	0.079	-1.64	1.01E-01	0.15	0.150	1.02	3.07E-01	0.20	0.169	1.15	2.50E-01
Apolipoprotein B	MAGNETIC	20690	27555778	2016	-0.10	0.055	-1.89	5.90E-02	0.21	0.150	1.41	1.58E-01	0.24	0.181	1.34	1.80E-01
Total fatty acids	MAGNETIC	24482	27555778	2016	-	-	-	-	-	-	-	-	-	-	-	-
Docosahexaenoic acid	MAGNETIC	13499	27555778	2016	-0.06	0.062	-0.91	3.65E-01	0.09	0.152	0.60	5.50E-01	0.16	0.171	0.96	3.37E-01
Linoleic acid	MAGNETIC	13527	27555778	2016	0.03	0.050	0.62	5.37E-01	0.00	0.123	0.02	9.81E-01	0.07	0.138	0.49	6.23E-01
Omega-3 fatty acids	MAGNETIC	13544	27555778	2016	0.01	0.059	-0.19	8.47E-01	0.09	0.143	0.64	5.22E-01	0.07	0.150	0.44	6.64E-01
Omega-6 fatty acids	MAGNETIC	13606	27555778	2016	-0.04	0.075	-0.53	5.98E-01	0.05	0.166	0.32	7.53E-01	0.10	0.191	0.51	6.08E-01
Polyunsaturated fatty acids	MAGNETIC	19270	27555778	2016	-	-	-	-	-	-	-	-	-	-	-	-
Monounsaturated fatty acids	MAGNETIC	13535	27555778	2016	0.05	0.057	0.85	3.95E-01	0.11	0.145	0.79	4.30E-01	0.06	0.161	0.39	6.98E-01
Average number of double bonds in a fatty acid chain	MAGNETIC	10728	27555778	2016	0.06	0.048	-1.16	2.46E-01	0.11	0.122	0.91	3.64E-01	0.05	0.143	0.34	7.31E-01
Average number of methylene groups per a double bond	MAGNETIC	13532	27555778	2016	0.08	0.047	1.64	1.02E-01	-0.17	0.118	-1.42	1.57E-01	-0.16	0.141	-1.10	2.70E-01
Description of average fatty acid chain length not actual carbon number	MAGNETIC	13476	27555778	2016	-0.03	0.058	-0.55	5.85E-01	0.06	0.162	0.39	7.00E-01	0.09	0.188	0.46	6.47E-01
Ratio of bis/allyls groups to total fatty acids	MAGNETIC	13171	27555778	2016	-0.05	0.043	-1.15	2.52E-01	0.11	0.107	1.00	3.18E-01	0.12	0.124	0.93	3.53E-01
Ratio of bis/allyls groups to double bonds	MAGNETIC	13534	27555778	2016	-0.02	0.045	-0.36	7.17E-01	0.04	0.111	0.33	7.39E-01	0.01	0.134	0.12	9.02E-01
Albumin	MAGNETIC	18993	27555778	2016	0.20	0.090	2.20	2.75E-02	0.15	0.160	0.95	3.41E-01	-0.25	0.186	-1.37	1.72E-01
Creatinine	MAGNETIC	24810	27555778	2016	0.09	0.049	1.92	5.43E-02	0.05	0.125	0.41	6.82E-01	0.06	0.145	0.53	5.95E-01
Alanine	MAGNETIC	24796	27555778	2016	-0.03	0.059	-0.54	5.90E-01	0.12	0.125	0.88	3.78E-01	0.17	0.153	1.12	2.62E-01
Glutamine	MAGNETIC	24482	27555778	2016	0.13	0.070	1.88	6.10E-02	0.00	0.157	0.00	9.99E-01	0.03	0.193	0.13	8.98E-01
Glycine	MAGNETIC	21555	27555778	2016	-	-	-	-	-	-	-	-	-	-	-	-
Histidine	MAGNETIC	19273	27555778	2016	-	-	-	-	-	-	-	-	-	-	-	-
Isoleucine	MAGNETIC	24778	27555778	2016	0.21	0.071	2.94	3.00E-03	0.13	0.140	0.89	3.71E-01	0.18	0.151	1.22	2.22E-01
Leucine	MAGNETIC	24728	27555778	2016	0.03	0.050	0.50	6.19E-01	0.05	0.129	0.41	6.85E-01	0.06	0.147	0.39	6.99E-01
Valine	MAGNETIC	24800	27555778	2016	0.15	0.070	2.08	3.80E-02	-0.04	0.154	-0.25	8.05E-01	-0.02	0.173	-0.14	8.90E-01
Phenylalanine	MAGNETIC	22663	27555778	2016	-0.01	0.064	-0.21	8.35E-01	0.29	0.164	1.78	7.63E-02	0.30	0.192	1.57	1.16E-01
Tyrosine	MAGNETIC	24805	27555778	2016	-0.01	0.057	-0.13	8.93E-01	0.22	0.127	1.72	8.63E-02	0.27	0.146	1.83	6.76E-02
Citrate	MAGNETIC	24778	27555778	2016	0.06	0.052	0.97	3.33E-01	-0.02	0.149	-0.16	8.80E-01	0.03	0.156	0.17	8.63E-01
Glucose	MAGNETIC	24678	27555778	2016	0.02	0.055	0.30	7.64E-01	-0.07	0.126	-0.53	5.94E-01	0.07	0.150	-0.48	6.48E-01
Acetoacetate	MAGNETIC	19282	27555778	2016	0.07	0.071	0.95	3.44E-01	0.07	0.163	0.42	6.78E-01	0.02	0.155	0.10	9.18E-01
Acetate	MAGNETIC	24748	27555778	2016	0.02	0.048	-0.36	7.17E-01	0.04	0.116	0.36	7.20E-01	0.01	0.134	0.12	9.02E-01
Glycoprotein acetyls mainly a1 acid glycoprotein	MAGNETIC	19270	27555778	2016	-0.04	0.060	-0.74	4.61E-01	0.20	0.138	1.46	1.44E-01	0.22	0.158	1.42	1.56E-01
Adiponectin	ADIPOGen	39883	23470002	2012	-0.07	0.045	-1.54	1.23E-01	0.23	0.111	1.88	6.30E-02	0.22	0.130	1.72	8.50E-02
Fasting glucose	MAGIC	53645	22561238	2012	0.04	0.038	1.03	3.02E-01	-0.01	0.092	-0.13	8.94E-01	0.05	0.094	0.49	6.27E-01
Fasting insulin	MAGIC	51750	22561238	2012	0.07	0.043	1.64	1.01E-01	0.16	0.104	0.07	9.44E-01	0.09	0.115	0.81	4.18E-01
Fasting proinsulin	MAGIC	10701	20081858	2011	-0.01	0.084	-0.17	8.65E-01	-0.08	0.158	-0.48	6.29E-01	0.00	0.175	0.02	9.85E-01
2hr glucose adjusted for body mass index	MAGIC	15234	20081857	2010	0.02	0.066	0.28	7.79E-01	0.18	0.164	1.12	2.62E-01	0.27	0.187	1.45	1.46E-01
Glycated hemoglobin HbA1C	MAGIC	46548	20858683	2010	0.05	0.044	1.18	2.39E-01	0.06	0.110	-0.71	4.79E-01	0.09	0.131	-0.65	5.15E-01
Homeostasis model assessment-B	MAGIC	46186	20081858	2011	0.06	0.063	1.27	2.05E-01	0.03	0.111	0.23	8.16E-01	0.05	0.130	0.35	7.27E-01
Homeostasis model assessment-IR	MAGIC	46186	20081858	2011	0.10	0.071	1.45	1.47E-01	0.05	0.122	0.41	6.85E-01	0.09	0.143	0.65	5.17E-01
Serum creatinine	CKDGen	133914	20651099	2015	-0.01	0.034	-0.42	6.76E-01	0.11	0.084	1.31	1.89E-01	0.14	0.101	1.39	1.64E-01
Urinary albumin-to-creatinine ratio-diabetes	CKDGen	118493	20651099	2015	-0.03	0.056	-0.52	3.03E-01	-0.01	0.056	-0.18	8.55E-01	0.01	0.072	0.11	9.11E-01
Urinary albumin-to-creatinine ratio	CKDGen	54450	26831737	2015	-0.01	0.049	-0.27	7.90E-01	0.03	0.121	0.23	8.01E-01	0.05	0.142	0.33	7.38E-01
Urinary albumin-to-creatinine ratio-non diabetes	CKDGen	46091	26831737	2015	-0.04	0.075	-0.53	5.93E-01	-0.08	0.155	-0.53	5.97E-01	-0.10	0.175	-0.59	5.58E-01
Serum cystatin c	CKDGen	33152	26831099	2015	-0.01	0.049	-0.19	8.52E-01	0.02	0.128	0.14	8.85E-01	0.06	0.148	0.43	6.68E-01
Serum/urine c-overweight all	GCKD	9445	25611787	2014	0.02	0.057	0.37	7.07E-01	0.06	0.090	0.60	5.71E-01	0.04	0.095	0.34	7.32E-01
Forearm bone mineral density	GEFOS	19805	26367754	2015	0.72	0.211	3.43

Supplementary Table 8. Variant Effect Predictor annotations for predicted deleterious genome-wide significant coding SNPs

CONDITIONALLY INDEPENDENT eBMD ASSOCIATED VARIANTS			PREDICTED DELETERIOUS SNP					eBMD GWAS SUMMARY STATISTICS			VEP ANNOTATIONS FOR PREDICTED DELETERIOUS SNPS					FINE MAPPING ANNOTATION
INDICES	RSIDS	P_{LEAD}	$RSID_{DEL}$	CHR	BP	EA	NEA	EAF	β	SE	P	CONSEQUENCE	IMPACT	GENE	BIOTYPE	AMINO ACID	CODON	PLAUSIBLE CAUSAL*
2	rs2708632	1.20E-18	rs2289732	1	8423877	G	C	0.83	-0.02	0.004	3.60E-09	missense_varian	MODERATE	*RERE*	non_stop_decay	S/C	tCt/tGt	No
2	rs2708632	1.20E-18	rs9628991	1	8424039	C	G	0.83	-0.02	0.004	5.00E-09	missense_varian	MODERATE	*RERE*	non_stop_decay	G/A	gGg/gCg	No
4	rs6701290	2.30E-14	rs848208	1	16256644	C	T	0.90	-0.04	0.006	1.50E-13	missense_varian	MODERATE	*SPEN*	protein_coding	A/V	gCa/gTa	No
5,6	**rs7519859,1:22483649_T_TGGGGGG**	**1.10E-50**	**rs10917051**	**1**	**22141206**	**A**	**C**	**0.31**	**0.02**	**0.004**	**2.90E-09**	**missense_variant**	**MODERATE**	*LDLRAD2*	**protein_coding**	**N/T**	**aAc/aCc**	**Yes**
11,12,13	**rs4397637,rs143243230,rs11209241**	**1.10E-26**	**rs983034**	**1**	**68603586**	**C**	**T**	**0.61**	**0.03**	**0.003**	**5.90E-17**	**missense_variant**	**MODERATE**	*WLS*	**protein_coding**	**V/I**	**Gtc/Atc**	**Yes**
23,24	rs201324539,rs2275707	1.20E-17	rs2230301	1	220197625	G	T	0.19	0.03	0.004	8.10E-15	missense_varian	MODERATE	*EPRS*	protein_coding	D/E	gaC/gaA	No
29	rs10490046	3.20E-17	2:40981770_G_GT	2	40981770	G	GT	0.63	-0.02	0.003	1.90E-09	splice_donor_variant,non_coding_transcript_variar	HIGH	*AC007317.1*	lincRNA	-	-	No
30,31	rs7576689,rs1550425	1.60E-38	rs187184761	2	42276664	T	C	0.86	0.03	0.005	7.00E-11	missense_varian	MODERATE	*PKDCC*	protein_coding	S/P	Tcc/Ccc	No
30,31	rs7576689,rs1550425	1.60E-38	rs11891676	2	42275726	C	G	0.77	-0.05	0.004	9.00E-36	missense_variant,NMD_transcript_varian	MODERATE	*PKDCC*	nonsense_mediated_decay	A/G	gCc/gGc	No
30,31	rs7576689,rs1550425	1.60E-38	rs11897440	2	42275819	T	C	0.62	-0.02	0.003	4.20E-10	missense_variant,NMD_transcript_varian	MODERATE	*PKDCC*	nonsense_mediated_decay	V/A	gTg/gCg	No
32	rs6761129	3.90E-11	rs7578597	2	43732823	T	C	0.89	-0.03	0.005	1.80E-10	missense_varian	MODERATE	*THADA*	protein_coding	T/A	Aca/Gca	No
33,34	rs4233969,rs34138475	2.40E-110	rs6574462	2	54582012	C	A	0.65	-0.03	0.003	4.10E-15	missense_varian	MODERATE	*C2orf73*	protein_coding	H/N	Cac/Aac	No
34	rs34138475	2.20E-44	rs11677096	2	55254165	T	A	0.98	0.07	0.011	1.90E-09	missense_varian	MODERATE	*RTN4*	protein_coding	D/V	gAt/gTt	No
42	**rs34588551**	**1.70E-09**	**rs34588551**	**2**	**159954175**	**C**	**T**	**0.63**	**-0.02**	**0.003**	**1.70E-09**	**missense_variant**	**MODERATE**	*TANC1*	**protein_coding**	**P/S**	**Cca/Tca**	**Yes**
48	rs183979857	6.30E-11	rs4675323	2	204062061	A	G	0.04	0.05	0.008	7.60E-11	missense_varian	MODERATE	*NBEAL1*	protein_coding	I/V	Atc/Gtc	No
48	rs183979857	6.30E-11	rs2043449	2	204116696	C	T	0.04	0.05	0.008	1.10E-10	missense_variant,splice_region_variar	MODERATE	*CYP20A1*	protein_coding	S/L	tCg/tTg	No
48	rs183979857	6.30E-11	rs2043449	2	204116696	C	T	0.04	0.05	0.008	1.10E-10	missense_variant,splice_region_variant,NMD_transcript_varia	MODERATE	*CYP20A1*	nonsense_mediated_decay	S/L	tCg/tTg	No
57,58	rs11915970,rs1352014	4.80E-16	rs12488237	3	56114861	T	C	0.94	-0.05	0.007	6.30E-12	missense_variant,NMD_transcript_varian	MODERATE	*ERC2*	nonsense_mediated_decay	N/S	aAt/aGt	No
57,58	rs11915970,rs1352014	4.80E-16	rs12488237	3	56114861	T	C	0.94	-0.05	0.007	6.30E-12	missense_varian	MODERATE	*ERC2*	protein_coding	N/S	aAt/aGt	No
61,62,63	rs6829296,rs4505759,rs11206992	5.50E-52	rs3759955	4	994414	G	A	0.85	0.07	0.005	2.70E-47	missense_varian	MODERATE	*IDUA*	protein_coding	R/Q	cGg/cAg	No
61,62,63	rs6829296,rs4505759,rs11206992	5.50E-52	rs114806891	4	995868	C	T	0.94	-0.08	0.007	4.90E-32	stop_gained	HIGH	*IDUA*	protein_coding	R/*	Cga/Tga	No
61,62,63	rs6829296,rs4505759,rs11206992	5.50E-52	rs6830825	4	995919	G	C	0.85	0.07	0.005	1.50E-48	missense_varian	MODERATE	*IDUA*	protein_coding	G/R	Gga/Cga	No
61,62,63	rs6829296,rs4505759,rs11206992	5.50E-52	rs6811373	4	995997	A	G	0.85	0.07	0.005	2.20E-48	missense_varian	MODERATE	*IDUA*	protein_coding	R/G	Aga/Gga	No
61,62,63	rs6829296,rs4505759,rs11206992	5.50E-52	rs6831021	4	996012	G	C	0.85	0.07	0.005	1.40E-48	missense_varian	MODERATE	*IDUA*	protein_coding	A/P	Gcg/Ccg	No
61,62,63	rs6829296,rs4505759,rs11206992	5.50E-52	rs6831280	4	996165	G	A	0.85	0.07	0.005	5.40E-48	missense_varian	MODERATE	*IDUA*	protein_coding	A/T	Gcg/Acg	No
61,62,63	rs6829296,rs4505759,rs11206992	5.50E-52	rs73066475	4	996690	G	A	0.85	0.07	0.005	1.40E-48	missense_varian	MODERATE	*IDUA*	protein_coding	V/I	Gtc/Atc	No
61,62,63	rs6829296,rs4505759,rs11206992	5.50E-52	rs4647932	4	1019011	C	T	0.94	-0.08	0.007	2.70E-30	missense_varian	MODERATE	*FGFRL1*	protein_coding	P/L	cCa/cTa	No
61,62,63	rs6829296,rs4505759,rs11206992	5.50E-52	rs4045481	4	1090625	G	A	0.32	0.02	0.004	6.60E-10	stop_gained,splice_region_variant,NMD_transcript_variar	HIGH	*RNF212*	nonsense_mediated_decay	R/*	Cga/Tga	No
69,70	rs35417399,rs7265579	2.50E-17	rs1054627	4	88732692	G	A	0.69	0.02	0.004	4.40E-11	missense_varian	MODERATE	*IBSP*	protein_coding	G/E	gGa/gAa	No
69,70	rs35417399,rs7265579	2.50E-17	rs1054629	4	88732918	A	T	0.69	0.02	0.004	2.00E-11	missense_varian	MODERATE	*IBSP*	protein_coding	E/D	gaA/gaT	No
77	rs2542710	2.70E-14	rs700233	5	39364554	G	A	0.60	-0.02	0.003	3.30E-09	missense_varian	MODERATE	*C9*	protein_coding	R/W	Cgg/Tgg	No
85,86	**rs525678,rs9379084**	**1.90E-20**	**rs1334576**	**6**	**7211818**	**G**	**A**	**0.57**	**-0.02**	**0.003**	**2.20E-09**	**missense_variant**	**MODERATE**	*RREB1*	**protein_coding**	**G/R**	**Ggg/Agg**	**Yes**
85,86	**rs525678,rs9379084**	**1.90E-20**	**rs9379084**	**6**	**7211843**	**G**	**A**	**0.88**	**0.04**	**0.005**	**3.00E-15**	**missense_variant**	**MODERATE**	*RREB1*	**protein_coding**	**D/N**	**Gac/Aac**	**Yes**
88	rs9260426	2.60E-11	rs1143146	6	29910358	C	G	0.54	0.02	0.003	9.70E-10	missense_varian	MODERATE	*HLA-A*	protein_coding	L/V	Ctc/Gtc	No
88	rs9260426	2.60E-11	rs1136695	6	29911064	A	G	0.42	0.02	0.003	3.00E-09	missense_varian	MODERATE	*HLA-A*	protein_coding	I/M	atA/atG	No
88	rs9260426	2.60E-11	rs2231119	6	29912856	A	T	0.42	0.02	0.003	2.60E-09	missense_varian	MODERATE	*HLA-A*	protein_coding	T/S	Act/Tct	No
89,90	rs113166754,rs14464727	5.20E-47	rs188622836	6	44922299	A	G	1.00	0.21	0.037	2.20E-09	missense_varian	MODERATE	*SUPT3H*	protein_coding	M/T	aTg/aCg	No
89,90	rs113166754,rs14464727	5.20E-47	rs188622836	6	44922299	A	G	1.00	0.21	0.037	2.20E-09	missense_variant,NMD_transcript_varian	MODERATE	*SUPT3H*	nonsense_mediated_decay	M/T	aTg/aCg	No
91,92,93,94	**rs1502199,rs76768932,rs191147097,rs721**	**6.40E-23**	**rs9370418**	**6**	**55266625**	**T**	**C**	**0.25**	**0.02**	**0.004**	**5.60E-10**	**missense_variant**	**MODERATE**	*GFRAL*	**protein_coding**	**S/P**	**Tcg/Ccg**	**Yes**
96	rs10943136	1.30E-12	rs10455097	6	74493432	A	C	0.49	0.02	0.003	2.70E-12	missense_variant,splice_region_variar	MODERATE	*CD109*	protein_coding	Y/S	tAc/tCc	No
97	rs6454314	4.90E-13	rs473267	6	83880167	C	T	0.74	-0.02	0.004	2.30E-09	missense_variant,NMD_transcript_varian	MODERATE	*PGM3*	nonsense_mediated_decay	D/N	Gat/Aat	No
97	rs6454314	4.90E-13	rs473267	6	83880167	C	T	0.74	-0.02	0.004	2.30E-09	missense_varian	MODERATE	*PGM3*	protein_coding	D/N	Gat/Aat	No
100	rs1415701	3.50E-14	rs9388768	6	130374102	C	A	0.33	-0.02	0.004	1.60E-10	missense_varian	MODERATE	*L3MBTL3*	protein_coding	T/N	aCc/aAc	No
102,103,104	rs10713212,rs9402490,rs54754	9.40E-67	rs9493627	6	133789722	G	A	0.68	0.02	0.004	1.40E-10	missense_varian	MODERATE	*EYA4*	protein_coding	G/S	Ggc/Agc	No
106,107,108,109,110	rs55784958,rs4869744,rs12525051,rs2941	4.40E-150	rs3734800	6	151766552	G	A	0.90	0.05	0.006	6.70E-21	missense_varian	MODERATE	*RWDD1*	protein_coding	T/M	aCg/aTg	No
106,107,108,109,110	**rs55784958,rs4869744,rs12525051,rs294**	**4.40E-150**	**rs12205837**	**6**	**151894344**	**C**	**T**	**0.89**	**0.07**	**0.005**	**3.30E-45**	**missense_variant**	**MODERATE**	*CCDC170*	**protein_coding**	**A/V**	**gCt/gTt**	**Yes**
106,107,108,109,110	rs55784958,rs4869744,rs12525051,rs2941	4.40E-150	rs55868408	6	151894567	G	A	0.99	0.10	0.016	7.10E-10	missense_varian	MODERATE	*CCDC170*	protein_coding	E/K	Gag/Aag	No
106,107,108,109,110	rs55784958,rs4869744,rs12525051,rs2941	4.40E-150	rs34430497	6	151917666	G	A	0.94	0.05	0.007	1.60E-16	missense_varian	MODERATE	*CCDC170*	protein_coding	R/Q	cGa/cAa	No
106,107,108,109,110	rs55784958,rs4869744,rs12525051,rs2941	4.40E-150	rs6829137	6	151936677	G	A	0.67	0.05	0.004	1.00E-44	missense_varian	MODERATE	*CCDC170*	protein_coding	V/I	Gtc/Atc	No
106,107,108,109,110	rs55784958,rs4869744,rs12525051,rs2941	4.40E-150	rs3734804	6	151939181	G	A	0.48	0.06	0.003	3.50E-71	missense_varian	MODERATE	*CCDC170*	protein_coding	V/I	Gtc/Atc	No
119,120	rs62454420,rs1750109	8.50E-23	rs34398255	7	27239201	G	T	0.98	0.07	0.011	3.90E-10	missense_varian	MODERATE	*HOXA13*	protein_coding	P/T	Ccc/Acc	No
124,125,126	rs17236600,rs1717731,rs9956941	1.10E-63	rs1802074	7	37947103	C	T	0.79	-0.05	0.004	6.90E-29	missense_varian	MODERATE	*SFRP4*	protein_coding	R/K	aGa/aAa	No
133,134,135,136,137	rs149333699,rs184953495,rs2536195,rs19	4.94066564584	rs41281692	7	120778097	C	G	0.55	0.06	0.003	6.50E-66	missense_varian	MODERATE	*CPED1*	protein_coding	A/G	gCa/gGa	No
133,134,135,136,137	rs149333699,rs184953495,rs2536195,rs19	4.94066564584	rs35793694	7	120876837	A	G	0.92	-0.06	0.006	1.80E-21	missense_varian	MODERATE	*CPED1*	protein_coding	E/G	gAa/gGa	No
133,134,135,136,137	rs149333699,rs184953495,rs2536195,rs19	4.94066564584	rs10953934	7	120901699	G	A	0.62	-0.10	0.003	7.30E-214	missense_varian	MODERATE	*CPED1*	protein_coding	D/N	Gat/Aat	No
133,134,135,136,137	**rs149333699,rs184953495,rs2536195,rs19**	**4.94066564584**	**rs2908004**	**7**	**120969766**	**G**	**A**	**0.56**	**-0.10**	**0.003**	**1.60E-199**	**missense_variant**	**MODERATE**	*WNT16*	**protein_coding**	**G/R**	**Ggg/Agg**	**Yes**
133,134,135,136,137	**rs149333699,rs184953495,rs2536195,rs19**	**4.94066564584**	**rs2707466**	**7**	**120970085**	**C**	**T**	**0.56**	**-0.10**	**0.003**	**6.10E-203**	**missense_variant**	**MODERATE**	*WNT16*	**protein_coding**	**T/I**	**aCa/aTa**	**Yes**
138	**rs62621812**	**2.50E-16**	**rs62621812**	**7**	**127015082**	**G**	**A**	**0.98**	**0.09**	**0.011**	**2.50E-16**	**missense_variant**	**MODERATE**	*ZNF800*	**protein_coding**	**P/S**	**Cct/Tct**	**Yes**
139	rs2929308	1.90E-39	rs7015700	8	9527707	G	A	0.82	-0.03	0.004	7.80E-12	splice_donor_variant,non_coding_transcript_variar	HIGH	*TNKS*	retained_intron	-	-	No
142	rs7003794	3.50E-18	rs35863913	8	71573259	C	T	0.57	0.02	0.003	1.20E-12	missense_varian	MODERATE	*RP11-382J12.1*	protein_coding	H/Y	Cac/Tac	No
150,151	rs10992867,rs143581991	2.50E-17	rs1460736720	9	96439004	C	CCCTGCCT	0.36	0.02	0.004	7.20E-12	inframe_insertior	MODERATE	*PHF2*	protein_coding	-/PASTT	-/CCTGCCTG	No
150,151	rs10992867,rs143581991	2.50E-17	rs191789925	9	96717287	C	T	0.88	-0.03	0.005	1.10E-11	missense_varian	MODERATE	*BARX1*	protein_coding	A/T	Gcc/Acc	No
170	**rs147048550**	**1.20E-10**	**rs17173698**	**10**	**89468953**	**G**	**A**	**0.97**	**-0.07**	**0.011**	**3.90E-10**	**missense_variant,splice_region_variant**	**MODERATE**	*PAPSS2*	**protein_coding**	**E/K**	**Gag/Aag**	**Yes**
176	**rs1133400**	**1.70E-17**	**rs1133400**	**10**	**134459388**	**A**	**G**	**0.78**	**-0.03**	**0.004**	**1.70E-17**	**missense_variant**	**MODERATE**	*INPP5A*	**protein_coding**	**K/R**	**aAg/aGg**	**Yes**
177	rs71059190	2.40E-15	rs11042127	11	8947586	C	G	0.84	0.03	0.005	5.40E-13	missense_varian	MODERATE	*C11orf16*	protein_coding	V/L	Gtc/Ctc	No
178	**rs17507577**	**1.40E-15**	**rs17507577**	**11**	**15243059**	**G**	**A**	**0.92**	**-0.05**	**0.006**	**1.40E-15**	**missense_variant**	**MODERATE**	*INSC*	**protein_coding**	**D/N**	**Gac/Aac**	**Yes**
185	rs12806687	2.60E-32	rs5896	11	46745003	C	T	0.86	-0.03	0.005	8.80E-11	missense_varian	MODERATE	*F2*	protein_coding	T/M	aCg/aTg	No
185	rs12806687	2.60E-32	rs3816614	11	46890165	C	T	0.23	0.04	0.004	1.60E-19	missense_varian	MODERATE	*LRP4*	protein_coding	R/Q	cGg/cAg	No
185	rs12806687	2.60E-32	rs2306029	11	46893108	T	C	0.46	0.03	0.003	8.30E-15	missense_varian	MODERATE	*LRP4*	protein_coding	S/G	Agc/Ggc	No
185	rs12806687	2.60E-32	rs2306033	11	46897446	G	A	0.87	-0.03	0.005	3.10E-12	missense_varian	MODERATE	*LRP4*	protein_coding	A/V	gCg/gTg	No
185	rs12806687	2.60E-32	rs6485702	11	46898771	T	C	0.34	0.04	0.004	4.20E-30	missense_varian	MODERATE	*LRP4*	protein_coding	I/V	Att/Gtt	No
185	rs12806687	2.60E-32	rs2242261	11	47266808	T	G	0.85	-0.03	0.005	9.80E-10	missense_variant,splice_region_variar	MODERATE	*ACP2*	protein_coding	Q/P	cAg/cCg	No
185	rs12806687	2.60E-32	rs2167079	11	47270255	C	T	0.70	-0.02	0.004	7.50E-10	missense_varian	MODERATE	*ACP2*	protein_coding	R/Q	cGg/cAg	No
185	rs12806687	2.60E-32	rs2167079	11	47270255	C	T	0.70	-0.02	0.004	7.50E-10	missense_variant,NMD_transcript_varian	MODERATE	*ACP2*	nonsense_mediated_decay	R/Q	cGg/cAg	No
185	rs12806687	2.60E-32	rs2279238	11	47282024	C	T	0.85	-0.03	0.005	9.90E-10	missense_variant,NMD_transcript_varian	MODERATE	*NR1H3*	nonsense_mediated_decay	A/V	gCg/gTg	No
186	**rs17602572**	**1.20E-19**	**rs7232**	**11**	**59940599**	**T**	**A**	**0.63**	**0.03**	**0.003**	**1.80E-19**	**missense_variant**	**MODERATE**	*MS4A6A*	**protein_coding**	**T/S**	**Act/Tct**	**Yes**
186	**rs17602572**	**1.20E-19**	**rs7232**	**11**	**59940599**	**T**	**A**	**0.63**	**0.03**	**0.003**	**1.80E-19**	**missense_variant**	**MODERATE**	*MS4A6A*	**protein_coding**	**N/I**	**aAc/aTc**	**Yes**
186	rs17602572	1.20E-19	rs583791	11	59947252	C	T	0.43	-0.03	0.003	2.90E-16	missense_varian	MODERATE	*MS4A6A*	protein_coding	A/T	Gcc/Acc	No
189	rs6686433	3.20E-16	rs4787	11	65359910	C	T	0.26	-0.03	0.004	7.10E-13	missense_varian	MODERATE	*AP001362.1*	protein_coding	V/I	Gta/Ata	No
189	rs6686433	3.20E-16	rs3741378	11	65408937	C	T	0.86	0.03	0.005	3.10E-11	missense_varian	MODERATE	*SIPA1*	protein_coding	S/F	tCc/tTc	No
189	rs6686433	3.20E-16	rs12362011	11	65547455	C	A	0.85	0.03	0.005	3.80E-10	missense_varian	MODERATE	*AP5B1*	protein_coding	G/V	gGg/gTg	No
190,191,192	**rs61887821,rs11228219,rs4988321**	**3.30E-23**	**rs41494349**	**11**	**68115489**	**A**	**G**	**0.99**	**0.19**	**0.021**	**3.80E-20**	**missense_variant,NMD_transcript_variant**	**MODERATE**	*LRP5*	**nonsense_mediated_decay**	**Q/R**	**cAg/cGg**	**Yes**
190,191,192	**rs61887821,rs11228219,rs4988321**	**3.30E-23**	**rs41494349**	**11**	**68115489**	**A**	**G**	**0.99**	**0.19**	**0.021**	**3.80E-20**	**missense_variant**	**MODERATE**	*LRP5*	**protein_coding**	**Q/R**	**cAg/cGg**	**Yes**
190,191,192	**rs61887821,rs11228219,rs4988321**	**3.30E-23**	**rs4988321**	**11**	**68174189**	**G**	**A**	**0.95**	**0.07**	**0.008**	**3.30E-23**	**missense_variant**	**MODERATE**	*LRP5*	**protein_coding**	**V/M**	**Gtg/Atg**	**Yes**
190,191,192,193	**rs61887821,rs11228219,rs4988321,rs5573**	**3.30E-23**	**rs61888960**	**11**	**68191036**	**G**	**A**	**0.99**	**0.20**	**0.024**	**3.00E-19**	**missense_variant**	**MODERATE**	*LRP5*	**protein_coding**	**R/Q**	**cGg/cAg**	**Yes**
190,191,192,193	rs61887821,rs11228219,rs4988321,rs5573	3.30E-23	rs3736228	11	68201295	C	T	0.85	0.04	0.005	6.50E-19	missense_varian	MODERATE	*LRP5*	protein_coding	A/V	gCg/gTg	No
193,194	rs557266652,rs3829241	4.50E-21	rs3750965	11	68840160	A	G	0.67	0.02	0.004	7.30E-10	missense_varian	MODERATE	*TPCN2*	protein_coding	K/R	aAa/aGa	No
193,194	**rs557266652,rs3829241**	**4.50E-21**	**rs3829241**	**11**	**68855363**	**G**	**A**	**0.60**	**-0.03**	**0.003**	**4.50E-21**	**missense_variant**	**MODERATE**	*TPCN2*	**protein_coding**	**G/E**	**gGg/gAg**	**Yes**
202	**rs10790255**	**1.30E-13**	**rs2276065**	**11**	**118530611**	**T**	**C**	**0.77**	**0.03**	**0.004**	**1.70E-13**	**missense_variant**	**MODERATE**	*TREH*	**protein_coding**	**T/A**	**Aca/Gca**	**Yes**
211,212	rs118115924,rs10875906	2.90E-36	rs11730071	12	49168798	C	A	0.97	0.09	0.010	3.00E-22	missense_varian	MODERATE	*ADCY6*	protein_coding	A/S	Gcc/Tcc	No
211,212	rs118115924,rs10875906	2.90E-36	rs11551274	12	49224108	G	C	0.97	0.10	0.010	1.50E-25	missense_varian	MODERATE	*DDX23*	protein_coding	Q/E	Cag/Gag	No
213	rs2279743	1.10E-11	rs35493121	12	57390038	T	C	0.92	0.04	0.006	6.20E-10	missense_varian	MODERATE	*GPR182*	protein_coding	C/R	Tgc/Cgc	No
213	rs2279743	1.10E-11	rs56298942	12	57391292	C	T	0.92	0.04	0.006	3.10E-10	missense_varian	MODERATE	*HBCBP*	protein_coding	T/I	aCa/aT	No
213	rs2279743	1.10E-11	rs17719344	12	57423934	G	A	0.92	0.04	0.006	6.60E-09	missense_varian	MODERATE	*MYO1A*	protein_coding	T/I	aCa/aTa	No
223,224	**rs58973023,rs2147166**	**2.60E-48**	**rs138818878**	**13**	**43148546**	**C**	**G**	**0.97**	**-0.07**	**0.010**	**8.20E-12**	**missense_variant**	**MODERATE**	*TNFSF11*	**protein_coding**	**P/R**	**cCt/cGt**	**Yes**
230	**rs1078514**	**1.40E-11**	**rs1805097**	**13**	**110435231**	**C**	**T**	**0.67**	**0.02**	**0.004**	**2.10E-11**	**missense_variant**	**MODERATE**	*IRS2*	**protein_coding**	**G/D**	**gGc/gAc**	**Yes**
231	**rs1042704**	**9.00E-14**	**rs1042704**	**14**	**23312594**	**G**	**A**	**0.79**	**0.03**	**0.004**	**9.00E-14**	**missense_variant**	**MODERATE**	*MMP14*	**protein_coding**	**D/N**	**Gat/Aat**	**Yes**
233,234	rs10130587,rs71446481	2.80E-72	rs17563	14	54417522	A	G	0.43	0.05	0.003	1.90E-50	stop_lost	HIGH	*BMP4*	protein_coding	*/R	Tga/Cga	No
233,234	rs10130587,rs71446481	2.80E-72	rs17563	14	54417522	A	G	0.43	0.05	0.003	1.90E-50	missense_varian	MODERATE	*BMP4*	protein_coding	V/A	gTg/gCg	No
236	rs35816040	3.40E-34	rs2272468	14	104029376	C	G	0.65	0.03	0.004	4.50E-17	missense_varian	MODERATE	*APOPT1*	protein_coding	P/A	Cct/Gct	No
236	rs35816040	3.40E-34	rs2272468	14	104029376	C	G	0.65	0.03	0.004	4.50E-17	missense_varian	MODERATE	*RP11-73M18.2*	protein_coding	P/A	Cct/Gct	No
236	rs35816040	3.40E-34	rs2272468	14	104029376	C	G	0.65	0.03	0.004	4.50E-17	missense_varian	MODERATE	*APOPT1*	protein_coding	P/R	cCc/cGc	No
236	rs35816040	3.40E-34	rs2272468	14	104029376	C	G	0.65	0.03	0.004	4.50E-17	missense_variant,NMD_transcript_varian	MODERATE	*APOPT1*	nonsense_mediated_decay	P/A	Cct/Gct	No
236	rs35816040	3.40E-34	rs861539	14	104165753	G	A	0.63	0.03	0.003	1.80E-14	missense_varian	MODERATE	*KRCC3*	protein_coding	T/M	aCg/aTg	No
242	rs11637971	1.20E-14	rs2589973	15	90892293	C	T	0.69	0.02	0.004	4.40E-11	missense_varian	MODERATE	*GABARAPL3*	protein_coding	R/K	aGg/aAg	No
242	rs11637971	1.20E-14	rs12589957	15	90903311	A	G	0.53	0.02	0.003	1.90E-10	missense_varian	MODERATE	*ZNF774*	protein_coding	N/S	aAt/aGt	No
242	rs11637971	1.20E-14	rs8033595	15	91083353	G	A	0.45	-0.02	0.003	2.40E-13	missense_varian	MODERATE	*CRTC3*	protein_coding	S/N	aGt/aAt	No
243,244	rs2301522,rs7137851	1.10E-25	rs117208012	16	347063	C	T	0.98	0.08	0.012	2.60E-11	missense_varian	MODERATE	*AXIN1*	protein_coding	G/S	Ggc/Agc	No
252	rs17680862	7.40E-20	rs61733768	16	67213950	G	A	0.97	0.08	0.010	2.00E-17	missense_variant,NMD_transcript_varian	MODERATE	*KIAA0895L*	nonsense_mediated_decay	S/F	tCc/tTc	No
252	**rs17680862**	**7.40E-20**	**rs17693761**	**16**	**67233243**	**G**	**A**	**0.97**	**0.08**	**0.010**	**6.30E-19**	**missense_variant**	**MODERATE**	*ELMO3*	**protein_coding**	**R/Q**	**cGg/cAg**	**Yes**
252	**rs17680862**	**7.40E-20**	**rs75193761**	**16**	**67233243**	**G**	**A**	**0.97**	**0.08**	**0.010**	**6.30E-19**	**missense_variant,NMD_transcript_variant**	**MODERATE**	*ELMO3*	**nonsense_mediated_decay**	**R/Q**	**cGg/cAg**	**Yes**
252	**rs17680862**	**7.40E-20**	**rs17680862**	**16**	**67322118**	**G**	**C**	**0.97**	**0.09**	**0.011**	**7.40E-20**	**missense_variant,NMD_transcript_variant**	**MODERATE**	*PLEKHG4*	**nonsense_mediated_decay**	**S/T**	**aGc/aCc**	**Yes**
252	**rs17680862**	**7.40E-20**	**rs17680862**	**16**	**67322118**	**G**	**C**	**0.97**	**0.09**	**0.011**	**7.40E-20**	**missense_variant**	**MODERATE**	*PLEKHG4*	**protein_coding**	**S/T**	**aGc/aCc**	**Yes**
256	rs35401268	2.10E-56	rs903160	17	2091765	C	T	0.69	-0.03	0.004	2.40E-15	missense_varian	MODERATE	*SMO6*	protein_coding	A/T	Gca/Aca	No
256	rs35401268	2.10E-56	rs216195	17	2203167	T	G	0.70	0.04	0.004	8.90E-33	missense_varian	MODERATE	*SMO6*	protein_coding	K/Q	Aag/Cag	No
257,258	**rs78180894,rs74439044**	**7.90E-10**	**rs34914463**	**17**	**7366619**	**T**	**C**	**0.87**	**0.03**	**0.005**	**7.70E-10**	**missense_variant**	**MODERATE**	*ZBTB4*	**protein_coding**	**N/S**	**aAt/aGt**	**Yes**
260	17:27961561_GATTATT_C	1.00E-15	rs2289629	17	27959903	G	A	0.66	0.03	0.004	5.60E-13	missense_varian	MODERATE	*SSH2*	protein_coding	S/L	tCg/tTg	No
260	17:27961561_GATTATT_C	1.00E-15	rs9897794	17	28296327	T	G	0.52	-0.02	0.003	1.20E-11	missense_varian	MODERATE	*EFCAB5*	protein_coding	L/V	Ttg/Gtg	No
260	17:27961561_GATTATT_C	1.00E-15	rs9897794	17	28296327	T	G	0.52	-0.02	0.003	1.20E-11	missense_variant,NMD_transcript_varian	MODERATE	*EFCAB5*	nonsense_mediated_decay	L/V	Ttg/Gtg	No
262	**rs143043662**	**4.20E-10**	**rs143043662**	**17**	**39913771**	**C**	**T**	**0.99**	**-0.09**	**0.015**	**4.20E-10**	**missense_variant**	**MODERATE**	*JUP*	**protein_coding**	**V/I**	**Gtc/Atc**	**Yes**
263,264,265	**rs7209826,rs188810925,rs17063**	**2.30E-36**	**rs228757**	**17**	**42164885**	**G**	**C**	**0.26**	**0.03**	**0.004**	**2.10E-16**	**missense_variant**	**MODERATE**	*HDAC5*	**protein_coding**	**D/E**	**gaC/gaG**	**Yes**
263,264,265	rs7209826,rs188810925,rs17063	2.30E-36	rs227584	17	42225547	A	C	0.70	-0.03	0.004	1.00E-12	missense_varian	MODERATE	*C17orf53*	protein_coding	T/P	Aca/Cca	No
263,264,265	rs7209826,rs188810925,rs17063	2.30E-36	rs7220138	17	42254011	C	G	0.70	-0.03	0.004	2.50E-12	splice_acceptor_variant,non_coding_transcript_variar	HIGH	*ASB16-AS1*	antisense	-	-	No
263,264,265	rs7209826,rs188810925,rs17063	2.30E-36	rs7212573	17	42254281	A	G	0.71	-0.03	0.004	1.80E-12	missense_varian	MODERATE	*ASB16*	protein_coding	T/A	Acg/Gcg	No
263,264,265	rs7209826,rs188810925,rs17063	2.30E-36	rs7212573	17	42254281	A	G	0.71	-0.03	0.004	1.80E-12	missense_variant,NMD_transcript_varian	MODERATE	*ASB16*	nonsense_mediated_decay	T/A	Acg/Gcg	No
263,264,265	rs7209826,rs188810925,rs17063

Supplementary Table 9.Results from statistical fine-mapping of autosomal loci using FINEMAP, functional annotation using Chisae I hypersensitivity site data from 115 cell types, CATO score annotation, and possible target genes identified from/in -eQTL analyses in 95 primary human osteoblasts

locus	snp	# s	snp	RSNP#	RSNP# PREDICTED CAUSAL	RSNP# PLAUSIBLE CAUSAL*	RSNP# OVERLAP SNP	FINE MAPPED RESULTS	RSNP# STRONG CATO** SCORE	GTEx EVIDENCE IN SYNTHBLAST***
1	rs2298633	1.56e-12	chr1:150839798-150910293	7925	1	4	3	chr1:150904994-150917439	0	CSDP1%2CMRTA1
1	rs2738632	1.97E-15	chr1:7864263-8964143	9264	3	11	5	chr1:8314199-8910555	0	SLC4A1%2CCNN1
1	rs10888896	1.98e-06	chr1:23510964-23530972	6761	1	1	1	chr1:23530972-23530972	0	ATP1A1
1	rs6701290	3.14e-11	chr1:16468729-16496201	6787	1	18	8	chr1:14957394-16511227	0	CSDP%2CMIR4539
1	rs7512869	1.36E-06	chr1:237159964-237571716	7394	6	42	17	chr1:23137964-23716581	2	ALPL%2CEIF2CL%2FSSU1A1A%2PHKA%2MRPS1 MRTA
1	1:23181834_T_C	3.16E-08	chr1:23180170-23180411	7262	6	43	17	chr1:23137964-23716581	2	ALPL%2CEIF2CL%2FSSU1A1A%2PHKA%2MRPS1 MRTA
1	rs28635398	1.27E-01	chr1:23310962-23318972	7229	6	42	17	chr1:23172506-23716581	2	ALPL%2CEIF2CL%2FSSU1A1A%2PHKA%2MRPS1 MRTA
1	rs11364302	1.19E-12	chr1:23229922-23229943	6971	6	41	17	chr1:23172506-23716581	2	ALPL%2CEIF2CL%2FSSU1A1A%2PHKA%2MRPS1 MRTA
1	rs6588535	3.19E-03	chr1:25621780-27412355	8871	2	10	3	chr1:27020212-27303864	0	CSDP1%2CSHOD1%2DHC18
1	rs6588536	3.19E-03	chr1:25621780-27412355	8872	2	10	3	chr1:27020212-27303864	0	-
1	rs2975257	6.76e-19	chr1:28331916-28329962	6368	5	31	9	chr1:30985253-30996716	0	-
1	rs10132370	1.45E-16	chr1:30164025-30164092	6366	5	31	9	chr1:30985253-30996716	0	-
1	rs11265618	9.85e-17	chr1:30253998-30259841	6371	5	31	9	chr1:30985253-30996716	0	-
1	rs34698212	7.96E-11	chr1:30971372-30971513	6981	1	22	1	chr1:30322234-30922832	0	CCBL2
1	rs2980888	1.96E-11	chr1:30971372-30971513	6981	1	22	1	chr1:30322234-30922832	0	CCBL2
1	rs6685737	1.43E-16	chr1:33822548-33931413	7276	2	18	8	chr1:33337619-33922832	0	TCTL
1	rs2800788	5.48E-12	chr1:33337429-34437466	6292	1	8	3	chr1:33337619-34437466	0	SPAG17
1	rs2853079	9.30E-01	chr1:17533619-17718132	6896	2	15	4	chr1:17533428-17989149	0	C1ORF126,KIF4PC1C1,SEPC
1	rs2316183	9.12E-14	chr1:17717536-17728216	6120	1	6	3	chr1:17432896-17728379	0	DNAH
1	rs2316182	1.12E-13	chr1:17717536-17728216	6121	1	6	3	chr1:17432896-17728379	0	DNAH,CHD1,PKP3
1	rs7514171	8.73E-12	chr1:28966679-28966679	6472	1	11	7	C1ORF127,MIA3,SMYD3	0	C1ORF127,MIA3,SMYD3
1	rs2741738	2.35E-11	chr1:216899953-216989997	8164	1	9	2	chr1:216952181-216989997	0	-
1	rs2811628	1.56E-16	chr1:235610526-235642161	6851	1	24	5	chr1:234778858-235011715	0	IRF6,TLR5,IRF6,1,TRAL4,1
1	rs2275707	3.43E-15	chr1:235660526-235687930	6827	3	33	5	chr1:234778858-235011715	1	IRF6,TLR5,IRF6,1,TRAL4,1
1	rs7527355	5.75E-18	chr1:235977984-235977192	6828	2	9	4	chr1:235161814-235187265	0	C1ORF116,IRAK3,IRF2
1	rs1410960	2.15E-05	chr1:235997764-235995320	7855	1	1	1	chr1:235820303-235820320	1	-
1	rs1410961	2.15E-05	chr1:235997764-235995320	7856	1	1	1	chr1:235820303-235820320	1	-
1	rs6414793	2.09E-12	chr1:28227321-29237513	6362	2	19	6	chr1:29031546-29041150	0	PLCB2%2P
1	rs2035958	2.20E-16	chr1:30155679-31153013	7973	2	19	3	chr1:30926705-30992688	0	-
1	rs2035957	1.17E-15	chr1:30155679-31153013	7974	2	19	3	chr1:30926705-30992688	0	-
1	rs2076680	1.17E-15	chr1:30155679-31153013	7975	2	19	3	chr1:30926705-30992688	0	-
1	rs2076682	1.20E-11	chr1:30155679-31153013	7976	2	19	3	chr1:30926705-30992688	0	-
1	rs2034329	1.26E-11	chr1:30155679-31153013	7977	2	19	3	chr1:30926705-30992688	0	-
1	rs2034328	1.26E-11	chr1:30155679-31153013	7978	2	19	3	chr1:30926705-30992688	0	-
1	rs2034327	1.26E-11	chr1:30155679-31153013	7979	2	19	3	chr1:30926705-30992688	0	-
1	rs2034326	1.26E-11	chr1:30155679-31153013	7980	2	19	3	chr1:30926705-30992688	0	-
1	rs2034325	1.26E-11	chr1:30155679-31153013	7981	2	19	3	chr1:30926705-30992688	0	-
1	rs2034324	1.26E-11	chr1:30155679-31153013	7982	2	19	3	chr1:30926705-30992688	0	-
1	rs2034323	1.26E-11	chr1:30155679-31153013	7983	2	19	3	chr1:30926705-30992688	0	-
1	rs2034322	1.26E-11	chr1:30155679-31153013	7984	2	19	3	chr1:30926705-30992688	0	-
1	rs2034321	1.26E-11	chr1:30155679-31153013	7985	2	19	3	chr1:30926705-30992688	0	-
1	rs2034320	1.26E-11	chr1:30155679-31153013	7986	2	19	3	chr1:30926705-30992688	0	-
1	rs2034319	1.26E-11	chr1:30155679-31153013	7987	2	19	3	chr1:30926705-30992688	0	-
1	rs2034318	1.26E-11	chr1:30155679-31153013	7988	2	19	3	chr1:30926705-30992688	0	-
1	rs2034317	1.26E-11	chr1:30155679-31153013	7989	2	19	3	chr1:30926705-30992688	0	-
1	rs2034316	1.26E-11	chr1:30155679-31153013	7990	2	19	3	chr1:30926705-30992688	0	-
1	rs2034315	1.26E-11	chr1:30155679-31153013	7991	2	19	3	chr1:30926705-30992688	0	-
1	rs2034314	1.26E-11	chr1:30155679-31153013	7992	2	19	3	chr1:30926705-30992688	0	-
1	rs2034313	1.26E-11	chr1:30155679-31153013	7993	2	19	3	chr1:30926705-30992688	0	-
1	rs2034312	1.26E-11	chr1:30155679-31153013	7994	2	19	3	chr1:30926705-30992688	0	-
1	rs2034311	1.26E-11	chr1:30155679-31153013	7995	2	19	3	chr1:30926705-30992688	0	-
1	rs2034310	1.26E-11	chr1:30155679-31153013	7996	2	19	3	chr1:30926705-30992688	0	-
1	rs2034309	1.26E-11	chr1:30155679-31153013	7997	2	19	3	chr1:30926705-30992688	0	-
1	rs2034308	1.26E-11	chr1:30155679-31153013	7998	2	19	3	chr1:30926705-30992688	0	-
1	rs2034307	1.26E-11	chr1:30155679-31153013	7999	2	19	3	chr1:30926705-30992688	0	-
1	rs2034306	1.26E-11	chr1:30155679-31153013	8000	2	19	3	chr1:30926705-30992688	0	-
1	rs2034305	1.26E-11	chr1:30155679-31153013	8001	2	19	3	chr1:30926705-30992688	0	-
1	rs2034304	1.26E-11	chr1:30155679-31153013	8002	2	19	3	chr1:30926705-30992688	0	-
1	rs2034303	1.26E-11	chr1:30155679-31153013	8003	2	19	3	chr1:30926705-30992688	0	-
1	rs2034302	1.26E-11	chr1:30155679-31153013	8004	2	19	3	chr1:30926705-30992688	0	-
1	rs2034301	1.26E-11	chr1:30155679-31153013	8005	2	19	3	chr1:30926705-30992688	0	-
1	rs2034300	1.26E-11	chr1:30155679-31153013	8006	2	19	3	chr1:30926705-30992688	0	-
1	rs2034299	1.26E-11	chr1:30155679-31153013	8007	2	19	3	chr1:30926705-30992688	0	-
1	rs2034298	1.26E-11	chr1:30155679-31153013	8008	2	19	3	chr1:30926705-30992688	0	-
1	rs2034297	1.26E-11	chr1:30155679-31153013	8009	2	19	3	chr1:30926705-30992688	0	-
1	rs2034296	1.26E-11	chr1:30155679-31153013	8010	2	19	3	chr1:30926705-30992688	0	-
1	rs2034295	1.26E-11	chr1:30155679-31153013	8011	2	19	3	chr1:30926705-30992688	0	-
1	rs2034294	1.26E-11	chr1:30155679-31153013	8012	2	19	3	chr1:30926705-30992688	0	-
1	rs2034293	1.26E-11	chr1:30155679-31153013	8013	2	19	3	chr1:30926705-30992688	0	-
1	rs2034292	1.26E-11	chr1:30155679-31153013	8014	2	19	3	chr1:30926705-30992688	0	-
1	rs2034291	1.26E-11	chr1:30155679-31153013	8015	2	19	3	chr1:30926705-30992688	0	-
1	rs2034290	1.26E-11	chr1:30155679-31153013	8016	2	19	3	chr1:30926705-30992688	0	-
1	rs2034289	1.26E-11	chr1:30155679-31153013	8017	2	19	3	chr1:30926705-30992688	0	-
1	rs2034288	1.26E-11	chr1:30155679-31153013	8018	2	19	3	chr1:30926705-30992688	0	-
1	rs2034287	1.26E-11	chr1:30155679-31153013	8019	2	19	3	chr1:30926705-30992688	0	-
1	rs2034286	1.26E-11	chr1:30155679-31153013	8020	2	19	3	chr1:30926705-30992688	0	-
1	rs2034285	1.26E-11	chr1:30155679-31153013	8021	2	19	3	chr1:30926705-30992688	0	-
1	rs2034284	1.26E-11	chr1:30155679-31153013	8022	2	19	3	chr1:30926705-30992688	0	-
1	rs2034283	1.26E-11	chr1:30155679-31153013	8023	2	19	3	chr1:30926705-30992688	0	-
1	rs2034282	1.26E-11	chr1:30155679-31153013	8024	2	19	3	chr1:30926705-30992688	0	-
1	rs2034281	1.26E-11	chr1:30155679-31153013	8025	2	19	3	chr1:30926705-30992688	0	-
1	rs2034280	1.26E-11	chr1:30155679-31153013	8026	2	19	3	chr1:30926705-30992688	0	-
1	rs2034279	1.26E-11	chr1:30155679-31153013	8027	2	19	3	chr1:30926705-30992688	0	-
1	rs2034278	1.26E-11	chr1:30155679-31153013	8028	2	19	3	chr1:30926705-30992688	0	-
1	rs2034277	1.26E-11	chr1:30155679-31153013	8029	2	19	3	chr1:30926705-30992688	0	-
1	rs2034276	1.26E-11	chr1:30155679-31153013	8030	2	19	3	chr1:30926705-30992688	0	-
1	rs2034275	1.26E-11	chr1:30155679-31153013	8031	2	19	3	chr1:30926705-30992688	0	-
1	rs2034274	1.26E-11	chr1:30155679-31153013	8032	2	19	3	chr1:30926705-30992688	0	-
1	rs2034273	1.26E-11	chr1:30155679-31153013	8033	2	19	3	chr1:30926705-30992688	0	-
1	rs2034272	1.26E-11	chr1:30155679-31153013	8034	2	19	3	chr1:30926705-30992688	0	-
1	rs2034271	1.26E-11	chr1:30155679-31153013	8035	2	19	3	chr1:30926705-30992688	0	-
1	rs2034270	1.26E-11	chr1:30155679-31153013	8036	2	19	3	chr1:30926705-30992688	0	-
1	rs2034269	1.26E-11	chr1:30155679-31153013	8037	2	19	3	chr1:30926705-30992688	0	-
1	rs2034268	1.26E-11	chr1:30155679-31153013	8038	2	19	3	chr1:30926705-30992688	0	-
1	rs2034267	1.26E-11	chr1:30155679-31153013	8039	2	19	3	chr1:30926705-30992688	0	-
1	rs2034266	1.26E-11	chr1:30155679-31153013	8040	2	19	3	chr1:30926705-30992688	0	-
1	rs2034265	1.26E-11	chr1:30155679-31153013	8041	2	19	3	chr1:30926705-30992688	0	-
1	rs2034264	1.26E-11	chr1:30155679-31153013	8042	2	19	3	chr1:30926705-30992688	0	-
1	rs2034263	1.26E-11	chr1:30155679-31153013	8043	2	19	3	chr1:30926705-30992688	0	-
1	rs2034262	1.26E-11	chr1:30155679-31153013	8044	2	19	3	chr1:30926705-30992688	0	-
1	rs2034261	1.26E-11	chr1:30155679-31153013	8045	2	19	3	chr1:30926705-30992688	0	-
1	rs2034260	1.26E-11	chr1:30155679-31153013	8046	2	19	3	chr1:30926705-30992688	0	-
1	rs2034259	1.26E-11	chr1:30155679-31153013	8047	2	19	3	chr1:30926705-30992688	0	-
1	rs2034258	1.26E-11	chr1:30155679-31153013	8048	2	19	3	chr1:30926705-30992688	0	-
1	rs2034257	1.26E-11	chr1:30155679-31153013	8049	2	19	3	chr1:30926705-30992688	0	-
1	rs2034256	1.26E-11	chr1:30155679-31153013	8050	2	19	3	chr1:30926705-30992688	0	-
1	rs2034255	1.26E-11	chr1:30155679-31153013	8051	2	19	3	chr1:30926705-30992688	0	-
1	rs2034254	1.26E-11	chr1:30155679-31153013	8052	2	19	3	chr1:30926705-30992688	0	-
1	rs2034253	1.26E-11	chr1:30155679-31153013	8053	2	19	3	chr1:30926705-30992688	0	-
1	rs2034252	1.26E-11	chr1:30155679-31153013	8054	2	19	3	chr1:30926705-30992688	0	-
1	rs2034251	1.26E-11	chr1:30155679-31153013	8055	2	19	3	chr1:30926705-30992688	0	-
1	rs2034250	1.26E-11	chr1:30155679-31153013	8056	2	19	3	chr1:30926705-30992688	0	-
1	rs2034249	1.26E-11	chr1:30155679-31153013	8057	2	19	3	chr1:30926705-30992688	0	-
1	rs2034248	1.26E-11	chr1:30155679-31153013	8058	2	19	3	chr1:30926705-30992688	0	-
1	rs2034247	1.26E-11	chr1:30155679-31153013	8059	2	19	3	chr1:30926705-30992688	0	-
1	rs2034246	1.26E-11	chr1:30155679-31153013	8060	2	19	3	chr1:30926705-30992688	0	-
1	rs2034245	1.26E-11	chr1:30155679-31153013	8061	2	19	3	chr1:30926705-30992688	0	-
1	rs2034244	1.26E-11	chr1:30155679-31153013	8062	2	19	3	chr1:30926705-30992688	0	-
1	rs2034243	1.26E-11	chr1:30155679-31153013	8063	2	19	3	chr1:30926705-30992688	0	-
1	rs2034242	1.26E-11	chr1:30155679-31153013	8064	2	19	3	chr1:30926705-30992688	0	-
1	rs2034241	1.26E-11	chr1:30155679-31153013	8065	2	19	3	chr1:30926705-30992688	0	-
1	rs2034240	1.26E-11	chr1:30155679-31153013	8066	2	19	3	chr1:30926705-30992688	0	-
1	rs2034239	1.26E-11	chr1:30155679-31153013	8067	2	19	3	chr1:30926705-30992688	0	-
1	rs2034238	1.26E-11	chr1:30155679-31153013	8068	2	19	3	chr1:30926705-30992688	0	-
1	rs2034237	1.26E-11	chr1:30155679-31153013	8069	2	19	3	chr1:30926705-30992688	0	-
1	rs2034236	1.26E-11	chr1:30155679-31153013	8070	2	19	3	chr1:30926705-30992688	0	-
1	rs2034235	1.26E-11	chr1:30155679-31153013	8071	2	19	3	chr1:30926705-30992688	0	-
1	rs2034234	1.26E-11	chr1:30155679-31153013	8072	2	19	3	chr1:30926705-30992688	0	-
1	rs2034233	1.26E-11	chr1:30155679-31153013	8073	2	19	3	chr1:30926705-30992688	0	-
1	rs2034232	1.26E-11	chr1:30155679-31153013	8074	2	19	3	chr1:30926705-30992688	0	-
1	rs2034231	1.26E-11	chr1:30155679-31153013	8075	2	19	3	chr1:30926705-30992688	0	-
1	rs2034230	1.26E-11	chr1:30155679-31153013	8076	2	19	3	chr1:30926705-30992688	0	-
1	rs2034229	1.26E-11	chr1:30155679-31153013	8077	2	19	3	chr1:30926705-30992688	0	-
1	rs2034228	1.26E-11	chr1:30155679-31153013	8078	2	19	3	chr1:30926705-30992688	0	-
1	rs2034227	1.26E-11	chr1:30155679-31153013	8079	2	19	3	chr1:30926705-30992688	0	-
1	rs2034226	1.26E-11	chr1:30155679-31153013	8080	2	19	3	chr1:30926705-30992688	0	-
1	rs2034225	1.26E-11	chr1:30155679-31153013	8081	2	19	3	chr1:30926705-30992688	0	-
1	rs2034224	1.26E-11	chr1:30155679-31153013	8082	2	19	3	chr1:30926705-30992688	0	-
1	rs2034223	1.26E-11	chr1:30155679-31153013	8083	2	19	3	chr1:30926705-30992688	0	-
1	rs2034222	1.26E-11	chr1:30155679-31153013	8084	2	19	3	chr1:30926705-30992688	0	-
1	rs2034221	1.26E-11	chr1:30155679-31153013	8085	2	19	3	chr1:30926705-30992688	0	-
1	rs2034220	1.26E-11	chr1:30155679-31153013	8086	2	19	3	chr1:30926705-30992688	0	-
1	rs2034219	1.26E-11	chr1:30155679-31153013	8087	2	19	3	chr1:30926705-30992688	0	-
1	rs2034218	1.26E-11	chr1:30155679-31153013	8088	2	19	3	chr1:30926705-30992688	0	-
1	rs2034217	1.26E-11	chr1:30155679-31153013	8089	2	19	3	chr1:30926705-30992688	0	-
1	rs2034216	1.26E-11	chr1:30155679-31153013	8090	2	19	3	chr1:30926705-30992688	0	-
1	rs2034215	1.26E-11	chr1:30155679-31153013	8091	2	19	3	chr1:30926705-30992688	0	-
1	rs2034214	1.26E-11	chr1:30155679-31153013	8092	2	19	3	chr1:30926705-30992688	0	-
1	rs2034213	1.26E-11	chr1:30155679-31153013	8093	2	19	3	chr1:30926705-30992688	0	-
1	rs2034212	1.26E-11	chr1:30155679-31153013	8094	2	19	3	chr1:30926705-30992688	0	-
1	rs2034211	1.26E-11	chr1:30155679-31153013	8095	2	19	3	chr1:30926705-30992688	0	-
1	rs2034210	1.26E-11	chr1:30155679-31153013	8096	2	19	3	chr1:30926705-30992688	0	-
1	rs2034209	1.26E-11	chr1:30155679-31153013	8097	2	19	3	chr1:30926705-30992688	0	-
1	rs2034208	1.26E-11	chr1:30155679-31153013	8098	2	19	3	chr1:30926705-30992688	0	-
1	rs2034207	1.26E-11	chr1:30155679-31153013	8099	2	19	3	chr1:30926705-30992688	0	-
1	rs2034206	1.26E-11	chr1:30155679-31153013	8100	2	19	3	chr1:30926705-30992688	0	-
1	rs2034205	1.26E-11	chr1:30155679-31153013	8101	2	19	3	chr1:30926705-30992688	0	-
1	rs2034204	1.26E-11	chr1:30155679-31153013	8102	2	19	3	chr1:30926705-30992688	0	-
1	rs2034203	1.26E-11	chr1:30155679-31153013	8103	2	19	3	chr1:30926705-30992688	0	-
1	rs2034202	1.26E-11	chr1:30155679-31153013	8104	2	19	3	chr1:30926705-30992688	0	-
1	rs2034201	1.26E-11	chr1:30155679-31153013	8105	2	19	3	chr1:30926705-30992688	0	-
1	rs2034200	1.26E-11	chr1:30155679-31153013	8106	2	19	3	chr1:30926705-30992688	0	-
1	rs2034199	1.26E-11	chr1:30155679-31153013	8107	2	19	3	chr1:30926705-30992688	0	-
1	rs2034198	1.26E-11	chr1:30155679-31153013	8108	2	19	3	chr1:30926705-30992688	0	-
1	rs2034197	1.26E-11	chr1:30155679-31153013	8109	2	19	3	chr1:30926705-30992688	0	-
1	rs2034196	1.26E-11	chr1:30155679-31153013	8110	2	19	3	chr1:30926705-30992688	0	-
1	rs2034195	1.26E-11	chr1:30155679-31153013	8111	2	19	3	chr1:30926705-30992688	0	-
1	rs2034194	1.26E-11	chr1:30155679-31153013	8112	2	19	3	chr1:30926705-30992688	0	-
1	rs2034193	1.26E-11	chr1:30155679-31153013	8113	2	19	3	chr1:30926705-30992688	0	-
1	rs2034192	1.26E-11	chr1:30155679-31153013	8114	2	19	3	chr1:30926705-30992688	0	-
1	rs2034191	1.26E-11	chr1:30155679-31153013	8115	2	19	3	chr1:30926705-30992688	0	-
1	rs2034190	1.26E-11	chr1:30155679-31153013	8116	2	19	3	chr1:30926705-30992688	0	-
1	rs2034189	1.26E-11	chr1:30155679-31153013	8117	2	19	3	chr1:30926705-30992688	0	-
1	rs2034188	1.26E-11	chr1:30155679-31153013	8118	2	19	3	chr1:30926705-30992688	0	-
1	rs2034187	1.26E-11	chr1:30155679-31153013	8119	2	19	3	chr1:30926705-30992688	0	-
1	rs2034186	1.26E-11	chr1:30155679-31153013	8120	2	19	3	chr1:30926705-30992688	0	-
1	rs2034185	1.26E-11	chr1:30155679-31153013	8121	2	19	3	chr1:30926705-30992688	0	-
1	rs2034184	1.26E-11	chr1:30155679-31153013	8122	2	19	3	chr1:30926705-30992688	0	-
1	rs2034183	1.26E-11	chr1:30155679-31153013	8123	2	19	3	chr1:30926705-30992688	0	-
1	rs2034182	1.26E-11	chr1:30155679-31153013	8124	2	19	3	chr1:30926705-30992688	0	-
1	rs2034181	1.26E-11	chr1:30155679-31153013	8125	2	19	3	chr1:30926705-30992688	0	-
1	rs2034180	1.26E-11	chr1:30155679-31153013	8126	2	19	3	chr1:30926705-30992688	0	-
1	rs2034179	1.26E-11	chr1:30155679-31153013	8127	2	19	3	chr1:30926705-30992688	0	-
1	rs2034178	1.26E-11	chr1:30155679-31153013	8128	2	19	3	chr1:30926705-30992688	0	-
1	rs2034177	1.26E-11	chr1:30155679-31153013	8129	2	19	3	chr1:30926705-30992688	0	-
1	rs2034176	1.26E-11	chr1:30155679-31153013	8130	2	19	3	chr1:30926705-30992688	0	-
1	rs2034175	1.26E-11	chr1:30155679-31153013	8131	2	19	3	chr1:30926705-30992688	0	-
1	rs2034174	1.26E-11	chr1:30155679-31153013	8132	2	19	3	chr1:30926705-30992688	0	-
1	rs2034173	1.26E-11	chr1:30155679-31153013	8133	2	19	3	chr1:30926705-30992688	0	-
1	rs2034172	1.26E-11	chr1:30155679-31153013	8134	2	19	3	chr1:30926705-30992688	0	-
1	rs2034171	1.26E-11	chr1:30155679-31153013	8135	2	19	3	chr1:30926705-30992688	0	-
1	rs2034170	1.26E-11	chr1:30155679-31153013	8136	2	19	3	chr1:30926705-30992688	0	-
1	rs2034169	1.26E-11	chr1:30155679-31153013	8137	2	19	3	chr1:30926705-30992688	0	-
1	rs2034168	1.26E-11	chr1:30155679-31153013	8138	2	19	3	chr1:30926705-30992688	0	-
1	rs2034167	1.26E-11	chr1:30155679-31153013	8139	2	19	3	chr1:30926705-30992688	0	-
1	rs2034166	1.26E-11	chr1:30155679-31153013	8140	2	19	3	chr1:30926705-30992688	0	-
1	rs2034165	1.26E-11	chr1:30155679-31153013	8141	2	19	3	chr1:30926705-30992688	0	-
1	rs2034164	1.26E-11	chr1:30155679-31153013	8142	2	19	3	chr1:30926705-30992688	0	-
1	rs2034163	1.26E-11	chr1:30155679-31153013	8143	2	19	3	chr1:30926705-30992688	0	-
1	rs2034162	1.26E-11	chr1:30155679-31153013	8144	2	19	3	chr1:30926705-30992688	0	-
1	rs2034161	1.26E-11	chr1:30155679-31153013	8145	2	19	3	chr1:30926705-30992688	0	-
1	rs2034160	1.26E-11	chr1:30155679-31153013	8146	2	19	3	chr1:30926705-30992688	0	-
1	rs2034159	1.26E-11	chr1:30155679-31153013	8147	2	19	3	chr1:30926705-30992688	0	-
1	rs2034158	1.26E-11	chr1:30155679-31153013	8148	2	19	3	chr1:30926705-30992688	0	-
1	rs2034157	1.26E-11	chr1:30155679-31153013	8149	2	19	3	chr1:30926705-30992688	0	-
1	rs2034156	1.26E-11	chr1:30155679-31153013	8150	2	19	3	chr1:30926705-30992688	0	-
1	rs2034155	1.26E-11	chr1:30155679-31153013	8151	2	19	3	chr1:30926705-30992688	0	-
1	rs2034154	1.26E-11	chr1:30155679-31153013	8152	2	19	3	chr1:30926705-30992688	0	-
1	rs2034153	1.26E-11	chr1:30155679-31153013	8153	2	19	3	chr1:30926705-30992688	0	-
1	rs2034152	1.26E-11	chr1:30155679-31153013	8154	2	19	3	chr1:30926705-30992688	0	-
1	rs2034151	1.26E-11	chr1:30155679-31153013	8155	2	19	3	chr1:30926705-30992688	0	-
1	rs2034150	1.26E-11	chr1:30155679-31153013	8156	2	19	3	chr1:30926705-30992688	0	-
1	rs2034149	1.26E-11	chr1:30155679-31153013	8157	2	19	3	chr1:30926705-30992688	0	-
1	rs2034148	1.26E-11	chr1:30155679-31153013	8158	2	19	3	chr1:30926705-30992688	0	-
1	rs2034147	1.26E-11	chr1:30155679-31153013	8159	2	19	3	chr1:30926705-30992688	0	-
1	rs2034146	1.26E-11	chr1:30155679-31153013	8160	2	19	3	chr1:30926705-30992688	0	-
1	rs2034145

Supplementary Table 10. Association results with subgroups of allele and of mean recombination

| Marker | Chromosome | Position | Reference allele | Effect allele | Effect allele frequency | Sample size | Beta | Standard error | P-value | Heterozygosity | Beta | Standard error | P-value | Mean recombination | Beta | Standard error | P-value | Mean recombination | Beta | Standard error | P-value | Mean recombination

Supplementary Table 11. DEPICT Gene prioritization (FDR < 5%).

DEPICT GENE PRIORITIZATION									ACTIONABLE CONDITIONALLY INDEPENDENT eSNP2 ASSOCIATED VARIANT			
RSID	ASSOC	P_{ASSOC}	#GENES	ENSEMBL GENE ID	GENE SYMBOL	P_{GENE}	FDR	INDEX	D_DIST	LOCUS SIZE	LOCUS_ID	
rs11200816-2685931	rs12960321	3.66E-14	2	ENSG00000171723	LRIC3/B3GAT3	1.98E-04	<=0.01	1	53412	1	LRIC3/B3GAT3	
rs4073868-68677702	rs17630826 or rs1581418	8.45E-10	2	ENSG00000145399	RERE	4.66E-04	<=0.01	0	0	2	RERE	
rs11027414-11595156	rs12585492	3.20E-10	8	ENSG00000171818	ANGPTL7	5.24E-06	<=0.01	0	0	3	ANGPTL7	
rs17850427-58139111	rs1391731	9.01e-10	1	ENSG00000284592	TARDBP	2.76e-01	<=0.01	1	none	4	SPATS1	
rs11161656-15320627	rs8121269	2.29E-10	3	ENSG00000265326	SPIDR	4.27E-13	<=0.01	0	0	4	SPIDR	
rs17630826-81569900	rs12454317	2.79E-10	5	ENSG00000182551	KLF5	3.99E-12	<=0.01	0	59765	5	WNT5*	
rs12220497-22410942	rs7515859 or rs12308811 or rs7137559	4.62E-10	5	ENSG00000162552	WNT5	2.99E-09	<=0.01	2	2044	5	WNT5*	
rs7734777-54947939	rs4766228 or rs6825958 or rs7736671	7.18E-10	2	ENSG00000124671	ZBTB40	6.63E-04	<=0.01	0	40852	6	WNT5*	
rs17252324-27327167	rs2010168	1.90E-11	8	ENSG00000117713	ARID3A	2.03E-09	<=0.01	0	0	4	ARID3A	
rs17252324-27327167	rs2010168	1.90E-11	8	ENSG00000117724	CCNT2	1.15E-03	<=0.01	0	0	4	ARID3A	
rs17252324-27327167	rs2010168	1.90E-11	8	ENSG00000275257	C1orf122	1.15E-03	<=0.01	0	0	4	ARID3A	
rs11262436-28012419	rs4430484	8.00E-10	3	ENSG00000163286	FRL2	1.88E-05	<=0.01	0	0	4	FRL2	
rs11466141-68588803	rs14243220 or rs1837512 or rs7552	1.18E-09	2	ENSG00000160339	WLS	6.18E-10	<=0.01	0	0	4	WLS*	
rs11891-68458826	rs284808	1.20E-11	4	ENSG00000002243	PKN2	2.05E-10	<=0.01	0	0	5	PKN2	
rs11726256-74113258	rs2296398	1.20e-10	6	ENSG00000138280	WWOX	2.01e-08	<=0.01	0	0	10	WWOX	
rs11535962-112505938	rs3760608	1.20E-10	6	ENSG00000134245	WNT5B	1.60E-07	<=0.01	10	0	10	WNT5B	
rs11535962-112505938	rs3760608	1.20E-10	6	ENSG00000138263	MTA3	9.57E-05	<=0.01	10	0	10	WNT5B	
rs11394386-119818586	rs6565137 or rs7139453	1.93E-10	3	ENSG00000213063	-	5.07E-04	<=0.01	0	0	11	TBX15	
rs11394386-119818586	rs6565137 or rs7139453	1.93E-10	3	ENSG00000265507	TBX15	4.15E-10	<=0.01	0	0	11	TBX15	
rs11726256-74113258	rs2414318	3.43E-10	6	ENSG00000197132	WWOX	9.98E-08	<=0.01	0	0	19	PAWR	
rs12220497-22410942	rs7515859	3.70E-10	5	ENSG00000162552	WNT5	2.99E-09	<=0.01	2	2044	5	WNT5*	
rs4073868-68677702	rs1581418	8.45E-10	2	ENSG00000145399	RERE	4.66E-04	<=0.01	0	0	2	RERE	
rs12957273-52168765	rs4844986	2.05E-10	3	ENSG00000259329	SNX9/CCR5	1.09E-05	<=0.01	0	0	14	CKAP2/SS	
rs12957273-52168765	rs7935122 or rs7935400	1.49E-10	2	ENSG00000118200	CKAP2/KY2	1.80E-07	<=0.01	0	20955	15	CKAP2/KY2	
rs11210156-119846438	rs7318171	9.85E-10	1	ENSG00000283360	HAAT	1.05E-03	<=0.01	0	34660	16	HAAT	
rs11210156-119846438	rs7327350	1.75E-10	1	ENSG00000188382	HLX	4.55E-06	<=0.01	25	418620	19	HLX	
rs12-42215160-42265648	rs7574668 or rs16722979	1.53E-09	1	ENSG00000163879	PKDCC	1.45E-12	<=0.01	24	48317	24	PKDCC*	
rs12-42265648-43822183	rs17230845	2.73E-11	2	ENSG00000152518	ZFP36L2	2.72E-09	<=0.01	0	0	25	ZFP36L2	
rs5012478-55126701	rs9635628 or rs7854854 or rs7843139	1.03E-10	10	ENSG00000138139	-	3.25E-07	<=0.01	0	0	26	SPTBN5*	
rs5012478-55228702	rs6533539 or rs73854854 or rs7427291	1.26E-10	10	ENSG00000152256	SPTBN2	1.23E-04	<=0.01	22	0	26	SPTBN5*	
rs11785936766-118652249	rs61738964 or rs78322224 or rs17850427	1.28E-10	1	ENSG00000163464	EIF3J	1.70E-06	<=0.01	23	59116	28	HNT	
rs11596263166-118599115	rs34588501	1.73E-09	1	ENSG00000151163	ITGA12	8.72E-03	<=0.01	40	0	29	TANK3	
rs11596263166-118599115	rs34588501	1.73E-09	1	ENSG00000151167	TANK3	1.00E-04	<=0.01	41	0	29	TANK3	
rs2891168-56222-56222	rs4722672 or rs62060882	2.05E-10	3	ENSG00000166862	SNTA1/LAX2	1.66E-07	<=0.01	42	0	31	GATA2

Supplementary Table 12. DEPICT Medical Subject Heading (MeSH) tissue and cell type annotations enrichment (FDR<0.05).

MeSH TERM	NAME	MeSH FIRST LEVEL TERM	MeSH SECOND LEVEL TERM	P_{NOM}	FDR
A11.329.171	Chondrocytes	Cells	Connective Tissue Cells	4.63E-08	<0.01
A02.165	Cartilage	Musculoskeletal System	Cartilage	1.39E-07	<0.01
A03.556.875	Upper Gastrointestinal Tract	Digestive System	Gastrointestinal Tract	4.02E-06	<0.01
A07.231.114	Arteries	Cardiovascular System	Blood Vessels	4.89E-06	<0.01
A03.556.875.875	Stomach	Digestive System	Gastrointestinal Tract	1.04E-05	<0.01
A05.360.319.679	Uterus	Urogenital System	Genitalia	1.66E-05	<0.01
A05.360.319.679.690	Myometrium	Urogenital System	Genitalia	1.81E-05	<0.01
A02.835.583.443	Joint Capsule	Musculoskeletal System	Skeleton	4.04E-05	<0.01
A02.835.583	Joints	Musculoskeletal System	Skeleton	4.04E-05	<0.01
A02.835.583.443.800	Synovial Membrane	Musculoskeletal System	Skeleton	4.04E-05	<0.01
A10.615	Membranes	Tissues	Membranes	5.79E-05	<0.01
A03.556.875.500	Esophagus	Digestive System	Gastrointestinal Tract	6.83E-05	<0.01
A10.690.467	Muscle Smooth	Tissues	Muscles	1.32E-04	<0.01
A05.360	Genitalia	Urogenital System	Genitalia	5.11E-04	<0.01
A07.231	Blood Vessels	Cardiovascular System	Blood Vessels	5.16E-04	<0.01
A05.360.319.679.490	Endometrium	Urogenital System	Genitalia	5.40E-04	<0.01
A03.556.249.249.209	Cecum	Digestive System	Gastrointestinal Tract	5.86E-04	<0.01
A11.872.580	Mesenchymal Stem Cells	Cells	Stem Cells	6.07E-04	<0.01
A17.815	Skin	Integumentary System	Skin	7.38E-04	<0.01
A03.556.249.249.356.668	Colon Sigmoid	Digestive System	Gastrointestinal Tract	7.94E-04	<0.01
A03.556	Gastrointestinal Tract	Digestive System	Gastrointestinal Tract	7.98E-04	<0.01
A05.360.319	Genitalia Female	Urogenital System	Genitalia	9.02E-04	<0.01
A15.145.846	Serum	Hemic and Immune Systems	Blood	1.03E-03	<0.01
A11.329.228	Fibroblasts	Cells	Connective Tissue Cells	1.36E-03	<0.01
A10.615.284.473	Chorion	Tissues	Membranes	1.90E-03	<0.05
A10.615.284	Extraembryonic Membranes	Tissues	Membranes	1.90E-03	<0.05
A10.615.550	Mucous Membrane	Tissues	Membranes	1.94E-03	<0.05
A11.329.830	Stromal Cells	Cells	Connective Tissue Cells	2.04E-03	<0.05
A03.556.249	Lower Gastrointestinal Tract	Digestive System	Gastrointestinal Tract	2.09E-03	<0.05
A03.556.249.249	Intestine Large	Digestive System	Gastrointestinal Tract	2.15E-03	<0.05
A03.556.249.249.356	Colon	Digestive System	Gastrointestinal Tract	2.46E-03	<0.05
A03.556.124.526.767	Rectum	Digestive System	Gastrointestinal Tract	2.90E-03	<0.05
A10.615.550.599	Mouth Mucosa	Tissues	Membranes	3.48E-03	<0.05
A03.556.124	Intestines	Digestive System	Gastrointestinal Tract	3.73E-03	<0.05
A05.360.319.679.256	Cervix Uteri	Urogenital System	Genitalia	4.00E-03	<0.05
A07.541.510	Heart Valves	Cardiovascular System	Heart	4.63E-03	<0.05
A07.541.510.110	Aortic Valve	Cardiovascular System	Heart	4.63E-03	<0.05
A07.231.908	Veins	Cardiovascular System	Blood Vessels	5.05E-03	<0.05
A10.165.114	Adipose Tissue	Tissues	Connective Tissue	5.73E-03	<0.05
A05.810.890	Urinary Bladder	Urogenital System	Urinary Tract	6.05E-03	<0.05
A11.872.190.260	Embryoid Bodies	Cells	Stem Cells	7.19E-03	<0.05
A10.165.114.830	Adipose Tissue White	Tissues	Connective Tissue	7.89E-03	<0.05
A10.165.114.830.750	Subcutaneous Fat	Tissues	Connective Tissue	7.89E-03	<0.05
A03.734.414	Islets of Langerhans	Digestive System	Pancreas	8.58E-03	<0.05
A07.231.908.670	Portal System	Cardiovascular System	Blood Vessels	8.96E-03	<0.05
A07.231.908.670.874	Umbilical Veins	Cardiovascular System	Blood Vessels	8.96E-03	<0.05
A11.436.275	Endothelial Cells	Cells	Epithelial Cells	8.99E-03	<0.05
A10.336	Exocrine Glands	Tissues	Exocrine Glands	0.01	<0.05
A11.436	Epithelial Cells	Cells	Epithelial Cells	0.01	<0.05
A02.835.232.834.151	Cervical Vertebrae	Musculoskeletal System	Skeleton	0.01	<0.05
A10.336.707	Prostate	Tissues	Exocrine Glands	0.01	<0.05
A02.835.232.834	Spine	Musculoskeletal System	Skeleton	0.01	<0.05
A11.620	Muscle Cells	Cells	Muscle Cells	0.01	<0.05
A11.620.520	Myocytes Smooth Muscle	Cells	Muscle Cells	0.01	<0.05
A10.165.114.830.500	Abdominal Fat	Tissues	Connective Tissue	0.01	<0.05
A10.165.114.830.500.750	Subcutaneous Fat Abdominal	Tissues	Connective Tissue	0.01	<0.05
A11.329	Connective Tissue Cells	Cells	Connective Tissue Cells	0.02	<0.05
A05.360.444	Genitalia Male	Urogenital System	Genitalia	0.02	<0.05
A11.329.114	Adipocytes	Cells	Connective Tissue Cells	0.02	<0.05
A14.549.167	Dentition	Stomatognathic System	Mouth	0.02	<0.05
A04.411	Lung	Respiratory System	Lung	0.02	<0.05
A10.615.789	Serous Membrane	Tissues	Membranes	0.02	<0.05

P_{NOM} Nominal P-value
FDR False discover rate

Supplementary Table 13. Magenta Gene set enrichment analysis

MAGENTA GENE SET ENRICHMENT ANALYSIS			95th PERCENTILE ENRICHMENT CUTOFF			75th PERCENTILE ENRICHMENT CUTOFF		
DATABASE	GENE SET	#GENES (MAPPED TO MAGENTA)	P	FDR	#GENES: EXPECTED (OBSERVED)	P	FDR	#GENES: EXPECTED (OBSERVED)
KEGG	KEGG_BASAL_CELL_CARCINOMA	55 (51)	9.90E-07	<1E-04	3 (15)	4.70E-04	0.02	13 (24)
KEGG	KEGG_HEDGEHOG_SIGNALING_PATHWAY	56 (52)	3.00E-06	8.50E-04	3 (12)	1.03E-02	0.14	13 (21)
BIOCARTA	ALK_PATHWAY	37 (37)	1.00E-04	0.005	2 (10)	1.20E-03	0.13	9 (18)
KEGG	KEGG_WNT_SIGNALING_PATHWAY	151 (142)	1.00E-04	0.024	7 (18)	7.00E-03	0.13	36 (49)
PANTHER	Oogenesis	65 (59)	2.00E-04	0.026	3 (10)	3.95E-01	0.86	15 (16)
PANTHER	Asymmetric_protein_localization	20 (19)	1.50E-03	0.027	1 (5)	8.70E-03	0.13	5 (10)
GOTERM	endochondral ossification	12 (12)	2.00E-04	0.028	1 (5)	1.43E-02	0.20	3 (7)
PANTHER	Endoderm_development	12 (12)	2.30E-03	0.032	1 (4)	5.71E-02	0.38	3 (6)
PANTHER	Developmental_processes	509 (448)	3.00E-04	0.036	22 (40)	9.90E-03	0.18	112 (133)
GOTERM	skeletal system development	126 (117)	1.00E-06	0.039	6 (20)	3.79E-04	0.08	29 (46)
PANTHER	Oncogenesis	182 (152)	2.00E-04	0.039	8 (18)	9.00E-04	0.03	38 (56)
GOTERM	positive regulation of osteoblast differentiation	24 (24)	1.00E-04	0.041	1 (7)	2.23E-02	0.29	6 (11)
PANTHER	Cadherin_signaling_pathway	29 (25)	1.20E-03	0.042	1 (6)	2.40E-03	0.10	6 (13)
GOTERM	positive regulation of bone mineralization	19 (19)	5.00E-04	0.042	1 (6)	2.77E-02	0.30	5 (9)
GOTERM	Wnt receptor signaling pathway	94 (89)	3.80E-05	0.042	4 (15)	2.86E-01	0.66	22 (25)
KEGG	KEGG_PATHWAYS_IN_CANCER	328 (312)	3.52E-04	0.042	16 (30)	9.90E-05	0.01	78 (107)
KEGG	KEGG_MELANOGENESIS	102 (96)	1.00E-03	0.044	5 (13)	9.54E-02	0.59	24 (30)

P_{NOM} Nominal P-value
FDR False discover rate

Supplementary Table 14. Skeletal phenotype data from the International Mouse Phenotyping Consortium and Mouse Genome Informatics databases and expression data from murine osteoblasts, osteocytes and osteoclas

				EXPRESSION			MOUSE GENOMIC DATABASE			INTERNATIONAL KNOCKOUT MOUSE CONSORTIUM		OMIM
REGION OF INTEREST	GENE SYMBOL	MOUSE HOMOLOG	KNOWN MURINE BONE PHENOTYPE?	EXPRESSED IN OSTEOBLASTS	EXPRESSED IN OSTEOCLASTS	EXPRESSED IN OSTEOCYTES	PHENOTYPE INFORMATION IN IMG	RELEVANT PHENOTYPE	IMG (MGI ID)	IMPC MOUSE STATUS	IMPC PHENOTYPE	PHENOTYPE
chr1:4,123,418-98,121,365	C1galt1	C1galt1	Yes	Yes	Yes	Yes	No			Mice Produced	decreased bone mineral density	
chr1:7,289,578-7,324,618	CDK11B	Cdk11b	Yes	Yes	Yes	Yes	Yes			Mice Produced	decreased femur length, decreased tibia length	
chr1:11,072,608-11,092,732	CLCN7	Clcn7	Yes	Yes	Yes	Yes	Yes	none relevant		Mice Produced	abnormal bone marrow cell morphology/development, abnormal osteoclast morphology, decreased bone mineral content, decreased bone strength, increased bone mineralization	osteopetrosis, tubular aggregate myopathy, and congenital bone marrow failure
chr1:11,092,732-11,107,743	CLCN7-AS1	Clcn7-ps1	No	No	No	No	No			No Data Available		
chr1:19,669,731-19,693,862	ANKRD13C	Ankrd13c	Yes	Yes	No	Yes	Yes	decreased bone mineral content	ABPC	Mice Produced	decreased BMC/body weight	
chr1:20,693,862-20,699,731	ANKRD13C	Ankrd13c	Yes	Yes	No	Yes	Yes	decreased bone mineral content	ABPC	Mice Produced	decreased BMC/body weight	
chr1:21,099,731-21,113,862	ANKRD13C	Ankrd13c	Yes	Yes	No	Yes	Yes	decreased bone mineral content	ABPC	Mice Produced	decreased BMC/body weight	
chr1:21,113,862-21,119,731	ANKRD13C	Ankrd13c	Yes	Yes	No	Yes	Yes	decreased bone mineral content	ABPC	Mice Produced	decreased BMC/body weight	
chr1:21,119,731-21,133,862	ANKRD13C	Ankrd13c	Yes	Yes	No	Yes	Yes	decreased bone mineral content	ABPC	Mice Produced	decreased BMC/body weight	
chr1:21,133,862-21,139,731	ANKRD13C	Ankrd13c	Yes	Yes	No	Yes	Yes	decreased bone mineral content	ABPC	Mice Produced	decreased BMC/body weight	
chr1:21,139,731-21,153,862	ANKRD13C	Ankrd13c	Yes	Yes	No	Yes	Yes	decreased bone mineral content	ABPC	Mice Produced	decreased BMC/body weight	
chr1:21,153,862-21,159,731	ANKRD13C	Ankrd13c	Yes	Yes	No	Yes	Yes	decreased bone mineral content	ABPC	Mice Produced	decreased BMC/body weight	
chr1:21,159,731-21,173,862	ANKRD13C	Ankrd13c	Yes	Yes	No	Yes	Yes	decreased bone mineral content	ABPC	Mice Produced	decreased BMC/body weight	
chr1:21,173,862-21,179,731	ANKRD13C	Ankrd13c	Yes	Yes	No	Yes	Yes	decreased bone mineral content	ABPC	Mice Produced	decreased BMC/body weight	
chr1:21,179,731-21,193,862	ANKRD13C	Ankrd13c	Yes	Yes	No	Yes	Yes	decreased bone mineral content	ABPC	Mice Produced	decreased BMC/body weight	
chr1:21,193,862-21,199,731	ANKRD13C	Ankrd13c	Yes	Yes	No	Yes	Yes	decreased bone mineral content	ABPC	Mice Produced	decreased BMC/body weight	
chr1:21,199,731-21,213,862	ANKRD13C	Ankrd13c	Yes	Yes	No	Yes	Yes	decreased bone mineral content	ABPC	Mice Produced	decreased BMC/body weight	
chr1:21,213,862-21,219,731	ANKRD13C	Ankrd13c	Yes	Yes	No	Yes	Yes	decreased bone mineral content	ABPC	Mice Produced	decreased BMC/body weight	
chr1:21,219,731-21,233,862	ANKRD13C	Ankrd13c	Yes	Yes	No	Yes	Yes	decreased bone mineral content	ABPC	Mice Produced	decreased BMC/body weight	
chr1:21,233,862-21,239,731	ANKRD13C	Ankrd13c	Yes	Yes	No	Yes	Yes	decreased bone mineral content	ABPC	Mice Produced	decreased BMC/body weight	
chr1:21,239,731-21,253,862	ANKRD13C	Ankrd13c	Yes	Yes	No	Yes	Yes	decreased bone mineral content	ABPC	Mice Produced	decreased BMC/body weight	
chr1:21,253,862-21,259,731	ANKRD13C	Ankrd13c	Yes	Yes	No	Yes	Yes	decreased bone mineral content	ABPC	Mice Produced	decreased BMC/body weight	
chr1:21,259,731-21,273,862	ANKRD13C	Ankrd13c	Yes	Yes	No	Yes	Yes	decreased bone mineral content	ABPC	Mice Produced	decreased BMC/body weight	
chr1:21,273,862-21,279,731	ANKRD13C	Ankrd13c	Yes	Yes	No	Yes	Yes	decreased bone mineral content	ABPC	Mice Produced	decreased BMC/body weight	
chr1:21,279,731-21,293,862	ANKRD13C	Ankrd13c	Yes	Yes	No	Yes	Yes	decreased bone mineral content	ABPC	Mice Produced	decreased BMC/body weight	
chr1:21,293,862-21,299,731	ANKRD13C	Ankrd13c	Yes	Yes	No	Yes	Yes	decreased bone mineral content	ABPC	Mice Produced	decreased BMC/body weight	
chr1:21,299,731-21,313,862	ANKRD13C	Ankrd13c	Yes	Yes	No	Yes	Yes	decreased bone mineral content	ABPC	Mice Produced	decreased BMC/body weight	
chr1:21,313,862-21,319,731	ANKRD13C	Ankrd13c	Yes	Yes	No	Yes	Yes	decreased bone mineral content	ABPC	Mice Produced	decreased BMC/body weight	
chr1:21,319,731-21,333,862	ANKRD13C	Ankrd13c	Yes	Yes	No	Yes	Yes	decreased bone mineral content	ABPC	Mice Produced	decreased BMC/body weight	
chr1:21,333,862-21,339,731	ANKRD13C	Ankrd13c	Yes	Yes	No	Yes	Yes	decreased bone mineral content	ABPC	Mice Produced	decreased BMC/body weight	
chr1:21,339,731-21,353,862	ANKRD13C	Ankrd13c	Yes	Yes	No	Yes	Yes	decreased bone mineral content	ABPC	Mice Produced	decreased BMC/body weight	
chr1:21,353,862-21,359,731	ANKRD13C	Ankrd13c	Yes	Yes	No	Yes	Yes	decreased bone mineral content	ABPC	Mice Produced	decreased BMC/body weight	
chr1:21,359,731-21,373,862	ANKRD13C	Ankrd13c	Yes	Yes	No	Yes	Yes	decreased bone mineral content	ABPC	Mice Produced	decreased BMC/body weight	
chr1:21,373,862-21,379,731	ANKRD13C	Ankrd13c	Yes	Yes	No	Yes	Yes	decreased bone mineral content	ABPC	Mice Produced	decreased BMC/body weight	
chr1:21,379,731-21,393,862	ANKRD13C	Ankrd13c	Yes	Yes	No	Yes	Yes	decreased bone mineral content	ABPC	Mice Produced	decreased BMC/body weight	
chr1:21,393,862-21,399,731	ANKRD13C	Ankrd13c	Yes	Yes	No	Yes	Yes	decreased bone mineral content	ABPC	Mice Produced	decreased BMC/body weight	
chr1:21,399,731-21,413,862	ANKRD13C	Ankrd13c	Yes	Yes	No	Yes	Yes	decreased bone mineral content	ABPC	Mice Produced	decreased BMC/body weight	
chr1:21,413,862-21,419,731	ANKRD13C	Ankrd13c	Yes	Yes	No	Yes	Yes	decreased bone mineral content	ABPC	Mice Produced	decreased BMC/body weight	
chr1:21,419,731-21,433,862	ANKRD13C	Ankrd13c	Yes	Yes	No	Yes	Yes	decreased bone mineral content	ABPC	Mice Produced	decreased BMC/body weight	
chr1:21,433,862-21,439,731	ANKRD13C	Ankrd13c	Yes	Yes	No	Yes	Yes	decreased bone mineral content	ABPC	Mice Produced	decreased BMC/body weight	
chr1:21,439,731-21,453,862	ANKRD13C	Ankrd13c	Yes	Yes	No	Yes	Yes	decreased bone mineral content	ABPC	Mice Produced	decreased BMC/body weight	
chr1:21,453,862-21,459,731	ANKRD13C	Ankrd13c	Yes	Yes	No	Yes	Yes	decreased bone mineral content	ABPC	Mice Produced	decreased BMC/body weight	
chr1:21,459,731-21,473,862	ANKRD13C	Ankrd13c	Yes	Yes	No	Yes	Yes	decreased bone mineral content	ABPC	Mice Produced	decreased BMC/body weight	
chr1:21,473,862-21,479,731	ANKRD13C	Ankrd13c	Yes	Yes	No	Yes	Yes	decreased bone mineral content	ABPC	Mice Produced	decreased BMC/body weight	
chr1:21,479,731-21,493,862	ANKRD13C	Ankrd13c	Yes	Yes	No	Yes	Yes	decreased bone mineral content	ABPC	Mice Produced	decreased BMC/body weight	
chr1:21,493,862-21,499,731	ANKRD13C	Ankrd13c	Yes	Yes	No	Yes	Yes	decreased bone mineral content	ABPC	Mice Produced	decreased BMC/body weight	
chr1:21,499,731-21,513,862	ANKRD13C	Ankrd13c	Yes	Yes	No	Yes	Yes	decreased bone mineral content	ABPC	Mice Produced	decreased BMC/body weight	
chr1:21,513,862-21,519,731	ANKRD13C	Ankrd13c	Yes	Yes	No	Yes	Yes	decreased bone mineral content	ABPC	Mice Produced	decreased BMC/body weight	
chr1:21,519,731-21,533,862	ANKRD13C	Ankrd13c	Yes	Yes	No	Yes	Yes	decreased bone mineral content	ABPC	Mice Produced	decreased BMC/body weight	
chr1:21,533,862-21,539,731	ANKRD13C	Ankrd13c	Yes	Yes	No	Yes	Yes	decreased bone mineral content	ABPC	Mice Produced	decreased BMC/body weight	
chr1:21,539,731-21,553,862	ANKRD13C	Ankrd13c	Yes	Yes	No	Yes	Yes	decreased bone mineral content	ABPC	Mice Produced	decreased BMC/body weight	
chr1:21,553,862-21,559,731	ANKRD13C	Ankrd13c	Yes	Yes	No	Yes	Yes	decreased bone mineral content	ABPC	Mice Produced	decreased BMC/body weight	
chr1:21,559,731-21,573,862	ANKRD13C	Ankrd13c	Yes	Yes	No	Yes	Yes	decreased bone mineral content	ABPC	Mice Produced	decreased BMC/body weight	
chr1:21,573,862-21,579,731	ANKRD13C	Ankrd13c	Yes	Yes	No	Yes	Yes	decreased bone mineral content	ABPC	Mice Produced	decreased BMC/body weight	
chr1:21,579,731-21,593,862	ANKRD13C	Ankrd13c	Yes	Yes	No	Yes	Yes	decreased bone mineral content	ABPC	Mice Produced	decreased BMC/body weight	
chr1:21,593,862-21,599,731	ANKRD13C	Ankrd13c	Yes	Yes	No	Yes	Yes	decreased bone mineral content	ABPC	Mice Produced	decreased BMC/body weight	
chr1:21,599,731-21,613,862	ANKRD13C	Ankrd13c	Yes	Yes	No	Yes	Yes	decreased bone mineral content	ABPC	Mice Produced	decreased BMC/body weight	
chr1:21,613,862-21,619,731	ANKRD13C	Ankrd13c	Yes	Yes	No	Yes	Yes	decreased bone mineral content	ABPC	Mice Produced	decreased BMC/body weight	
chr1:21,619,731-21,633,862	ANKRD13C	Ankrd13c	Yes	Yes	No	Yes	Yes	decreased bone mineral content	ABPC	Mice Produced	decreased BMC/body weight	
chr1:21,633,862-21,639,731	ANKRD13C	Ankrd13c	Yes	Yes	No	Yes	Yes	decreased bone mineral content	ABPC	Mice Produced	decreased BMC/body weight	
chr1:21,639,731-21,653,862	ANKRD13C	Ankrd13c	Yes	Yes	No	Yes	Yes	decreased bone mineral content	ABPC	Mice Produced	decreased BMC/body weight	
chr1:21,653,862-21,659,731	ANKRD13C	Ankrd13c	Yes	Yes	No	Yes	Yes	decreased bone mineral content	ABPC	Mice Produced	decreased BMC/body weight	
chr1:21,659,731-21,673,862	ANKRD13C	Ankrd13c	Yes	Yes	No	Yes	Yes	decreased bone mineral content	ABPC	Mice Produced	decreased BMC/body weight	
chr1:21,673,862-21,679,731	ANKRD13C	Ankrd13c	Yes	Yes	No	Yes	Yes	decreased bone mineral content	ABPC	Mice Produced	decreased BMC/body weight	
chr1:21,679,731-21,693,862	ANKRD13C	Ankrd13c	Yes	Yes	No	Yes	Yes	decreased bone mineral content	ABPC	Mice Produced	decreased BMC/body weight	
chr1:21,693,862-21,699,731	ANKRD13C	Ankrd13c	Yes	Yes	No	Yes	Yes	decreased bone mineral content	ABPC	Mice Produced	decreased BMC/body weight	
chr1:21,699,731-21,713,862	ANKRD13C	Ankrd13c	Yes	Yes	No	Yes	Yes	decreased bone mineral content	ABPC	Mice Produced	decreased BMC/body weight	
chr1:21,713,862-21,719,731	ANKRD13C	Ankrd13c	Yes	Yes	No	Yes	Yes	decreased bone mineral content	ABPC	Mice Produced	decreased BMC/body weight	
chr1:21,719,731-21,733,862	ANKRD13C	Ankrd13c	Yes	Yes	No	Yes	Yes	decreased bone mineral content	ABPC	Mice Produced	decreased BMC/body weight	
chr1:21,733,862-21,739,731	ANKRD13C	Ankrd13c	Yes	Yes	No	Yes	Yes	decreased bone mineral content	ABPC	Mice Produced	decreased BMC/body weight	
chr1:21,739,731-21,753,862	ANKRD13C	Ankrd13c	Yes	Yes	No	Yes	Yes	decreased bone mineral content	ABPC	Mice Produced	decreased BMC/body weight	
chr1:21,753,862-21,759,731	ANKRD13C	Ankrd13c	Yes	Yes	No	Yes	Yes	decreased bone mineral content	ABPC	Mice Produced	decreased BMC/body weight	
chr1:21,759,731-21,773,862	ANKRD13C	Ankrd13c	Yes	Yes	No	Yes	Yes	decreased bone mineral content	ABPC	Mice Produced	decreased BMC/body weight	
chr1:21,773,862-21,779,731	ANKRD13C	Ankrd13c	Yes	Yes	No	Yes	Yes	decreased bone mineral content	ABPC	Mice Produced	decreased BMC/body weight	
chr1:21,779,731-21,793,862	ANKRD13C	Ankrd13c	Yes	Yes	No	Yes	Yes	decreased bone mineral content	ABPC	Mice Produced	decreased BMC/body weight	
chr1:21,793,862-21,799,731	ANKRD13C	Ankrd13c	Yes	Yes	No	Yes	Yes	decreased bone mineral content	ABPC	Mice Produced	decreased BMC/body weight	
chr1:21,799,731-21,813,862	ANKRD13C	Ankrd13c	Yes	Yes	No	Yes	Yes	decreased bone mineral content	ABPC	Mice Produced	decreased BMC/body weight	
chr1:21,813,862-21,819,731	ANKRD13C	Ankrd13c	Yes	Yes	No	Yes	Yes	decreased bone mineral content	ABPC	Mice Produced	decreased BMC/body weight	
chr1:21,819,731-21,833,862	ANKRD13C	Ankrd13c	Yes	Yes	No	Yes	Yes	decreased bone mineral content	ABPC	Mice Produced	decreased BMC/body weight	
chr1:21,833,862-21,839,731	ANKRD13C	Ankrd13c	Yes	Yes	No	Yes	Yes	decreased bone mineral content	ABPC	Mice Produced	decreased BMC/body weight	
chr1:21,839,731-21,853,862	ANKRD13C	Ankrd13c	Yes	Yes	No	Yes	Yes	decreased bone mineral content	ABPC	Mice Produced	decreased BMC/body weight	
chr1:21,853,862-21,859,731	ANKRD13C	Ankrd13c	Yes	Yes	No	Yes	Yes	decreased bone mineral content	ABPC	Mice Produced	decreased BMC/body weight	
chr1:21,859,731-21,873,862	ANKRD13C	Ankrd13c	Yes	Yes	No	Yes	Yes	decreased bone mineral content	ABPC	Mice Produced	decreased BMC/body weight	
chr1:21,873,862-21,879,731	ANKRD13C	Ankrd13c	Yes	Yes	No	Yes	Yes	decreased bone mineral content	ABPC	Mice Produced	decreased BMC/body weight	
chr1:21,879,731-21,893,862	ANKRD13C	Ankrd13c	Yes	Yes	No	Yes	Yes	decreased bone mineral content	ABPC	Mice Produced	decreased BMC/body weight	
chr1:21,893,862-21,899,731	ANKRD13C	Ankrd13c	Yes	Yes	No	Yes	Yes	decreased bone mineral content	ABPC	Mice Produced	decreased BMC/body weight	
chr1:21,899,731-21,913,862	ANKRD13C	Ankrd13c	Yes	Yes	No	Yes	Yes	decreased bone mineral content	ABPC	Mice Produced	decreased BMC/body weight	
chr1:21,913,862-21,919,731	ANKRD13C	Ankrd13c	Yes	Yes	No	Yes	Yes	decreased bone mineral content	ABPC	Mice Produced	decreased BMC/body weight	
chr1:21,919,731-21,933,862	ANKRD13C	Ankrd13c	Yes	Yes	No	Yes	Yes	decreased bone mineral content	ABPC	Mice Produced	decreased BMC/body weight	
chr1:21,933,862-21,939,731	ANKRD13C	Ankrd13c	Yes	Yes	No	Yes	Yes	decreased bone mineral content	ABPC	Mice Produced	decreased BMC/body weight	
chr1:21,939,731-21,953,862	ANKRD13C	Ankrd13c	Yes	Yes	No	Yes	Yes	decreased bone mineral content	ABPC	Mice Produced	decreased BMC/body weight	
chr1:21,953,862-21,959,731	ANKRD13C	Ankrd13c	Yes	Yes	No	Yes	Yes	decreased bone mineral content	ABPC	Mice Produced	decreased BMC/body weight	
chr1:21,959,731-21,973,862	ANKRD13C	Ankrd13c	Yes	Yes	No	Yes	Yes	decreased bone mineral content	ABPC	Mice Produced	decreased BMC/body weight	
chr1:21,973,862-21,979,731	ANKRD13C	Ankrd13c	Yes	Yes	No	Yes	Yes	decreased bone mineral content	ABPC	Mice Produced	decreased BMC/body weight	
chr1:21,979,731-21,993,862	ANKRD13C	Ankrd13c	Yes	Yes	No	Yes	Yes	decreased bone mineral content	ABPC	Mice Produced	decreased BMC/body weight	
chr1:21,993,862-21,999,731	ANKRD13C	Ankrd13c	Yes	Yes	No	Yes	Yes	decreased bone mineral content	ABPC	Mice Produced	decreased BMC/body weight	
chr1:21,999,731-22,013,862	ANKRD13C	Ankrd13c	Yes	Yes	No	Yes	Yes	decreased bone mineral content	ABPC	Mice Produced	decreased BMC/body weight	
chr1:22,013,862-22,019,731	ANKRD13C	Ankrd13c	Yes	Yes	No	Yes	Yes	decreased bone mineral content	ABPC	Mice Produced	decreased BMC/body weight	
chr1:22,019,731-22,033,862	ANKRD13C	Ankrd13c	Yes	Yes	No	Yes	Yes	decreased bone mineral content	ABPC	Mice Produced	decreased BMC/body weight	
chr1:22,033,862-22,039,731	ANKRD13C	Ankrd13c	Yes	Yes	No	Yes	Yes	decreased bone mineral content	ABPC	Mice Produced	decreased BMC/body weight	
chr1:22,039,731-22,053,862	ANKRD13C	Ankrd13c	Yes	Yes	No	Yes	Yes	decreased bone mineral content	ABPC	Mice Produced	decreased BMC/body weight	
chr1:22,053,862-22,059,731	ANKRD13C	Ankrd13c	Yes	Yes	No	Yes	Yes	decreased bone mineral content	ABPC	Mice Produced	decreased BMC/body weight	
chr1:22,059,731-22,073,862	ANKRD13C	Ankrd13c	Yes	Yes	No	Yes	Yes	decreased bone mineral content	ABPC	Mice Produced	decreased BMC/body weight	
chr1:22,073,862-22,079,731	ANKRD13C	Ankrd13c	Yes	Yes	No	Yes	Yes	decreased bone mineral content	ABPC	Mice Produced	decreased BMC/body weight	
chr1:22,079,731-22,093,862	ANKRD13C	Ankrd13c	Yes	Yes	No	Yes	Yes	decreased bone mineral content	ABPC	Mice Produced	decreased BMC/body weight	
chr1:22,093,862-22,099,731	ANKRD13C	Ankrd13c	Yes	Yes	No	Yes	Yes	decreased bone mineral content	ABPC	Mice Produced	decreased BMC/body weight	
chr1:22,099,731-22,113,862	ANKRD13C	Ankrd13c	Yes	Yes	No	Yes	Yes	decreased bone mineral content	ABPC	Mice Produced	decreased BMC/body weight	
chr1:22,113,862-22,119,731	ANKRD13C	Ankrd13c	Yes	Yes	No	Yes	Yes	decreased bone mineral content	ABPC	Mice Produced	decreased BMC/body weight	
chr1:22,119,731-22,133,862	ANKRD13C	Ankrd13c	Yes	Yes	No	Yes	Yes	decreased bone mineral content	ABPC	Mice Produced	decreased BMC/body weight	
chr1:22,133,862-22,139,731	ANKRD13C	Ankrd13c	Yes	Yes	No	Yes	Yes	decreased bone mineral content	ABPC	Mice Produced	decreased BMC/body weight	
chr1:22,139,731-22,153,862	ANKRD13C	Ankrd13c	Yes	Yes	No	Yes	Yes	decreased bone mineral content	ABPC	Mice Produced	decreased BMC/body weight	
chr1:22,153,862-22,159,731	ANKRD13C	Ankrd13c	Yes	Yes	No	Yes	Yes	decreased bone mineral content	ABPC	Mice Produced	decreased BMC/body weight	
chr1:22,159,731-22,173,862	ANKRD13C	Ankrd13c	Yes	Yes	No	Yes	Yes	decreased bone mineral content	ABPC	Mice Produced	decreased BMC/body weight	
chr1:22,173,862-22,179,731	ANKRD13C	Ankrd13c	Yes	Yes	No	Yes	Yes	decreased bone mineral content	ABPC	Mice Produced	decreased BMC/body weight	
chr1:22,179,731-22,193,862	ANKRD13C	Ankrd13c	Yes	Yes	No	Yes	Yes	decreased bone mineral content	ABPC	Mice Produced	decreased BMC/body weight	
chr1:22,193,862-22,199,731	ANKRD13C	Ankrd13c	Yes	Yes	No	Yes	Yes	decreased bone mineral content	ABPC	Mice Produced	decreased BMC/body weight	
chr1:22,199,731-22,213,862	ANKRD13C	Ankrd13c	Yes	Yes	No	Yes	Yes	decreased bone mineral content	ABPC	Mice Produced	decreased BMC/body weight	
chr1:22,213,862-22,219,731	ANKRD13C	Ankrd13c	Yes	Yes	No	Yes	Yes	decreased bone mineral content	ABPC	Mice Produced	decreased BMC/body weight	
chr1:22,219,731-22,233,862	ANKRD13C	Ankrd13c	Yes	Yes	No	Yes	Yes	decreased bone mineral content	ABPC	Mice Produced	decreased BMC/body weight	
chr1:22,233,862-22,239,731	ANKRD13C	Ankrd13c	Yes	Yes	No	Yes	Yes	decreased bone mineral content	ABPC	Mice Produced	decreased BMC/body weight	
chr1:22,239,731-22,253,862	ANKRD13C	Ankrd13c	Yes	Yes	No	Yes	Yes	decreased bone mineral content	ABPC	Mice Produced	decreased BMC/body weight	
chr1:22,253,862-22,259,731	ANKRD13C	Ankrd13c	Yes	Yes	No	Yes	Yes	decreased bone mineral content	ABPC	Mice Produced	decreased BMC/body weight	
chr1:22,259,731-22,273,862	ANKRD13C	Ankrd13c	Yes	Yes	No	Yes	Yes	decreased bone mineral content	ABPC	Mice Produced	decreased BMC/body weight	
chr1:22,273,862-22,279,731	ANKRD13C	Ankrd13c	Yes	Yes	No	Yes	Yes	decreased bone mineral content	ABPC	Mice Produced	decreased BMC/body weight	
chr1:22,279,731-22,293,862	ANKRD13C	Ankrd13c	Yes	Yes	No	Yes	Yes	decreased bone mineral content	ABPC	Mice Produced	decreased BMC/body weight	
chr1:22,293,862-22,299,731	ANKRD13C	Ankrd13c	Yes	Yes	No	Yes	Yes	decreased bone mineral content	ABPC	Mice Produced	decreased BMC/body weight	
chr1:22,299,731-22,313,862	ANKRD13C	Ankrd13c	Yes	Yes	No	Yes	Yes	decreased bone mineral content	ABPC	Mice Produced	decreased BMC/body weight	
chr1:22,313,862-22,319,731	ANKRD13C	Ankrd13c	Yes	Yes	No	Yes	Yes	decreased bone mineral content	ABPC	Mice Produced	decreased BMC/body weight	
chr1:22,319,731-22,333,862	ANKRD13C	Ankrd13c	Yes	Yes	No	Yes	Yes	decreased bone mineral content	ABPC	Mice Produced	decreased BMC/body weight	
chr1:22,333,862-22,339,731	ANKRD13C	Ankrd13c	Yes	Yes	No	Yes	Yes	decreased bone mineral content	ABPC	Mice Produced	decreased BMC/body weight	
chr1:22,339,731-22,353,862	ANKRD13C	Ankrd13c	Yes	Yes	No	Yes	Yes	decreased bone mineral content	ABPC	Mice Produced	decreased BMC/body weight	
chr1:22,353,862-22,359,731	ANKRD13C	Ankrd13c	Yes	Yes	No	Yes	Yes	decreased bone mineral content	ABPC	Mice Produced	decreased BMC/body weight	
chr1:22,359,731-22,373,862	ANKRD13C	Ankrd13c	Yes	Yes	No	Yes	Yes	decreased bone mineral content	ABPC	Mice Produced	decreased BMC/body weight	
chr1:22,373,862-22,379,731	ANKRD13C	Ankrd13c	Yes	Yes	No	Yes	Yes	decreased bone mineral content	ABPC	Mice Produced	decreased BMC/body weight	
chr1:22,379,731-22,393,862	ANKRD13C	Ankrd13c	Yes	Yes	No	Yes	Yes	decreased bone mineral content	ABPC	Mice Produced	decreased BMC/body weight	
chr1:22,393,862-22,399,731	ANKRD13C	Ankrd13c	Yes	Yes	No	Yes	Yes	decreased bone mineral content	ABPC	Mice Produced	decreased BMC/body weight	
chr1:22,399,731-22,413,862	ANKRD13C	Ankrd13c	Yes	Yes	No	Yes	Yes	decreased bone mineral content	ABPC	Mice Produced	decreased BMC/body weight	
chr1:22,413,862-22,419,731	ANKRD13C	Ankrd13c	Yes	Yes	No	Yes	Yes	decreased bone mineral content	ABPC	Mice Produced	decreased BMC/body weight	
chr1:22,419,731-22,433,862	ANKRD13C	Ankrd13c	Yes	Yes	No	Yes	Yes	decreased bone mineral content	ABPC	Mice Produced	decreased BMC/body weight	
chr1:22,433,862-22,439,731	ANKRD13C	Ankrd13c	Yes	Yes	No	Yes	Yes	decreased bone mineral content	ABPC	Mice Produced	decreased BMC/body weight	
chr1:22,439,731-22,453,862	ANKRD13C	Ankrd13c	Yes	Yes	No	Yes	Yes	decreased bone mineral content	ABPC	Mice Produced	decreased BMC/body weight	
chr1:22,453,862-22,459,731	ANKRD13C	Ankrd13c	Yes	Yes	No	Yes	Yes	decreased bone mineral content	ABPC	Mice Produced	decreased BMC/body weight	
chr1:22,459,731-22,473,862	ANKRD13C	Ankrd13c	Yes	Yes	No	Yes	Yes	decreased bone mineral content	ABPC	Mice Produced	decreased BMC/body weight	
chr1:22,473,862-22,479,731	ANKRD13C	Ankrd13c	Yes	Yes	No	Yes	Yes	decreased bone mineral content	ABPC	Mice Produced	decreased BMC/body weight	
chr1:22,479,731-22,493,862	ANKRD13C	Ankrd13c	Yes	Yes	No	Yes	Yes	decreased bone mineral content	ABPC	Mice Produced	decreased BMC/body weight	
chr1:22,493,862-22,499,731	ANKRD13C	Ankrd13c	Yes	Yes	No	Yes	Yes	decreased bone mineral content	ABPC	Mice Produced	decreased BMC/body weight	
chr1:22,499,731-22,513,862	ANKRD13C	Ankrd13c	Yes	Yes	No	Yes	Yes	decreased bone mineral content	ABPC	Mice Produced	decreased BMC/body weight	
chr1:22,513,862-22,519,731	ANKRD13C	Ankrd13c	Yes	Yes	No	Yes	Yes	decreased bone mineral content	ABPC	Mice Produced	decreased BMC/body weight	
chr1:22,519,731-22,533,862	ANKRD13C	Ankrd13c	Yes	Yes	No	Yes	Yes	decreased bone mineral content	ABPC	Mice Produced	decreased BMC/body weight	
chr1:22,533,862-22,539,731	ANKRD13C	Ankrd13c	Yes	Yes	No	Yes	Yes	decreased bone mineral content	ABPC	Mice Produced	decreased BMC/body weight	
chr1:22,539,731-22,553,862	ANKRD13C	Ankrd13c	Yes	Yes	No	Yes	Yes	decreased bone mineral content	ABPC	Mice Produced	decreased BMC/body weight	
chr1:22,553,862-22,559,731	ANKRD13C	Ankrd13c	Yes	Yes	No	Yes	Yes	decreased bone mineral content	ABPC	Mice Produced	decreased BMC/body weight	
chr1:22,559,731-22,573,862	ANKRD13C	Ankrd13c	Yes	Yes	No	Yes	Yes	decreased bone mineral content	ABPC	Mice Produced	decreased BMC/body weight	
chr1:22,573,862-22,579,731	ANKRD13C	Ankrd13c	Yes	Yes	No	Yes	Yes	decreased bone mineral content	ABPC	Mice Produced	decreased BMC/body weight	
chr1:22,579,731-22,593,862	ANKRD13C	Ankrd13c	Yes	Yes	No	Yes	Yes	decreased bone mineral content	ABPC	Mice Produced	decreased BMC/body weight	
chr1:22,593,862-22,599,731	ANKRD13C	Ankrd13c	Yes	Yes	No	Yes	Yes	decreased bone mineral content	ABPC	Mice Produced	decreased BMC/body weight	
chr1:22,599,731-22,613,862	ANKRD13C	Ankrd13c	Yes	Yes	No	Yes	Yes	decreased bone mineral content	ABPC	Mice Produced	decreased BMC/body weight	
chr1:22,613,862-22,619,731	ANKRD13C	Ankrd13c	Yes	Yes	No	Yes	Yes	decreased bone mineral content	ABPC	Mice Produced	decreased BMC/body weight	
chr1:22,619,731-22,633,862	ANKRD13C	Ankrd13c	Yes	Yes	No	Yes	Yes	decreased bone mineral content	ABPC	Mice Produced	decreased BMC/body weight	
chr1:22,633,862-22,639,731	ANKRD13C	Ankrd13c	Yes	Yes	No	Yes	Yes	decreased bone mineral content	ABPC	Mice Produced	decreased BMC/body weight	
chr1:22,639,731-22,653,862	ANKRD13C	Ankrd13c	Yes	Yes	No	Yes	Yes	decreased bone mineral content	ABPC	Mice Produced	decreased BMC/body weight	
chr1:22,653,862-22,659,731	ANKRD13C	Ankrd13c	Yes	Yes	No	Yes	Yes	decreased bone mineral content	ABPC	Mice Produced	decreased BMC/body weight	
chr1:22,659,731-22,673,862	ANKRD13C	Ankrd13c	Yes	Yes	No	Yes	Yes	decreased bone mineral content	ABPC	Mice Produced	decreased BMC/body weight	
chr1:22,673,862-22,679,731	ANKRD13C	Ankrd13c	Yes	Yes	No	Yes	Yes	decreased bone mineral content	ABPC	Mice Produced	decreased BMC/body weight	
chr1:22,679,731-22,693,862	ANKRD13C	Ankrd13c	Yes	Yes	No	Yes	Yes	decreased bone mineral content	ABPC	Mice Produced	decreased BMC/body weight	
chr1:22,693,862-22,699,731	ANKRD13C	Ankrd13c	Yes	Yes	No	Yes	Yes	decreased bone mineral content	ABPC	Mice Produced	decreased BMC/body weight	
chr1:22,699,731-22,713,862	ANKRD13C	Ankrd13c	Yes	Yes	No	Yes	Yes	decreased bone mineral content	ABPC	Mice Produced	decreased BMC/body weight	
chr1:22,713,862-22,719,731	ANKRD13C	Ankrd13c	Yes	Yes	No	Yes	Yes	decreased bone mineral content	ABPC	Mice Produced	decreased BMC/body weight	
chr1:22,719,731-22,733,862	ANKRD13C	Ankrd13c	Yes	Yes	No	Yes	Yes	decreased bone mineral content	ABPC	Mice Produced	decreased BMC/body weight	
chr1:22,733,862-22,739,731	ANKRD13C	Ankrd13c	Yes	Yes	No	Yes	Yes	decreased bone mineral content	ABPC	Mice Produced	decreased BMC/body weight	
chr1:22,739,731-22,753,862	ANKRD13C	Ankrd13c	Yes	Yes	No	Yes	Yes	decreased bone mineral content	ABPC	Mice Produced	decreased BMC/body weight	
chr1:22,753,862-22,759,731	ANKRD13C	Ankrd13c	Yes	Yes	No	Yes	Yes	decreased bone mineral content	ABPC	Mice Produced	decreased BMC/body weight	
chr1:22,759,731-22,773,862	ANKRD13C	Ankrd13c	Yes	Yes	No	Yes	Yes	decreased bone mineral content	ABPC	Mice Produced	decreased BMC/body weight	
chr1:22,773,862-22,779,731	ANKRD13C	Ankrd13c	Yes	Yes	No	Yes	Yes	decreased bone mineral content	ABPC	Mice Produced	decreased BMC/body weight	
chr1:22,779,731-22,793,862	ANKRD13C	Ankrd13c	Yes	Yes	No	Yes	Yes	decreased bone mineral content	ABPC	Mice Produced	decreased BMC/body weight	
chr1:22,793,862-22,799,731	ANKRD13C	Ankrd13c	Yes	Yes	No	Yes	Yes	decreased bone mineral content	ABPC	Mice Produced	decreased BMC/body weight	
chr1:22,799,731-22,813,862	ANKRD13C	Ankrd13c	Yes	Yes	No	Yes	Yes	decreased bone mineral content	ABPC	Mice Produced	decreased BMC/body weight	
chr1:22,813,862-22,819,731	ANKRD13C	Ankrd13c	Yes	Yes	No	Yes	Yes	decreased bone mineral content	ABPC	Mice Produced	decreased BMC/body weight	
chr1:22,819,731-22,833,862	ANKRD13C	Ankrd13c	Yes	Yes	No	Yes	Yes	decreased bone mineral content	ABPC	Mice Produced	decreased BMC/body weight	
chr1:22,833,862-22,839,731	ANKRD

Supplementary Table 15. Mouse knockouts from the OBDC Study and their mean scores on a variety of bone related phenotypes.

							FEMUR										VERTEBRAE				
							TRABECULAR				CORTICAL		3-POINT BENDING						COMPRESSION		
							BMC	LENGTH	BV/TV	Tb.Th	Tb.N	Tb.Sp	Ct.Th	Int.Di	Ct.BMD	YIELD LOAD	MAX LOAD	FRACTURE LOAD	STIFFNESS	DE #	BMC	LENGTH	YIELD LOAD	MAX LOAD	STIFFNESS
							(Grey level)	(mm)	%	(mm)	(mm-1)	(mm)	(mm)	(mm)	(mg HA/cm3)	(N)	(N)	(N)	(N/mm)	(%)	(Grey level)	(mm)	(N)	(N)	(N/mm)
							176.72	15.10	8.3%	3.24	0.053	0.30	0.19	0.81	1018.8	11.77	19.05	13.45	107.27	75%	169.02	3.96	60.85	77.35	318.43
eBMD RSID	eBMD P	HUMAN CHR	HUMAN POS	MOUSE GENE	DEPCT	ZYGOSITY	3.53	0.32	1.5%	0.24	0.004	0.03	0.01	0.05	40.8	1.61	1.89	3.95	14.63	20%	3.69	0.09	7.92	8.25	42.11
rs75077112	1.20E-10	1	107145852	*Mtor*		HET	0.04	-0.17	0.36	0.60	0.15	-0.26	-0.19	1.44	-1.24	-0.60	0.29	0.15	0.75	0.47	0.02	1.18	-0.51	-0.35	-0.49
rs6701290	2.30E-14	1	156869691	*Pkd1rs2*		HOM	-0.10	-0.39	-1.18	-2.56	-0.48	2.85	-0.11	-0.43	0.08	-1.16	-0.61	-0.77	-1.48	0.56	-0.39	-0.16	-0.55	-0.42	-0.23
rs4589135	4.10E-11	1	26541714	*Sh3bgrl3*		HOM	-2.25	0.70	-2.09	-2.32	-1.83	2.19	-0.54	-0.61	-0.54	0.09	-1.03	-0.89	-0.40	0.72	0.30	0.02	2.04	1.98	0.51
rs4360494	8.20E-10	1	37955891	*Cdca8*		HET	0.40	-1.15	1.20	1.30	0.52	-0.46	0.12	1.61	1.77	0.38	1.06	0.83	0.32	0.05	-0.91	0.21	0.38	0.14	0.51
rs4360494	8.20E-10	1	37955891	*Snip1*		HET	1.00	-0.60	0.40	0.40	0.10	No data	0.40	No data	No data	1.10	1.60	-0.20	0.70	0.50	No data	No data	No data	No data	No data
rs4360494	8.20E-10	1	37955891	*Maneal*		HOM	0.48	-0.60	1.05	1.30	-0.13	0.05	0.90	0.20	1.00	-0.36	0.38	0.87	0.89	-0.10	-0.80	-0.15	-0.30	-0.12	0.61
rs6680737	1.60E-14	1	119021631	*Hao2*		HOM	-0.01	0.42	-0.62	-0.73	-0.24	0.21	-0.11	0.02	-0.49	0.67	-0.12	0.44	0.08	-0.30	-0.03	-0.29	-0.05	-0.47	-0.91
rs53630378	8.20E-11	1	170183707	*Mrvh9*		HOM	-1.96	1.05	-0.44	-0.81	-0.03	0.06	0.72	-0.63	0.66	1.27	-0.76	-0.35	0.28	0.19	0.23	0.30	0.26	0.49	-0.50
rs7535122	1.40E-12	1	200172699	*5730559C18Rik*		HOM	-1.01	0.67	-1.48	-1.17	-0.71	0.79	-0.12	0.03	0.37	0.94	-0.36	-0.76	-0.14	0.69	-0.58	0.14	-0.07	-0.45	-0.08
rs7535122	1.40E-12	1	200172699	*Kif21b*		HOM	2.19	0.02	1.43	1.53	-0.19	0.29	0.34	1.18	-0.69	1.17	0.24	-1.06	0.98	0.95	-0.41	-1.89	0.52	0.16	0.21
rs7535122	1.40E-12	1	200172699	*Tmem9*		HOM	-0.50	-0.81	0.06	0.02	0.56	-0.47	-2.01	0.74	-0.68	-1.70	-1.64	-0.53	0.50	0.62	-2.65	0.49	-1.12	-1.51	-0.21
rs17514738	1.50E-11	1	218488754	*Lysmd1*		HOM	-1.26	-0.76	0.29	-1.02	1.47	-1.25	-1.48	0.20	0.03	-0.76	-2.17	-0.78	-2.12	0.38	-0.65	1.01	-0.07	-0.09	-0.31
rs127144411	4.00E-09	2	151430	*Tmem18*		HOM	-0.67	0.60	-1.68	-0.79	-1.37	1.72	-0.46	-0.02	-0.19	0.05	-0.37	-0.94	-0.24	0.52	-0.31	-0.14	-0.46	-0.63	-0.77
rs6761129	3.90E-11	2	43235712	*Lrpprc*		HET	-1.21	-1.49	-0.42	-0.13	-0.32	0.13	-0.59	0.92	0.09	-0.44	0.49	0.36	0.76	0.24	-1.89	-0.60	-0.89	-1.04	-0.92
rs4233949	2.40E-11	2	54159760	*Sptbn1*	YES	HET	-0.50	-3.80	-1.40	-1.20	-1.00	No data	0.70	No data	No data	-1.60	-1.90	-0.90	-1.50	0.10	No data	No data	No data	No data	No data
rs183979857	6.30E-11	2	203223050	*Cyp20a1*		HOM	-0.26	0.02	-0.47	-0.80	0.10	-0.07	0.37	-1.08	0.35	-0.16	-0.98	-0.09	-0.68	-0.08	1.02	-1.30	0.86	-0.06	0.16
rs2675952	1.40E-12	2	233290522	*Atg16l1*		HET	-0.08	-0.95	0.37	0.45	0.44	-0.53	-0.86	0.94	-0.80	-0.15	-0.11	-0.47	-0.16	0.63	-1.62	-2.23	-0.47	-1.29	-0.79
rs2675952	1.40E-12	2	233290522	*Sap*		HOM	0.92	0.03	-0.63	-0.13	-0.10	0.24	0.50	-0.58	-0.98	0.50	-0.61	0.57	0.02	-0.65	-0.06	-0.39	-0.19	0.18	0.50
rs58057291	2.90E-09	2	237895479	*Rab17*		HOM	-0.34	0.94	-1.32	-1.09	-1.14	1.36	0.49	-0.75	-0.33	0.78	0.23	0.08	0.18	0.27	0.35	-0.37	0.11	0.02	-0.84
rs2624847	1.80E-11	3	49674197	*Cish*		HOM	-0.48	-0.72	-0.48	-0.42	-0.27	0.22	-0.25	0.03	0.06	-0.68	0.13	0.31	-0.05	0.11	-0.85	0.87	0.08	-0.21	-0.17
rs2624847	1.80E-11	3	49674197	*Mrs1*		HOM	-2.68	0.06	-0.94	-0.29	-0.39	0.39	-1.54	0.68	-0.61	0.47	0.44	-0.29	0.40	0.53	-1.76	0.70	-0.05	-0.94	-1.17
rs11729027	4.70E-10	4	71491184	*Grsf1*		HOM	-0.86	0.46	-1.83	-0.83	-2.68	3.59	-1.43	0.00	-1.06	-0.22	-0.80	-0.98	-0.43	0.74	-0.29	-0.29	-0.20	-0.29	-0.76
rs72976751	1.30E-11	4	86226956	*Mapk10*		HOM	-0.65	-1.40	0.46	-0.18	0.68	-0.62	-0.73	-0.91	1.00	-1.26	-0.67	-0.29	0.36	-0.16	-1.01	-0.55	-0.73	-0.51	0.47
rs9327301	2.10E-10	5	122360170	*Crnkl1p3*	YES	HOM	-2.08	-1.04	-2.29	-1.13	-2.45	3.25	-0.73	-0.05	-0.43	0.33	-0.42	-0.24	-0.35	0.20	-0.25	-0.36	-0.17	0.05	0.05
rs4959677	8.10E-16	6	2000820	*Gmds*		HOM	-1.62	-4.33	-2.75	-2.30	-1.95	2.17	-3.39	2.02	0.30	0.25	-0.58	0.62	0.35	-0.78	-0.39	-3.89	-0.34	-0.66	-0.99
rs113166754	5.20E-47	6	44177173	*Supt3*		HET	-1.53	-0.09	-1.79	-1.01	-1.51	1.70	0.13	-0.64	0.13	0.30	-0.24	0.04	0.50	0.15	0.72	0.54	0.87	1.07	0.25
rs113166754	5.20E-47	6	44177173	*Tcte1*		HOM	-0.22	-1.33	1.36	-0.11	1.36	-1.21	1.03	-1.32	0.82	0.18	-1.44	0.99	0.01	-2.85	-0.12	-3.47	-0.45	-1.21	-1.13
rs11415701	3.50E-14	6	129845835	*Arhgap18*		HOM	0.80	0.10	0.00	0.20	-0.20	No data	1.30	No data	No data	0.20	0.10	0.40	0.20	0.10	No data	No data	No data	No data	No data
rs55784956	1.40E-01	6	151269853	*Mtmr6l1*		HET	-1.89	-2.14	-0.93	-0.79	-0.76	0.73	-1.55	0.16	1.61	-0.53	-0.47	-0.52	-0.03	0.50	-1.46	-0.61	-1.18	-1.02	0.06
rs62454422	5.80E-11	7	26691804	*Hibadh*		HOM	-0.81	0.86	-1.52	-1.24	-0.85	0.82	-0.96	0.47	-1.06	-0.88	-0.66	-0.15	0.14	-0.09	0.58	0.58	1.37	1.22	0.02
rs17236806	1.30E-11	7	37444375	*Elmo1*		HOM	0.04	0.68	1.29	-0.83	1.73	-1.32	-1.61	3.16	0.83	-1.60	0.00	-0.12	-0.90	0.20	-0.47	0.10	-0.07	-0.04	0.93
rs12154498	4.20E-12	7	91723518	*Akap9*		HET	-0.61	-1.69	0.36	-0.44	0.83	0.38	0.53	-1.92	-0.04	-1.18	-1.28	-0.61	-1.59	0.35	-0.25	-2.05	-0.20	-0.53	-0.43
rs149333699	1.10E-19	7	120418863	*Wnt16*	YES	HET	0.27	0.61	0.27	-0.21	0.53	-0.73	-1.18	0.37	0.17	0.28	-0.83	0.27	-1.47	-1.08	0.05	0.44	0.17	0.40	1.32
rs62621812	2.50E-16	7	126515083	*Esrrd*		HOM	-0.11	-0.40	-0.28	-0.06	-0.25	0.12	-0.34	0.19	-0.28	2.72	-0.11	1.22	-1.54	-2.17	-0.52	0.79	1.29	1.29	1.46
rs1005502	6.40E-11	8	116667843	*Evl9h*		HOM	-0.38	0.08	-1.55	-1.18	-1.15	1.12	-0.21	-0.03	-0.80	0.81	1.14	1.19	1.79	-0.57	0.12	-0.17	0.55	0.71	0.49
rs537120594	1.70E-18	9	132941613	*Lsmc3*		HOM	-0.01	0.57	-1.20	-0.94	-1.04	1.09	-0.74	0.50	0.43	-2.23	-0.32	0.24	-0.20	-0.34	0.61	-0.67	0.49	0.95	1.04
rs587729126	1.60E-15	9	135638765	*Med22*		HET	No data	No data	-0.18	-0.18	-0.53	0.46	-1.40	0.71	-0.42	-1.00	-1.11	0.05	-1.96	-0.52	-1.12	-0.48	-0.60	-0.90	0.64
rs587729126	1.60E-15	9	135638765	*Gtf3c5*		HET	-0.22	-0.27	-0.97	-0.55	-0.77	0.96	-1.13	0.71	-0.27	-1.40	-0.17	-0.89	0.66	0.79	-1.70	0.28	0.54	0.25	-0.31
rs70074558	3.70E-15	10	27376397	*Acbd5*		HOM	-1.21	-0.26	-1.99	-0.54	-1.86	2.28	-0.71	-0.26	0.05	0.04	-0.75	-0.08	-0.10	-0.16	0.32	-0.13	0.86	0.91	-0.12
rs11224192	4.70E-16	10	27939915	*Wac*		HET	1.19	2.19	1.06	-1.16	-0.54	0.53	1.84	-0.86	-0.75	2.94	1.01	1.00	-0.29	-0.81	2.23	-0.24	1.34	1.02	0.89
rs17662822	7.00E-27	10	53912481	*Mbd2*		HOM	-0.53	0.72	-1.03	-0.58	-0.68	0.63	0.55	-0.37	-1.19	0.31	0.19	-0.26	0.00	0.49	1.08	0.85	1.42	1.40	0.40
rs603424	2.50E-12	10	101575479	*Ndufb8*		HOM	-1.67	-0.70	-1.67	-1.52	-1.12	1.16	-0.76	-0.71	-0.69	-0.06	-0.66	-0.19	-0.24	-0.17	-0.52	-0.39	-0.54	-1.20	-1.44
rs11196177	7.00E-12	10	114224473	*Tcf7l2*	YES	HET	-0.60	-1.21	-0.29	-0.64	0.39	-0.61	-0.54	1.76	0.43	0.60	0.28	0.38	0.13	-0.45	0.00	0.13	1.59	0.95	0.20
rs10885441	2.30E-10	10	114666770	*Nhlrc2*		HET	-0.67	1.40	0.58	-1.07	1.59	-1.15	0.60	-0.62	0.57	2.30	1.57	0.59	1.04	-0.59	0.58	0.09	0.51	0.84	0.92
rs70693028	2.30E-08	10	123530741	*4933402N03Rik*		HOM	-0.08	1.13	-0.44	-1.12	0.11	-0.17	0.31	-0.18	0.18	-0.13	-0.24	0.21	-0.46	-0.05	-0.44	-0.46	0.40	-0.18	0.87
rs71059192	2.40E-15	11	84239372	*Trim66*		HOM	-1.10	-1.67	-0.13	0.36	-0.80	0.79	0.54	-0.59	0.41	-0.17	0.41	1.47	0.35	-1.74	0.30	-0.01	0.49	0.01	-1.01
rs17507571	1.40E-15	11	14743058	*Cyp2c1*		HOM	0.09	-0.04	-0.20	-0.15	0.08	-0.14	0.31	-0.40	0.26	1.70	-0.78	-0.11	-0.46	0.21	0.44	0.34	-0.45	-0.85	-0.30
rs34136481	1.50E-18	11	34594864	*Aplp*		HOM	-0.24	0.20	-0.48	0.17	-0.51	0.47	-0.28	-0.28	-1.04	1.52	-0.16	-0.81	0.17	0.78	0.25	0.57	0.48	0.24	-0.31
rs11806681	2.60E-32	11	46424665	*Pacsin3*	YES	HOM	0.64	0.66	-0.16	0.29	0.24	-0.36	-0.02	0.22	0.32	-0.95	1.18	-0.04	0.94	0.31	0.46	0.01	0.05	0.72	1.63
rs11806681	2.60E-32	11	46424665	*Zfp418*		HOM	-0.67	-0.86	-1.65	-2.58	-0.78	0.71	1.17	-1.05	1.41	1.97	0.59	-0.90	0.84	0.92	0.30	0.22	-0.08	-0.45	-0.77
rs117602572	1.20E-19	11	59448374	*Gif*		HOM	0.80	0.20	0.10	1.30	-0.50	No data	0.40	No data	No data	-0.30	0.40	0.70	0.40	-0.30	No data	No data	No data	No data	No data
rs174574	5.00E-09	11	61100342	*Fads3*		HOM	0.62	0.22	-1.15	-1.17	-0.64	0.73	1.15	-1.44	1.18	2.30	0.24	-0.11	0.49	0.11	1.68	-0.07	1.91	1.79	0.61
rs56864438	3.20E-16	11	64890693	*Ehbp1l1*		HET	-0.22	-0.65	-0.54	-1.49	0.09	-0.18	-0.53	1.03	0.33	0.26	-0.03	1.15	0.29	-0.91	0.03	-1.22	1.85	1.77	1.60
rs56864338	3.20E-16	11	64890803	*Rnaseh2c*		HET	0.32	-1.70	-0.71	-0.42	0.29	-0.36	-0.26	-0.15	-0.24	0.54	-0.63	-0.98	-0.24	0.75	-1.00	-1.89	-0.27	-0.32	-0.59
rs61887823	2.00E-20	11	67599622	*Aldh3b1*		HOM	-0.07	-0.33	1.09	-0.43	0.79	-0.79	-0.15	1.51	1.76	0.24	-0.08	0.95	1.82	-0.14	-0.83	-0.01	0.27	-0.37	0.15
rs61887823	2.00E-20	11	67599622	*Chka*		HET	1.48	0.14	-0.29	-1.03	0.86	-0.69	1.43	0.52	-0.88	0.28	3.44	0.16	3.67	0.81	0.58	0.23	0.94	0.39	-0.81
rs1048932	1.80E-33	11	114544850	*Cadm1*	YES	HOM	-3.20	0.10	-1.10	0.30	-1.30	No data	-1.90	No data	No data	-1.20	-2.00	-0.90	-1.40	0.70	No data	No data	No data	No data	No data
rs6489548	2.10E-12	12	88604	*Ccdc77*		HOM	-0.66	0.05	-0.21	-0.91	0.04	-0.10	-0.73	1.20	-0.17	1.93	-0.67	0.27	0.21	0.01	-1.08	0.47	0.56	0.42	0.80
rs6489548	2.10E-12	12	88604	*Ndng1*		HOM	0.11	-0.07	0.25	-1.14	0.39	-0.44	-0.01	-0.75	0.24	1.34	0.47	-0.15	0.54	0.10	0.53	-2.05	-0.80	-0.55	-0.94
rs11148821	4.00E-10	13	50637525	*Rnaseh2b*		HET	-0.74	-0.10	-0.46	-0.17	-0.44	0.33	-0.41	1.12	-0.54	-0.45	0.20	1.42	0.58	-0.99	0.35	0.44	-0.50	-0.08	-0.12
rs72635653	6.00E-09	13	93398697	*Gpc5*		HOM	1.59	0.52	-0.47	-0.44	0.08	-0.13	0.51	-0.81	-0.01	-1.86	-0.06	1.04	-0.75	-1.21	0.82	-0.87	-0.30	0.96	0.63
rs72635653	6.00E-09	13	93398697	*Gpc5*	YES	HOM	2.43	-1.95	1.15	1.56	-0.72	0.70	2.33	0.99	1.27	2.13	0.76	0.06	0.81	0.49	-0.25	-2.17	-1.01	-0.76	0.27
rs1042704	9.00E-14	14	22812594	*Pmf5*		HET	-1.42	-1.45	-0.87	0.59	-0.96	0.91	-1.01	0.58	-0.61	-0.32	-0.58	-0.92	-1.13	0.69	-0.97	-0.81	0.18	-0.16	0.05
rs1042704	9.00E-14	14	22812594	*Homez*		HOM	-1.96	-0.09	-1.82	-0.25	-2.67	5.50	-0.69	-1.34	0.64	0.86	-1.44	0.43	-0.57	-1.19	-0.39	-1.83	-0.40	-0.83	-0.57
rs1042704	9.00E-14	14	22812594	*1700123O20Rik*		HOM	-0.22	0.44	-1.57	0.04	-2.00	2.39	1.72	-0.97	1.10	1.52	0.19	0.32	0.58	-0.28	0.82	-0.31	1.05	0.42	0.07
rs11636402	6.80E-23	15	51048744	*Aplp1*		HOM	-0.53	-0.46	-1.74	-0.08	-2.26	2.96	-0.77	0.14	-0.89	-0.28	-0.61	-1.21	-1.06	0.85	-0.59	-0.46	-0.48	-0.40	-0.40
rs11636402	6.80E-23	15	51048744	*Dmxl2*		HET	-0.14	-0.26	-1.05	-1.24	-0.44	0.40	-1.00	1.63	0.88	0.35	0.15	-0.85	-0.91	0.54	0.01	-0.23	-0.77	0.12	0.56
rs8023466	1.10E-08	15	63341675	*Dapk2*		HOM	-0.96	-0.37	-1.47	-1.29	-1.36	1.73	0.10	-0.67	-0.25	-0.01	-0.66	-1.18	-0.25	0.74	0.07	-0.14	0.49	0.35	-0.37
rs8023466	1.10E-08	15	63341676	*Herc1*		HOM	-0.43	-0.35	-2.04	-0.87	-1.98	1.36	-0.12	-0.26	0.23	1.96	0.23	0.31	0.98	0.24	1.31	-1.18	0.81	0.04	-0.31
rs8023466	1.10E-08	15	63341675	*Usp3*		HET	-0.59	-0.79	-0.11	-0.96	1.39	-1.36	-1.48	1.90	-0.25	-0.29	-0.43	-1.09	0.46	0.83	-0.34	0.41	-1.35	-0.99	-0.21
rs11637971	1.20E-14	15	90578863	*Ngrn*		HET	-0.40	1.21	-0.91	-0.23	-0.55	0.43	0.43	0.01	0.59	0.56	0.66	-0.10	0.92	0.35	-0.59	0.56	-0.89	-1.17	-1.31
rs11637971	1.20E-14	15	90578863	*Vps33b*		HET	-0.59	-0.79	-0.11	-0.96	1.39	-1.36	-1.48	1.90	-0.25	-0.29	-0.43	-1.09	0.46	0.83	-0.34	0.41	-1.35	-0.99	-0.21
rs2301522	1.60E-16	16	309953	*Nme4*	YES	HOM	0.32	0.58	-1.31	-1.02	-1.30	1.37	0.27	0.46	0.88	1.83	0.43	0.29	-0.59	0.05	No data	No data	No data	No data	No data
rs2301522	1.60E-16	16	309953	*Rhod*		HOM	-1.59	-2.21	-1.27	0.09	-1.62	1.72	-2.26	1.18	-0.58	-1.83	-0.49	-0.97	0.33	0.84	-2.32	-0.28	-0.42	-1.20	-0.91
rs2301522	1.60E-16	16	309953	*Mpg*		HOM	-0.96	-0.33	-1.67	-1.66	-0.91	0.88	-0.10	-0.05	-0.80	0.14	0.55	-1.13	0.65	0.93	0.85	-0.58	0.17	0.59	0.41
rs1131996631	3.90E-10	16	22652702	*Dclre1b*		HET	-0.87	-0.77	-1.10	-0.19	-1.16	1.13	-1.27	0.87	-0.26	-0.81	0.00	1.61	1.30	-2.35	-0.61	0.41	-0.71	-0.48	0.12
rs1131996631	3.90E-10	16	22652702	*Eanz*		HET	0.32	-1.68	0.14	2.54	-1.50	1.74	-0.35	-0.17	-0.79	0.31	0.62	0.97	0.10	-0.24	1.13	-0.32	-0.02	-0.28	0.29
rs9972653	7.30E-10	16	53314363	*Chd9*		HOM	-0.65	-0.82	0.35	-0.01	0.16	-0.18	-0.60	-1.45	-1.33	-0.54	-1.54	0.53	-1.20	-1.42	-0.13	-0.34	-1.08	-1.32	-1.40
rs9972653	7.30E-10	16	53314363	*Fto*		HOM	0.29	-0.25	-0.84	0.18	-1.99	2.94	0.94	1.36	0.31	-0.67	-0.17	-0.09	0.32	0.35	-0.13	1.52	-0.48	-0.03	-0.75
rs9972653	7.30E-10	16	53314363	*Rpgrip1l*		HET	-0.15	0.20	-1.61	0.06	-1.24	1.29	-0.20	0.24	-0.62	0.92	-0.35	0.06	0.44	0.25	-1.52	0.89	-0.57	-0.61	0.38
rs17680862	7.40E-20	16	66822118	*Cbl2*		HET	-2.17	-0.18	-0.62	-0.06	-2.08	2.69	-2.65	2.75	-0.99	-1.65	-0.20	-0.40	-0.74	0.41	-1.10	-0.05	-0.94	-1.34	-0.54
rs4888151	8.80E-11	16	81059006	*Cmip*		HET	0.37	1.62	-1.03	0.42	-1.54	1.49	1.10	-0.61	0.37	0.89	0.40	0.45	0.66	-0.01	-0.59	1.90	0.03	-0.77	0.26
rs2376600	1.80E-15	17	428078	*Vps53*		HET	-1.44	-0.52	-0.46	-0.47	-0.37	0.18	-0.18	0.02	-0.89	1.14	-0.17	-0.13	-0.23	0.24	0.34	-0.90	-0.92	-1.04	-0.22
rs2376600	1.80E-15	17	428078	*Nsn*		HET	-2.82	-0.97	-1.74	-0.42	-2.48	2.94	-0.75	0.06	-1.12	0.47	0.53	0.33	1.00	0.14	0.44	0.26	-0.25	-0.02	-0.22
rs78180894	7.90E-10	17	6983662	*Dlg4*		HOM	-0.09	-0.83	3.12	2.87	0.23	-0.07	-1.70	1.10	-1.33	-0.91	-1.35	-1.06	-0.47	0.71	-0.65	-1.34	-0.57	-1.42	-0.95
rs78180894	7.90E-10	17	6983662	*Wrap53*		HET	-1.24	-0.45	-1.51	-0.41	-2.34	2.77	-1.03	0.19	-0.97	0.27	-0.43	-0.56	-0.24	0.61	1.82	0.98	1.13	1.30	0.58
rs56235411	7.60E-11	17	8642846	*Sbdl*		HOM	-2.35	1.09	-1.71	0.42	-2.68	2.54	-1.04	1.73	-0.93	-0.31	0.87	1.24	1.21	-0.84	-1.34	0.23	-0.86	-0.74	-0.38
rs72790163	1.00E-15	17	27401561	*Coro6*		HOM	-0.74	-0.01	-1.43	-1.56	-0.80	0.84	0.27	-0.47	0.45	0.60	-0.57	0.15	0.08	0.02	0.36	-0.14	0.53	0.28	0.00
rs4239232	4.10E-10	17	29319146	*Nf1*		HET	-1.34	-0.16	-0.44	0.09	-1.13	1.31	-1.17	0.36	0.17	-0.12	-0.10	0.79	-1.26	-0.86	-1.07	0.17	-1.20	-1.60	-1.14
rs143043662	4.20E-10	17	39413771	*Nkiras2*		HOM	-0.63	-1.30	-1.85	-0.06	-2.13	3.80	-1.32	-0.09	-0.40	-0.07	-1.53	-0.65	-1.35	0.32	-1.63	-2.14	-0.27	-0.73	-0.51
rs143043662	4.20E-10	17	39413771	*Rab5c*		HOM	-0.74	0.18	-1.74	-0.33	1.80	-1.55	-1.42	0.08	1.21	0.79	-1.15	0.39	-1.02	-0.41	-0.64	0.29	-1.17	-1.10	-1.07
rs143043662	4.20E-10	17	39413771	*Kcnh4*		HOM	-3.38	-0.86	-2.62	-2.39	-1.53	1.51	0.10	-0.24	0.32	0.49	0.96	-0.55	0.88	0.69	0.16	0.55	0.53	0.87	0.72
rs7209826	2.30E-36	17	41296408	*Arl4d*		HOM	-0.22	-2.25	-1.08	-0.35	-1.82	2.29	-1.55	1.03	-0.33	-2.94	-1.36	-1.37	-1.40	0.84	-0.97	-2.84	-0.49	-0.82	-0.35
rs7209826	2.30E-36	17	41296408	*Cd300lg*	YES	HOM	-1.80	-0.94	-0.86	-0.28	-0.61	0.44	-0.94	1.44	-0.50	-0.77	-0.39	-0.33	0.87	0.53	-1.03	0.21	-0.95	-0.93	-0.16
rs7209826	2.30E-36	17	41296408	*Dusp3*		HOM	0.06	-0.09	0.02	-0.15	0.49	-0.48	-0.25	0.04	-0.48	-0.26	-0.31	0.52	0.71	0.18	-1.57	0.04	-0.50	-1.12	-0.64
rs2696264	3.70E-18	17	47833348	*Rsad1*		HOM	-0.11	-0.08	0.14	0.59	0.20	-0.31	-0.05	0.28	0.76	-0.29	0.50	-0.67	0.86	0.71	-0.77	-1.89	-0.05	-0.57	-1.30
rs34202212	6.40E-10	17	78926021	*Ccdc137*		HET	0.68	0.02	-0.22	-0.06	0.19	-0.24	0.51	0.95	-0.29	-0.85	0.20	0.57	0.56	0.17	0.23	0.31	-0.66	-0.96	-1.12
rs34202212	6.40E-10	17	78926021	*Chmp6*		HET	-0.76	-0.19	-1.79	-0.91	-1.66	1.99	-0.27	-0.57	-0.43	0.57	-0.24	-0.12	-0.17	-0.05	0.26	0.52	-0.42	-0.61	-1.03
rs34202212	6.40E-10	17	78926021	*Enthd2*		HOM	0.05	0.78	-1.99	-1.77	-0.87	0.91	0.55	-0.63	-0.65	1.18	0.25	1.03	0.68	-1.10	0.35	0.40	0.75	0.96	1.09
rs34202212	6.40E-10	17	78926021	*Nploc4*		HET	-1.60	-1.00	-0.70

Supplementary Table 16. Summary of the evidence implicating GPC6 in the pathophysiology of osteoporosis

RSID	MAF	GPC6 LOCATION	EA	P_{GWAS}	FINEMAP: log_{10} BAYES FACTOR	DHS CELL TYPES	$P_{CIS-eQTL}$	MURINE CELL EXPRESSION	MURINE KNOCKOUT MODEL DATA
rs1933784	0.051	Intronic	G	$2.3x10^{-10}$	2.4	AG04450; BE2_C; GM04504A; HNPCEpiC; HSMM_D; IMR90; LHCN_M2_D4; NHDF_Ad; NHDF_Neo; WERI_Rb1; fAdrenal; fHeart; fIntestine_Lg; fKidney; fMuscle; hTH17; iPS_19_11	$4.7x10^{-7}$	Osteoblasts, Osteocytes	Increased femoral BMC, increased femoral yield load, increased femoral cortical thickness, decreased vertebral height

RSID Reference SNP cluster ID
MAF Minor allele frequency (Same as the effect allele frequency)
EA Effect allele (G allele is associated with decreased eBMD)
P_{GWAS} Strength of evidence against the null hypothesis of no association between rs1933784 and eBMD (i.e. P-value)
$P_{CIS-eQTL}$ Strength of evidence against the null hypothesis of no association between rs1933784 and GPC6 expression in human osteoblasts (i.e. P-value)